

11163

NATIONAL LIBRARY
OTTAWA



BIBLIOTHÈQUE NATIONALE
OTTAWA

NAME OF AUTHOR...Mr....Robin....Roman.....
TITLE OF THESIS...The...kinetics...of...the...Oxidation
 . Reactions...Catalyzed...by...Horse radish
 .. Peroxidase.....
UNIVERSITY...University...of...Alberta.....
DEGREE FOR WHICH THESIS WAS PRESENTED.....Ph.D.....
YEAR THIS DEGREE GRANTED...1972.....

Permission is hereby granted to THE NATIONAL LIBRARY
OF CANADA to microfilm this thesis and to lend or sell copies
of the film.

The author reserves other publication rights, and
neither the thesis nor extensive extracts from it may be
printed or otherwise reproduced without the author's
written permission.

(Signed)...Robin...Roman.....

PERMANENT ADDRESS:

..9852...86...Ave.....
..Edmonton...Alberta.
.....

DATED...April...28.....1972

NL-91 (10-68)

THE UNIVERSITY OF ALBERTA

THE KINETICS OF THE OXIDATION REACTIONS
CATALYZED BY HORSERADISH PEROXIDASE

by



ROBIN S. ROMAN

A THESIS

SUBMITTED TO THE FACULTY OF GRADUATE STUDIES AND RESEARCH
IN PARTIAL FULFILMENT OF THE REQUIREMENTS FOR THE DEGREE
OF DOCTOR OF PHILOSOPHY

DEPARTMENT OF CHEMISTRY

EDMONTON, ALBERTA

SPRING, 1972

THE UNIVERSITY OF ALBERTA
FACULTY OF GRADUATE STUDIES AND RESEARCH

The undersigned certify that they have read, and
recommend to the Faculty of Graduate Studies and Research,
for acceptance, a thesis entitled

"THE KINETICS OF THE OXIDATION REACTIONS CATALYZED BY
HORSE RADISH PEROXIDASE"

Submitted by ROBIN S. ROMAN in partial fulfilment of the
requirements for the degree of Doctor of Philosophy.

H.B. Dufford
.....
Supervisor

W.H. H. H. H.
.....

W. G. Graham
.....

George Kotowicz
.....

W. H. H. H.
.....

Keith J. Cairns
.....
External Examiner

Date

Abstract

The kinetics of the reactions of compounds I and II of horseradish peroxidase with iodide, sulfite and nitrite were studied as a function of pH at 25° and ionic strength 0.11. The rate law for the reactions of both compounds with all three substrates was the same; the reactions were first order in both the enzyme species and the substrate. The pH dependence for every reaction showed a general trend of increasing rate with increasing acidity, although there were differences in the detailed pH dependences for the reactions.

For the reactions of compounds I and II with iodide, it was possible to demonstrate, using the diffusion controlled limit, that iodide ion and not hydriodic acid was the reacting species. The second-order rate constant for the reaction between compound II and iodide increases linearly with increasing hydrogen ion concentration from a value of $0.10 \text{ M}^{-1}\text{sec}^{-1}$ at pH 9.05 to $2.3 \times 10^5 \text{ M}^{-1}\text{sec}^{-1}$ at pH 2.71. The pH dependence for the reaction is interpreted in terms of an acid dissociation on compound II the pK_a value of which is lower than the lowest pH of the kinetic study. This enzyme ionization has a large effect on the reaction rate and is assumed to have an intimate relation to the heme group. The second-order rate constant for the reaction between compound I and iodide increases with increasing acidity from a value of $7.7 \text{ M}^{-1}\text{sec}^{-1}$ at pH 9.87 to a value of

$2.1 \times 10^6 \text{ M}^{-1}\text{sec}^{-1}$, at pH 2.70. The pH dependence of the reaction is interpreted in terms of two enzyme ionizations on compound I; one pK_a is 4.6 and the other lies outside the pH range of the study. It is established that the reaction of compound I proceeds without the intermediate formation of compound II and involves a two electron transfer from iodide.

The second-order rate constant for the reaction between compound II and sulfite increases with increasing acidity from a value of $1.8 \times 10^2 \text{ M}^{-1}\text{sec}^{-1}$ at pH 6.92 to $6.8 \times 10^5 \text{ M}^{-1}\text{sec}^{-1}$ at pH 2.43. The pH dependence of the reaction is interpreted in terms of an enzyme ionization with a pK_a value of 3.9. The second-order rate constant for the reaction between compound I and sulfite increases with increasing acidity from a value of $76 \text{ M}^{-1}\text{sec}^{-1}$ at pH 7.22 to a value of $1.2 \times 10^5 \text{ M}^{-1}\text{sec}^{-1}$ at pH 2.28. The pH dependence of the reaction is interpreted in terms of two enzyme ionizations with pK_a values of 5.1 and 3.3. It is shown that the reaction of compound I proceeds without the intermediate formation of compound II and involves a two electron transfer from sulfite.

The second-order rate constants for the reactions of compounds I and II with nitrite increase linearly with increasing hydrogen ion concentration from a value of $8.2 \text{ M}^{-1}\text{sec}^{-1}$ at pH 8.84 to a value of $6.5 \times 10^3 \text{ M}^{-1}\text{sec}^{-1}$ at pH 5.97 for the compound I reaction and from a value of $4.5 \text{ M}^{-1}\text{sec}^{-1}$ at pH 7.53 to a value of $1.8 \times 10^2 \text{ M}^{-1}\text{sec}^{-1}$ at pH 5.98 for the compound II reaction. The reaction

between compound I and nitrite produces compound II with the transfer of a single electron from nitrite to compound I.

The high resolution NMR spectrum of the horseradish peroxidase-cyanide complex was recorded. No resonances shifted outside the range normally observed for protons on diamagnetic molecules were detected and possible explanations of this phenomenon are discussed.



Acknowledgements

I would like to thank my research director, Prof. H. B. Dunford, for the encouragement and advice he has given me throughout the course of my research. I would also like to thank Dr. J. Critchlow and Dr. M. Evett for their helpful discussions and suggestions. I am indebted to my fellow graduate students, Meredith Cotton and James Maguire for their help in performing the NMR experiments and their co-operation in performing the routine activities necessary for the smooth operation of the laboratory.

I would like to make an acknowledgement to Dr. G. Kotowycz for his collaboration on the NMR experiments.

CONTENTS

	Page
Abstract	i
Acknowledgements	iv
List of Tables	viii
List of Figures	x

Chapter 1

Introduction

1.01 Peroxidases	1
1.02 Physical Properties of Horseradish Peroxidase	5
1.03 Catalysis by Horseradish Peroxidase	17
1.04 Nature of the Oxidized Compounds of Horseradish Peroxidase	21
1.05 Kinetic Measurements of the Reactions of HRP-I and HRP-II	28

Chapter 2

Oxidation of Iodide by Horseradish
Peroxidase Compounds I and II

2.01 Introduction	37
2.02 Experimental	38
2.03 Results	48
2.04 Discussion	103

Chapter 3

Oxidation of Sulfite by Horseradish Peroxidase
Compounds I and II

3.01	Introduction	117
3.02	Experimental	118
3.03	Results	126
3.04	Discussion	140

Chapter 4

Oxidation of Nitrite by Horseradish Peroxidase
Compounds I and II

4.01	Introduction	150
4.02	Experimental	150
4.03	Results	153
4.04	Discussion	162

Chapter 5

High Resolution NMR Studies on HRP

5.01	Introduction	165
5.02	Experimental	170
5.03	Results	172
5.04	Discussion	177
	Summary, Conclusions and Suggestions for Further Work	183
	Bibliography	189

Appendix 1

Purification of Crude HRP 197

Appendix 2

The pH Dependence of the Second-Order Rate Constant
for the Reaction of HRP-I with Iodide 202

Appendix 3

Error Estimates on the Parameters Calculated from the
Nonlinear Least-Squares Analysis of the Kinetic pH
Dependence 205

Appendix 4

Descriptions of Photomultiplier Circuit Modifications
and the Analog-to-Digital Converter used with the
Stopped-Flow Apparatus 216

List of Tables

Table	Page
1.01 Amino Acid Composition of HRP Isozymes	15
1.02 Magnetic and ESR Properties of HRP and Its Complexes and Compounds	25
2.01 Second-Order Rate Constants for the HRP-I- Iodide Reaction at 25°	52
2.02 Ground State and Transition State Ionization Constants Obtained by the Nonlinear Least- Squares Analyses of Equations 2.18 and 2.19 ..	73
2.03 Second-Order Rate Constants for the HRP-II- Iodide Reaction at 25°	77
2.04 Comparison of the Rate Constants Measured Directly and by the Steady-State Method for the HRP Catalyzed Oxidation of Iodide	88
2.05 Molar Absorptivity Values for the Spectrum of HRP-I	97
3.01 Second-Order Rate Constants for the HRP-I- Sulfite Reaction at 25°	128
3.02 Ground State and Transition State Ionization Constants Obtained by the Nonlinear Least-Squares Analysis of Equation 3.04 for the HRP-I-Sulfite Reaction	131
3.03 Second-Order Rate Constants for the HRP-II- Sulfite Reaction at 25°	134

List of Tables

Table	Page
3.04 Ground State and Transition State Ionization Constants Obtained by the Nonlinear Least-Squares Analyses of Equations 3.08 and 3.09 for the HRP-II-Sulfite Reaction	136
3.05 Observed First-Order Rate Constants for the Decay of the Transient Enzymatic Species Formed from the HRP-II-Sulfite Reaction	139
4.01 Second-Order Rate Constants for the HRP-I-Nitrite and HRP-II-Nitrite Reactions at 25°	155
A 3.01 Errors Resulting from the Analysis of Equation 2.18 with K_2 as an Invariant Parameter for the Reaction of HRP-I with Iodide	211
A 3.02 Errors Resulting from the Analysis of Equation 3.04 with K_5 as an Invariant Parameter for the Reaction of HRP-I with Sulfite	212
A 3.03 Errors Resulting from the Analysis of Equation A 3.01 with K_7 as an Invariant Parameter	213
A 3.04 Errors Resulting from the Analysis of Equation 3.04 with K_4 as an Invariant Parameter for the Reaction of HRP-I with Sulfite	215

List of Figures

Figure	Page
1.01 Structure of ferriprotoporphyrin IX	7
1.02 Spectra of HRP, HRP-I and HRP-II	23
2.01 Plot of $k_{1,obs}$ <u>vs.</u> $[I^-]$ for the HRP-I-iodide reaction at pH 4.99	50
2.02 Plot of $\log k_1$ <u>vs.</u> pH for the HRP-I-iodide reaction at 25°	54
2.03 Schematic plot of $\log k_1$ <u>vs.</u> pH for the HRP-I- iodide reaction	57
2.04 Schematic plot of $\log k_1$ <u>vs.</u> pH for the HRP-I- iodide reaction	68
2.05 Plot of $k_{2,obs}$ <u>vs.</u> $[I^-]$ for the HRP-II-iodide reaction at pH 3.41	75
2.06 Plot of $\log k_2$ <u>vs.</u> pH for the HRP-II-iodide reaction at 25°	76
2.07 Experimental traces of absorbance at 411 nm <u>vs.</u> time for the HRP-I-iodide reaction with varying $[H_2O_2]$	80
2.08 Plot of the molar absorptivity difference between HRP:HRP-I and HRP-II:HRP-I <u>vs.</u> wavelength	82
2.09 Experimental trace of absorbance at 411 nm <u>vs.</u> time for the HRP-I-iodide reaction with successive additions of hydrogen peroxide ..	84

List of Figures

Figure	Page
2.10 Plot of $[\text{HRP}]_0/v$ <u>vs.</u> $1/[\text{I}^-]$ at pH 4.0	87
2.11 Plot of $[\text{HRP}]_0$ <u>vs.</u> dA_{353}/dt at pH 7.0	91
2.12 Experimental traces of absorbances <u>vs.</u> time for the HRP-iodide steady-state cycle	93
2.13 Spectrum of HRP-I compared to HRP	96
2.14 Plot of the change in absorbance at 353 nm <u>vs.</u> $[\text{H}_2\text{O}_2]$	99
2.15 Plot of the change in absorbance at 411 nm <u>vs.</u> $[\text{I}^-]$ for the titration of HRP-I with iodide ..	101
2.16 Plot of the change in absorbance at 425 nm <u>vs.</u> $[\text{I}^-]$ for the titration of HRP-II with iodide..	102
3.01 Plot of $k_{3,\text{obs}}$ <u>vs.</u> [sulfite] for the HRP-I- sulfite reaction at pH 3.81	127
3.02 Plot of $\log k_3$ <u>vs.</u> pH for the HRP-I-sulfite reaction	130
3.03 Plot of $k_{4,\text{obs}}$ <u>vs.</u> [sulfite] for the HRP-II- sulfite reaction at pH 5.38	133
3.04 Plot of $\log k_4$ <u>vs.</u> pH for the HRP-II-sulfite reaction	135
3.05 Spectrum of the enzymatic species present in the steady state for the HRP catalyzed oxidation of sulfite	138
4.01 Plot of $k_{5,\text{obs}}$ <u>vs.</u> [nitrite] for the HRP-I- nitrite reaction at pH 6.92.....	154

List of Figures

Figure	Page
4.02 Plot of $k_{6,obs}$ <u>vs.</u> [nitrite] for the HRP-II-nitrite reaction at pH 5.98.....	157
4.03 Spectrum of the enzymatic species present in the steady state for the HRP catalyzed oxidation of nitrite	158
4.04 Plot of the changes in absorbance at 355 nm and 300 nm <u>vs.</u> $[H_2O_2]$, for the HRP catalyzed reaction between nitrite and hydrogen peroxide.	160
4.05 Plot of the changes in absorbance at 411 nm <u>vs.</u> [nitrite] for the titration of HRP-I with nitrite	161
5.01 NMR spectra of the low field region for My-CN and ferriprotoporphyrin IX-cyanide complex ...	173
5.02 NMR spectrum of HRP-CN from -10 to + 5 ppm ...	174
5.03 NMR spectrum of HRP-CN from -25 to -5 ppm	175
5.04 NMR spectrum of HRP-CN from -10 to 10 ppm	176
A 1.01 Plot of the absorbance of various fractions from the HRP purification	199
A 4.01 Circuit diagram for the photomultiplier amplifier	218

CHAPTER 1

Introduction

1.01 Peroxidases

Peroxidases are heme-containing enzymes that are found widely distributed in both plants and animals. These enzymes catalyze the reaction between hydrogen peroxide and a wide variety of organic and inorganic compounds. The wide distribution of peroxidases and the extensive variety of reactions catalyzed by them, suggests that their biological functions may vary according to the source of the enzyme (Paul, 1963).

The first recorded indication of peroxidase activity was a report that guaiacum turned to an intense blue color in the presence of fresh root of horseradish (Planche, 1810). Later it was recorded that the oxidation of certain organic compounds by dilute solutions of hydrogen peroxide could be catalyzed by "substances" occurring in plants and animals (Schönbein, 1855). The name peroxidase was first given by Linossier who isolated an oxidase-free preparation of peroxidase from pus (Linossier, 1898). In the early 1900's peroxidases from horseradish (Bach and Chodat, 1903) and beet roots (Ernest and Berger, 1907) were obtained free from other enzymes and the presence of peroxidases in many plant and animal tissues was demonstrated (Battelli and Stern, 1908). Although Willstätter suspected a relationship between peroxidase activity and iron content (1923), this

fact was not proven until a proportional relationship between peroxidase activity and the Soret band (characteristic of iron porphyrins) was shown (Kuhn et al. 1931). Later Keilin and Mann obtained a reasonably pure sample of horseradish peroxidase and confirmed the observations of Kuhn (Keilin and Mann, 1937). Subsequent work on the cleavage and re-synthesis of horseradish peroxidase showed that the prosthetic group was ferriprotoporphyrin IX (Theorell, Bergstrom and Akeson, 1942).

Peroxidases are believed to be present in all higher plants. Horseradish roots and the sap of fig trees are the richest sources of peroxidase. Partially as a result of this fact, horseradish peroxidase (EC 1.11.17; donor: H_2O_2 oxidoreductase), subsequently referred to as HRP, has been the most extensively studied peroxidase. HRP is a heme-containing glycoprotein of molecular weight 40,000 (Maehly, 1955) with an amino acid content of about 300 residues and a carbohydrate content of about 18% (Shannon et al., 1966). HRP is an efficient catalyst for the oxidation of phenols and aromatic amines. The product formation from such reactions has been extensively studied with the hope that this knowledge could give insight into the mechanism of peroxidatic reactions. Although these studies have uncovered many interesting phenomena, they have left the fundamental questions of reaction mechanism unanswered (Saunders et al., 1964). HRP has been implicated in both the oxygen and hydrogen peroxide catalyzed oxidation of the plant

hormone indole acetic acid (Hinman and Lang, 1965), raising the possibility that the biological function of HRP might be related to the control of plant growth and metabolism.

In addition to the higher plants, peroxidases are also found in molds, microorganisms and animals. Due primarily to the studies of Hager and co-workers a peroxidase from the mold *Caldariomyces fumago*, chloroperoxidase, has been isolated and characterized. Chloroperoxidase has a molecular weight of about 42,000, contains about 25% carbohydrate and like HRP has ferriprotoporphyrin IX as the heme prosthetic group (Thomas et al., 1970). In many of its chemical and physical properties chloroperoxidase is similar to HRP, however chloroperoxidase has the unique ability among peroxidases, to catalyze the oxidation of chloride ions. The biological function of chloroperoxidase is believed to be related to the oxidation of chloride in the biosynthesis of the fungal metabolite Caldariomycin (2,2-dichloro-1,3-cyclopentanediol).

Cytochrome c peroxidase has been the most extensively studied peroxidase isolated from microorganisms. Obtained from aerobically grown baker's yeast, cytochrome c peroxidase has a molecular weight of 34,100 and contains ferriprotoporphyrin IX as its prosthetic heme group. It is unique among peroxidases in that it contains no carbohydrate (Yonetani, 1970).

Cytochrome c peroxidase catalyzes most typical peroxidase reactions, however its specific activity toward ferrocytochrome c is exceedingly high compared to other reducing agents. Although other peroxidases including HRP have been shown to oxidize ferrocytochrome c to ferricytochrome c (Chance, 1952a), they are much less efficient catalysts than cytochrome c peroxidase.

A peroxidase isolated from cows' milk, lactoperoxidase, has been the most extensively studied animal peroxidase. Lactoperoxidase is a glycoprotein with a molecular weight between 75,000 and 80,000 (Rombauts et al., 1967). The heme group in lactoperoxidase has not been unequivocally established, however it is known that the heme is covalently bonded to the protein and that it is not ferriprotoporphyrin IX. Despite the major differences in the physical properties of lactoperoxidase and HRP, the two enzymes have remarkably similar catalytic properties. The recent studies in our laboratory dealing with the oxidation of iodide (Maguire and Dunford, 1972a) and p-cresol (Maguire and Dunford, 1972b) by lactoperoxidase compound II bear a striking resemblance to the analogous oxidations observed for HRP (Roman et al., 1971; Critchlow and Dunford, 1972a).

Thyroid peroxidase, found in mammalian thyroid glands, is a heme protein of molecular weight 62,000 (Taurog et al., 1970). To date thyroid peroxidase has not been isolated in sufficient quantity or purity to determine its amino acid or carbohydrate content. The nature of the heme group

is uncertain, however recent evidence indicates that it may not be ferriprotoporphyrin IX (Taurog et al., 1970). Thyroid peroxidase is one of the few peroxidases that has a well defined biological function. There is good evidence to indicate that it functions in the biosynthesis of the growth hormone thyroxine through the oxidation of iodide (Hosoya, 1968). Thyroid peroxidase has also been implicated in the iodination of the tyrosine residues of thyroglobulin and the coupling of diiodotyrosines necessary for thyroxine formation (Taurog, 1970). The fact that HRP can catalyze the oxidation of iodotyrosine and thyroxine, suggests a possible feedback mechanism involving thyroid peroxidase in the control of thyroxine levels (Saunders et al., 1964).

1.02 Physical Properties of Horseradish Peroxidase

There is strong evidence to indicate that the heme iron is an essential site in peroxidase catalysis. This concept is based partly on the analogy between HRP and the respiratory proteins, myoglobin and hemoglobin, which contain the same heme group as HRP and are known to bind oxygen to the iron, and partly to the inhibition of peroxidase activity caused by the addition of cyanide and fluoride, two ions known to be strongly co-ordinated to iron. Because of its importance in the catalytic process, the configuration of the iron in HRP has been extensively studied. The high paramagnetic susceptibility observed for native HRP at neutral pH, 5.5 Bohr magnetons (Keilin and Hartree, 1951),

provides good evidence that the iron is in the ferric high spin form with five unpaired electrons. The ESR studies of Blumberg *et al.* (1968) on HRP verified the high spin ferric nature of native HRP, and in addition, revealed that the iron in HRP does not possess axial symmetry as normally observed for hemoglobin, myoglobin and ferriprotoporphyrin IX. At pH values above 11, marked changes in the magnetic moment and absorption spectrum of HRP are observed. This reversible transition to a ferric low spin compound with magnetic moment, 2.7 Bohr magnetons, has been attributed to the formation of an iron-hydroxide complex. HRP forms spectrally distinct compounds with cyanide and fluoride, and the magnetic moments for these complexes (2.7 Bohr magnetons for the cyanide complex and 5.9 for the fluoride complex) are as would be expected from the known ligand-field splitting ability of the two ions (Brill, 1966).

The iron in HRP is contained in the prosthetic group ferriprotoporphyrin IX, the structure of which is illustrated in Fig. 1.01. The chelation of the iron ion by the porphyrin involves the displacement of two protons from the pyrrole nitrogens to form a structure that is almost square planar. The positions above and below the plane of the nitrogen atoms are available for further co-ordination. The structure of the metmyoglobin molecule at a resolution of 1.4 Å shows the iron atom to lie 0.3-0.5 Å on one side of the plane of the porphyrin ring, and equally distant from the four pyrrole nitrogen atoms (Watson, 1968). Until there is

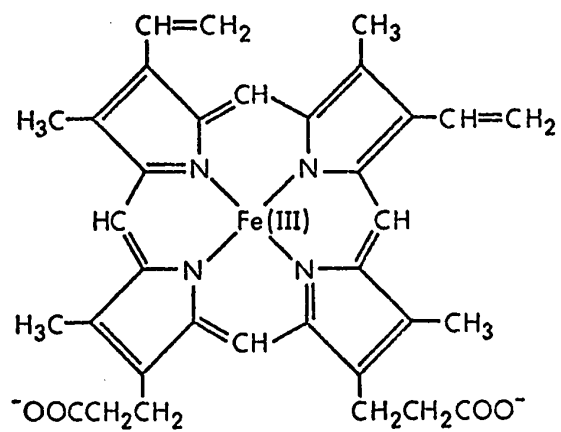


Fig. 1.01: Structure of ferriprotoporphylin IX.

evidence to indicate the contrary, it seems a reasonable assumption that iron in the heme group of HRP should also be very nearly in the tetrapyrrole plane and centrally located. The positions of the six ligands of the octahedral iron complexes found in hemoproteins are conventionally numbered one through four for the pyrrole nitrogens, five for the donor group which is bound to the protein and six for the site which is accessible to the aqueous medium. In general, for a particular hemoprotein, the ligands at positions 1-5 remain the same.

Hemoproteins are most frequently characterized by their distinctive visible and u.v. absorption spectra. The spectra and interpretation of the spectra for a wide variety of hemoproteins (including HRP) have recently been reviewed by Smith and Williams (1969). The spectra of metalloporphyrins have been well characterized in terms of three bands resulting from $\pi \rightarrow \pi^*$ transitions in the porphyrin. Two bands are in the visible region (molar absorptivity $\sim 10^4 \text{ M}^{-1} \text{ cm}^{-1}$) and give rise to the characteristic color of the porphyrin, the third more intense band is in the near u.v. (molar absorptivity $\sim 10^5 \text{ M}^{-1} \text{ cm}^{-1}$) and is referred to as the Soret band. The spectra of most heme proteins are more complicated than the simple porphyrins with several additional bands in the visible region. Although the nature of these bands have not been established with certainty, Smith and Williams suggest that they may be charge transfer

bands. In the present work the Soret band was used to determine concentrations of HRP. The various Soret bands of complexes and compounds of HRP were also used to distinguish between the enzymatic species. The great intensity of the bands in the Soret region facilitated work at the low concentrations of enzyme that were desired.

The mode of attachment of the heme group to the protein in HRP is not known with certainty, however the ease with which the heme group can be reversibly detached from the apoprotein is good evidence to indicate that the heme is not covalently bonded to the protein backbone. Because myoglobin has an identical heme group and a similar visible spectrum to that observed for HRP, it has long been thought that the heme attachment in myoglobin would be a reasonable model for that observed in HRP. In myoglobin the heme is held in a crevice with the non-polar vinyl groups buried in the hydrophobic interior of the protein. The iron atom is attached to the imidazole of a histidine in the fifth position and a water molecule in close proximity to a distal histidine in the sixth position. The propionic acid groups are on the outside of the protein and are weakly bound to some basic amino acids (Kendrew, 1962). In myoglobin the heme is held in place primarily by hydrophobic interactions in the interior of the molecule. In HRP, however, there is evidence to indicate that the propionic acid groups are implicated in the binding. The maximum of the Soret band

obtained when protoporphyrin IX reacts with the apo-horseradish peroxidase is very nearly the same as the maximum and extinction coefficient observed for the native enzyme. However, when the carboxyl groups are blocked by forming the dimethyl esters, there is no spectrophotometric indication of binding upon addition of the modified prosthetic group to the apoenzyme (Maehly, 1951). The same phenomenon was observed by Paul et al. (1959) who (1) replaced the propionic acid residues with H or COOH groups and (2) prepared an isomer of ferriprotoporphyrin IX with one propionic acid group shifted on the porphyrin skeleton. In both cases they found the modified hemes entirely inactive. Changes in structure of the vinyl groups, however, left the activity of the reconstituted enzyme unmodified or slightly enhanced (Paul, 1960).

The recent titration studies of Phelps et al. (1971) on native and apo-horseradish peroxidase suggest that in many respects the two proteins are dissimilar. Since the removal of the heme group is solely responsible for a change which is restored by its replacement, the heme group must contribute essentially to the structure of the peroxidase protein. Removal of the heme group leads to a change in the protein far beyond what would reasonably be expected on the sole grounds of steric cover by the heme group. The titration studies were complimented by sedimentation and O.R.D. experiments which confirmed a major structural difference between the native and apoenzyme. These findings coupled with the observations of Blumberg et al., from their ESR

studies, that the native HRP does not possess axial symmetry, suggest that the protein-heme interaction for HRP may be sufficiently strong to distort the structure of the heme group.

Since myoglobin and HRP possess the same heme group and have similar spectral and magnetic properties, it has often been suggested that the difference in the chemical behavior for the two hemoproteins must lie in the nature of the protein-heme interactions for the two species and, in particular, the nature the amino acids bound in the fifth and possible the sixth co-ordination positions of the iron. As pointed out by Brill (1966), the ligands available on the protein for the binding of iron are limited to: carboxylate anions, imidazoles of histidine residues, amino groups, the phenolate anion of tyrosine and, perhaps, the sulfhydryl group of cysteine. Of these groups only the sulfhydryl group could seem to be excluded, since the work of Welinder et al. (1972), indicates that all the cysteine groups are present in HRP as disulfide bridges.

There have been a variety of attempts to define the ligands in the fifth and sixth co-ordination positions of the iron in HRP using different techniques. The first such attempt was that of Theorell (1943) who suggested, on the basis of titration data that the iron was bound to a carboxyl group in the protein component. The more recent titration study by Phelps et al. (1971) on the native and apoenzyme suggests that the fifth position is occupied by histidine,

with the implication of a tyrosine residue in the sixth position. Tohjo et al. (1961) using ferriprotoporphylin IX as a model compound observed peroxidatic activity for the heme complexes with histidine and arginine but found other ligands including acetic acid ineffective in activating the heme. Comparison of the visible spectra observed for HRP and compounds like myoglobin and hemoglobin, where the co-ordination of the iron is well established, has been used as a basis for speculation on the nature of the groups in the fifth and sixth co-ordination positions of HRP. This approach has been recently reviewed by Smith and Williams (1969), who conclude that the iron is bound on one side by imidazole (or possibly some other neutral nitrogen base) and by water on the other just as in myoglobin. The difference in the chemical functions of the two proteins is explained in terms of a carboxylate group in close vicinity to the heme in HRP, replacing the distal imidazole of myoglobin. Using difference spectroscopy below 250 nm, Brill and Sandberg conclude that histidine is the group bound in the fifth co-ordination position of the iron in HRP (Brill and Sandberg, 1968). Brill points out that both proximal and distal histidines, like that observed for myoglobin, could be ruled out for HRP because the ferrous form (HRP reduced with sodium dithionite or other strong reducing agents) does not have a hemochrome spectrum (Brill, 1966).

The studies of Wüthrich and co-workers on heme proteins have shown that it is possible to identify the groups co-ordinated to the iron in these proteins by high resolution NMR. The authors were able to verify the presence of a histidine group co-ordinated to the iron in myoglobin (Wüthrich et al., 1970) and a methionyl residue co-ordinated to the iron in cytochrome c (Wüthrich, 1970). With the hope of elucidating the nature of the group co-ordinated to iron in HRP, a similar but unsuccessful NMR study was undertaken in this laboratory (see Chapter 5).

HRP extracted from horseradish roots has been shown to contain a number of isozymes (Shannon et al., 1966; Paul and Stigbrand, 1970). The term isozyme was proposed by Markert and Maller (1959) to describe different molecular forms of proteins which possess the same enzymatic specificity. The present concept of the term is very broad and primarily emphasizes the existence of two or more forms of an enzyme within a single species. Isozymes may catalyze the same reactions but possess wide variations in their physical and catalytic properties (Chen, 1968). It has long been thought that the tertiary structure of proteins was unambiguously defined by the primary sequence of amino acids in the polypeptide chain. The work of Kaplan and co-workers on the multiple enzyme forms of chicken mitochondrial malate dehydrogenase suggested that this concept may not be universally applicable (Kitto et al., 1966). The authors were not able to distinguish the enzyme forms on the basis

of amino acid composition. Since it was possible to cause an interconversion of the different forms of the enzyme, it was suggested that the forms differed only in conformation.

The HRP used in the present studies was always obtained from the same supplier (Boehringer-Mannheim). Purification of the crude HRP obtained from this source (described in Appendix 1) indicated that the enzyme was mainly present as the B and C isozymes described by Shannon (1966) or isozyme III described by Paul and Stigbrand (1970). The fact that no kinetic effects could be attributed to different isozymes in the present study implies either that the isozymes present react at the same rate or that various batches of enzyme contained the same ratio of isozymes. In all, about 30 different batches of enzyme were used in the present studies.

The amino acid analysis of various HRP isozymes have been performed by several workers and these are summarized in Table 1.01. The only amino acids not detected in the analyses are asparagine, glutamine, hydroxylysine and hydroxyproline. A partial amino acid sequence has been completed and the results indicate that HRP has four disulfide bridges and eight sites of carbohydrate attachment (Welinder et al., 1972).

HRP along with most peroxidases is a glycoprotein. However, the purpose of the carbohydrate in these enzymes is uncertain. Lee and Hager (1970) have reported that the

Table 1.01

Amino Acid Composition of HRP Isozymes
(Residue/mole)

	Isozyme B Shannon <u>et al.</u>	Isozyme C Shannon <u>et al.</u>	Isozyme III _b Paul and Stigbrand	Mann HRP ^a Welinder <u>et al.</u>
Lysine	6	6	6	6
Histidine	3	3	3	3
Arginine	22	21	18	20
Aspartic Acid	54	50	47	47
Threonine	27	23	25	25
Serine	23	22	26	26
Glutamic Acid	20	19	21	20
Proline	17	17	17	17
Glycine	18	15	17	17
Alanine	25	23	22	23
Half-cystine	4	4	-	8
Valine	18	17	16	18
Methionine	3	3	4	4
Isoleucine	13	13	13	12
Leucine	39	36	34	35
Tyrosine	5	5	6	6

Table 1.01 (continued)

Phenylalanine	24	23	20	20
Tryptophan	0	0	0	1 ^b

^aHRP purchased from Mann Research Laboratories.

^bOnly observed in amino acid sequence.

activity of chloroperoxidase is unchanged even when 90% of the carbohydrate has been removed, thus implying that the carbohydrate moiety may not be associated with the catalytic properties of peroxidases. In his early preparative work on HRP, Theorell (1942) observed a second type of peroxidase which he referred to as paraperoxidase. This peroxidase had an identical composition to that of native HRP, except that it lacked the carbohydrate moiety (Theorell and Akeson, 1943). The fact that paraperoxidase was found to be much more fragile than normal HRP suggests that the function of the carbohydrate might be to lend structural integrity to the tertiary structure of the native enzyme. HRP has long been known to be a very stable enzyme, even under conditions of elevated temperatures, and this property could be due in part to the carbohydrate associated with the enzyme.

1.03 Catalysis by Horseradish Peroxidase

HRP is an efficient catalyst for the oxidation of aromatic amines, phenols and a variety of inorganic reducing agents. The reactions of HRP have been studied mainly in terms of reactants and not products. The production of reactive free radical intermediates in HRP oxidations has been demonstrated by ESR measurements (Yamazaki *et al.*, 1960). It is generally believed that the nature of the oxidation products is related to the limited reactivity and favored reaction sites of substrate free radicals, and not to

enzymatic function.

The mechanism of HRP catalysis has frequently been compared to the peroxidatic function of other heme proteins and model inorganic compounds. Catalase is a hemoprotein of molecular weight 250,000 that contains four ferri-protoporphyrin IX groups per molecule. Catalase catalyzes the rapid decomposition of hydrogen peroxide to oxygen and water. HRP possesses some catalytic activity, however it is about 10^{-4} times as efficient as catalase in the catalysis of the decomposition of hydrogen peroxide (Brill, 1966). Catalase can catalyze various oxidation reactions similar to those observed for HRP. In addition catalase can catalyze the oxidation of formic acid, methanol, ethanol and n-propanol, reactions which are not observed for HRP. With respect to typical peroxidase substrates like phenols, catalase is only 10^{-4} - 10^{-6} times as efficient in its catalysis as is HRP (Brill, 1966). Generally the distinction between catalase and peroxidases is kinetically well defined, however chloroperoxidase is an exception to this general rule since it possesses both peroxidatic and catalytic properties (Thomas *et al.*, 1970).

Although they possess the same heme group as HRP the respiratory proteins myoglobin and hemoglobin have only feeble peroxidatic activity. It was observed that this activity could be enhanced by denaturing the protein either by exposing the protein to extremes of pH or with the use of the organic denaturing agents formamide and guanidine

(Kurozumi et al., 1961). One reason for the poor peroxidatic ability of the respiratory proteins may be related to the observation in our laboratory that the reaction between hydrogen peroxide and myoglobin results in the irreversible degradation of the heme group (Critchlow and Dunford, 1972d). A similar degradation was observed in the reaction between hydrogen peroxide and ferriprotoporphyrin IX (Brown and Jones, 1968).

The oxidations of phenols and aromatic amines by hydrogen peroxide with ferrous sulfate as a catalyst have been known for many years. Analysis of the products from such reactions generally results in different products and different distributions of products than observed for the HRP catalyzed reactions (Daniels et al., 1951). This difference is particularly evident for the oxidation of mesidine where the iron catalyzed reaction is known to produce an ill defined dark mass (Paul, 1963), whereas the HRP catalyzed reaction produces a quantitative yield of a single product (Chapman and Saunders, 1941). The results of these studies would indicate that the catalysis by HRP and simple inorganic models proceed via different mechanisms, thus the information concerning the nature of HRP catalyzed reactions that can be obtained from model studies is limited.

Although the reactions of HRP are ideally suited for chemical studies *in vivo* where the reaction can be initiated by the addition of hydrogen peroxide, the generation of hydrogen peroxide *in situ* is a mystery. Enzyme systems

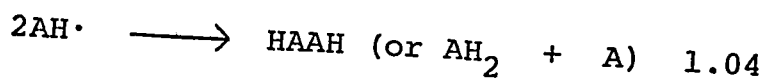
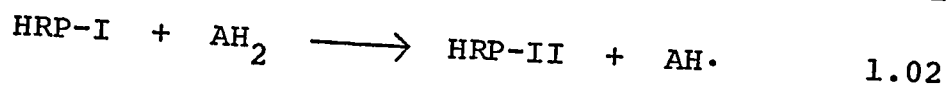
capable of generating hydrogen peroxide are known, such as glucose oxidase, and reactions of HRP have been studied using this source of hydrogen peroxide (Nunez and Pommier, 1968). To date however, there has been no evidence to indicate that any known hydrogen peroxide generating system is present in horseradish roots. Since hydrogen peroxide is toxic, its transfer from another part of the plant would appear unlikely. The uncertainty about the nature of the source of hydrogen peroxide in situ has led to the investigation of the possible oxidase function of HRP. The first observation of HRP oxidase activity was that of Swedin and Theorell (1940) who reported the oxidation of dihydroxyfumarate without the addition of hydrogen peroxide. More recently a number of studies have been reported of the HRP-catalyzed reaction between oxygen and the plant hormone indole acetic acid. The work of Fox et al. (1965) is particularly interesting since these authors have observed that indole acetic acid can form spectroscopically distinct compounds with HRP that closely resemble the compounds formed with hydrogen peroxide. George (1953a) had previously shown that a variety of inorganic oxidizing agent in addition to hydrogen peroxide could form these compounds. Fox et al. also observed that these compounds formed in the absence of hydrogen peroxide, could oxidize indole acetic acid. Thus it would appear that studies of the HRP compounds formed from hydrogen peroxide in vivo could make valuable contributions to the understanding of the HRP mechanism in situ, even

if hydrogen peroxide is not present under these conditions.

1.04 Nature of the Oxidized Compounds of Horseradish Peroxidase.

HRP was first observed to form spectroscopically distinct compounds with hydrogen peroxide by Keilin and Mann (1937). When hydrogen peroxide is added to a dilute solution of highly purified HRP, the brown color of the native enzyme rapidly changes to green. Upon standing for several minutes or on adding a small amount of reducing agent such as p-cresol the green color changes to red. With an enzyme preparation that is less pure, the reducing agent present in the preparation causes the green color to disappear immediately. If an excess of reducing agent is added to the green solution, the original brown color of the native enzyme is returned. The green compound was first observed by Theorell (1941), and is known as horseradish peroxidase compound I (HRP-I). The red compound observed following HRP-I decay is known as horseradish peroxidase compound II (HRP-II). Chance (1949) showed that HRP-I precedes HRP-II and that HRP-II is formed only from HRP-I. George (1953b) titrated HRP-II with ferrocyanide and showed that HRP-II was converted to HRP by a one-electron reduction. Similarly Chance (1952b) showed that the conversion from HRP-I to HRP-II also involved a one electron reduction. Thus HRP-I retains the two oxidizing equivalents of hydrogen peroxide and HRP-II only one. Two other enzymatic compounds referred to as horseradish peroxidase compounds III and IV are formed under

conditions of very high hydrogen peroxide concentration, however these compounds are not thought to be important intermediates in peroxidase catalyzed oxidations. The general mechanism for HRP catalyzed oxidation, as established by Chance and George, is usually written:



where AH_2 represents the reducing substrate. The nature of the free radical intermediate symbolized by $\text{AH}\cdot$ in equations 1.02-1.04 was demonstrated by Yamazaki *et al.* (1960), who observed typical free radical ESR spectra for the products of hydroquinone and ascorbic acid oxidations. Their studies also showed that the radicals usually reacted with each other and not with the enzyme again. Accurate spectra of HRP-I and HRP-II in the Soret region have recently been determined in our laboratory and are illustrated in Fig. 1.02 (Roman and Dunford, 1972; Critchlow and Dunford 1972b). The spectrum of HRP-II in Fig. 1.02 is very similar to one previously published by Chance (1967).

There has been considerable controversy concerning the structure of HRP-I and HRP-II and many questions about the nature of the two compounds are still unresolved. Chance (1949) originally believed that HRP-I and HRP-II were enzyme-substrate complexes of the type postulated by

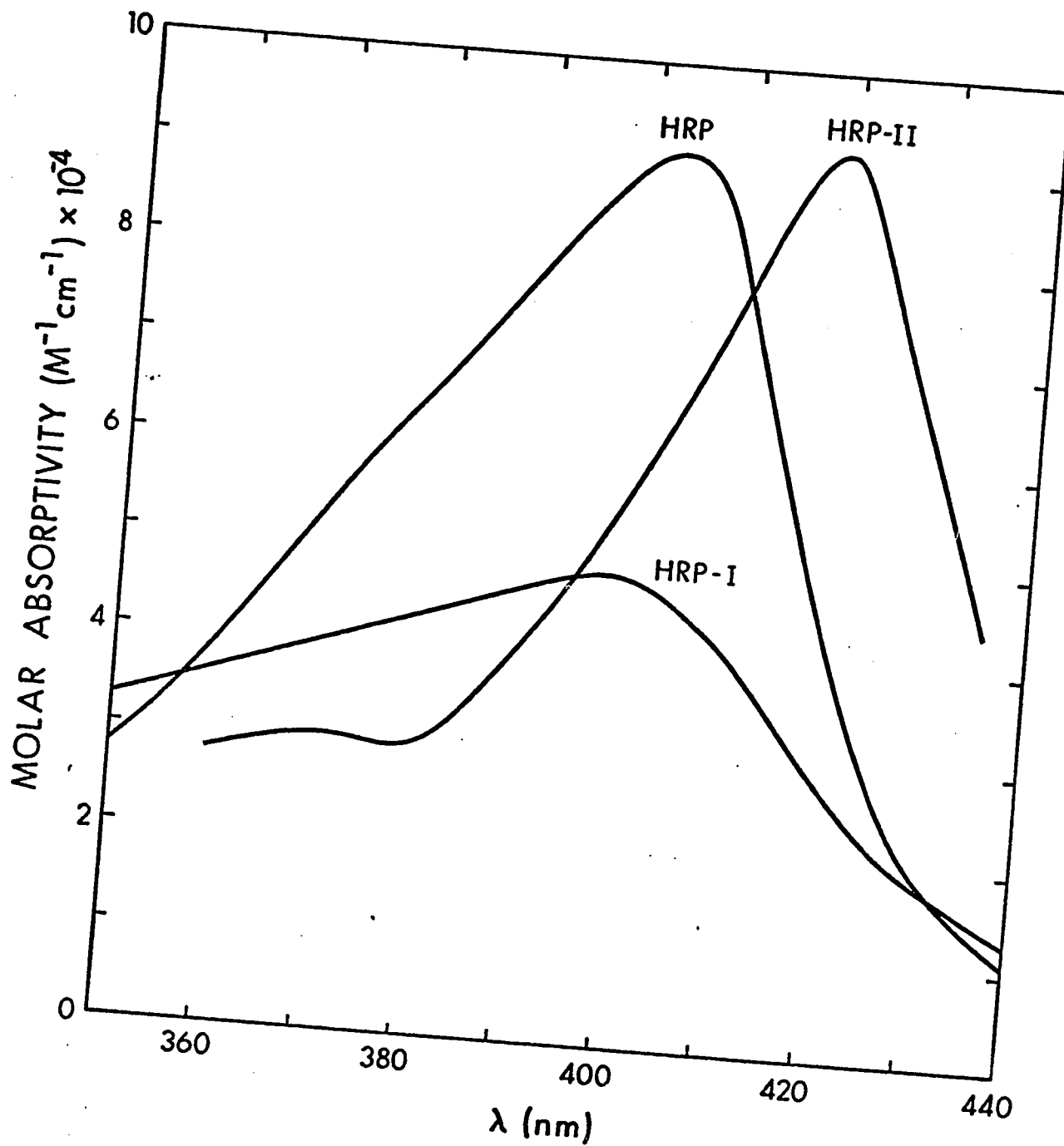


Fig. 1.02: Spectra of the oxidized compounds of HRP, HRP-I and HRP-II, compared to the spectrum of HRP.

Michaelis and Menten. This concept was disproved by George (1953a) who showed that hydrogen peroxide was not a unique oxidizing agent for HRP and that spectrally similar compounds could be produced with a variety of oxidizing agents. This finding has recently been put on a more quantitative basis by the observation in our laboratory that the reaction of HRP-I and HRP-II formed with hydrogen peroxide, ethyl hydrogen peroxide and p-chloroperbenzoic acid have identical reaction rates with the substrate ferrocyanide over a wide pH range (Cotton and Dunford, 1972).

The determination of the structures of HRP-I and HRP-II by most physical measurements is complicated by the lability of these compounds. The half lives of HRP-I and HRP-II depend to a large extent on the purity of the enzyme preparation. Even with the purest samples reported, the spontaneous decay of these compounds is sufficient to make many physical measurements something less than quantitative.

The electronic configurations of the heme iron in HRP-I and HRP-II have been deduced from magnetic susceptibility and ESR measurements. The results of these studies are compared to the corresponding measurements for native HRP, the HRP-cyanide complex and the HRP-fluoride complex in Table 1.02. The magnetic moment of HRP-I is very close to the value expected for three unpaired electrons. This has led Brill and Sandberg (1968) to predict that the structure of HRP-I must be one of five possibilities: (1) a mixture of low and high-spin ferric states which could exhibit any

Table 1.02
Magnetic and ESR Properties of HRP and
Its Complexes and Compounds

	Magnetic Moment (Bohr Magnetons)	ESR Signature	Number of Unpaired Electrons
HRP	5.5 ^a	High Spin ^c	5
HRP-hydroxide	2.7 ^a	Low Spin ^c	1
HRP-cyanide	2.7 ^a	Low Spin ^c	1
HRP-fluoride	5.9 ^a	Not measured	5
HRP-I	4.0 ^b	None ^c	3(?)
HRP-II	3.5 ^b	None ^c	2(?)

^aKeilin and Hartree, 1951.

^bTheorell and Ehrenberg, 1952.

^cPeisach et al., 1968.

intermediate magnetic susceptibility; (2) a low-spin ferric compound plus a biradical in the porphyrin or protein which would contribute susceptibilities which could sum to the appropriate value; (3) a low spin quadrivalent iron compound plus a free radical which would exhibit the same spin as (2); (4) pentavalent iron which would most likely have a spin of $3/2$; (5) a ferric compound with lower and upper orbital singlets and an orbital triplet of intermediate energy which would also have a spin of $3/2$. Knowledge of the magnetic susceptibility of HRP-I coupled with its similarity to the visible spectrum of various model systems led Brill and Williams (1961) to favor a mixture of compounds with average spin $3/2$. The structure of HRP-I proposed by the authors was an equilibrium mixture of compounds, one of which had a hydroperoxide molecule as the sixth ligand co-ordinated to the iron and the other having a meso carbon atom of the porphyrin substituted with a hydroxyl group. Using the same criteria of visible spectra and magnetic susceptibility data, Brill (1966) concludes that HRP-II is a low spin iron IV compound. A quadrivalent iron compound with oxygen bound in the sixth position is referred to as a ferryl ion and was first suggested as a structure for HRP-II by George (1953b). Brill concludes that the only simple alternative to a ferryl structure for HRP-II would involve a low spin ferric compound with a stable free radical in the porphyrin. He points out that such a structure would be expected to have a reduction in the

intensity of its Soret band and such a phenomenon is not observed.

Based on their studies of ESR and visible spectra at low temperature, Peisach et al. (1968) have suggested a ferric complex for HRP-I in which the two oxidizing equivalents are temporarily stored at a methine bridge carbon or at a pyrrole α -carbon atom of the porphyrin. The authors suggest a ferrous low spin compound for HRP-II with an oxygen molecule, or an oxygen containing ligand, in the sixth co-ordination position possessing the two oxidizing equivalents necessary to give HRP-II its known oxidation level.

Both Brill (1966) and Peisach et al. (1968) consider HRP-I to be too stable for any radical type structure. However the recent work of Dolphin et al. (1971) has shown that metalloporphyrin π -cation radicals are stable and have similar visible spectra to that observed for HRP-I. The authors conclude that the two oxidizing equivalents of HRP-I can be accounted for by the loss of one electron from the iron and one from the porphyrin π orbitals. The conversion of HRP-I to HRP-II is thought to involve the transfer of an electron to the π -cation radical to produce a quadrivalent iron porphyrin. The quadrivalent structures proposed for HRP-I and HRP-II by Dolphin et al. are in agreement with the studies of Moss et al. (1969) who have shown by Mössbauer spectroscopy that the electronic configuration of the iron is the same in both HRP-I and HRP-II.

Recent work in our laboratory has shown that cyanide does not bind appreciably to HRP-I or HRP-II (Cotton et al., 1972). If the structure of either HRP-I or HRP-II was such that the sixth co-ordination position of the iron was accessible to the aqueous medium, cyanide binding would be expected to occur. If the iron was present in an oxidation state greater than three, this binding would be expected to be very strong due to the added positive charge on the iron. The lack of cyanide binding to HRP-I and HRP-II indicates that whatever the structure of these two compounds may be, a tightly bound ligand must be present in the iron co-ordination position.

1.05 Kinetic Measurements of the Reactions of HRP-I and HRP-II.

Most physical studies on an enzyme aim to define various aspects of its structure, knowledge of which helps to limit the possible range of descriptions of the catalytic process. However in order to gain a complete understanding of the mechanisms for the enzyme action kinetic studies are required, since these are the only type of experiments directly related to the catalytic process itself. The present work is part of an overall research program designed to elucidate the mechanism of HRP catalysis. It primarily involves a kinetic study of the reactions of HRP-I and HRP-II with three inorganic reducing agents over as wide a

range of pH as is experimentally feasible.

The kinetic technique employed in the present study involves direct kinetic measurements of HRP-I and HRP-II reactions in isolation from the HRP reaction cycle described by equations 1.01-1.04. The majority of kinetic studies that have been performed on HRP catalysis have utilized the steady-state technique, where either the consumption of substrate or the formation of product is measured as a function of time. The steady-state technique has several advantages over the method used in the present study. The quantity of enzyme required for steady-state studies is usually much smaller than that required for direct studies. For the readily available HRP this is not a serious problem, however for thyroid peroxidase sufficient enzyme has not been isolated to perform non-steady-state kinetic measurements. The equipment necessary to monitor steady-state reactions is usually less complicated than that required for making direct measurements. The reason is that under the conditions of low enzyme concentrations used in the steady-state work, the overall reaction is slow enough that it can be monitored by conventional spectrophotometric instruments. In the present studies, where reactions with half lives as short as 10 milliseconds were observed, a device for the rapid mixing of solutions, the stopped-flow apparatus, was necessary to measure the reaction rates.

The disadvantages of the steady-state technique arise primarily in the interpretation of the kinetic data. In

general, on a well defined system, the results of steady-state kinetics and those obtained by direct kinetic measurement should give the same results. Such behavior has been observed for the HRP-catalyzed oxidation of ferrocyanide, where the two techniques yielded values of the second-order rate constant for the reaction of HRP-II and ferrocyanide that agreed within 20% (Hasinoff and Dunford, 1970). Steady-state studies on the HRP-ferrocyanide system were also performed with regard to a kinetic study in D_2O (Critchlow and Dunford, 1972b) and a study with a variety of oxidizing agents (Cotton and Dunford, 1972) and all three independently performed studies indicated that the results obtained by direct kinetic measurement were 20% higher than the steady-state results. Although the reason for the deviation between the two methods is still uncertain, the most likely explanation is that the enzyme concentration (determined by spectroscopic measurement) was incorrect due to an incorrect value for the molar absorptivity of the enzyme. Under the conditions employed for the direct kinetic measurements the measured rate constants are independent of the enzyme concentration. A further disadvantage of the steady-state technique in the HRP-ferrocyanide system is that no information can be gained on the reaction of HRP-I with ferrocyanide since it is much more rapid than the corresponding HRP-II reaction. This can be illustrated with respect to the HRP mechanism in equations 1.01-1.03 from which the steady-state equation can be calculated to be

$$\frac{[\text{HRP}]_0}{v} = \frac{1}{k^1[\text{H}_2\text{O}_2]} + \frac{1}{k^2[\text{AH}_2]} + \frac{1}{k^3[\text{AH}_2]} \quad 1.05$$

where v is the initial velocity; $[\text{HRP}]_0$ is the initial concentration of HRP; and k^1 , k^2 and k^3 are the second-order rate constants for the reactions in equations 1.01, 1.02 and 1.03. Since the rate constant for the HRP-I reaction with a given substrate, k^2 , is generally much greater than the rate constant for the reaction of HRP-II, k^3 , the term $\frac{1}{k^2[\text{AH}_2]}$ can never make an appreciable contribution to the rate and the steady-state technique can not be used to investigate this rate constant.

For the reactions catalyzed by HRP, the interpretation of steady-state kinetics is inherently more complicated than those observed by direct kinetic measurements. The rate of product formed as measured by steady-state kinetics may depend on any of the three rate constants or combinations of the three for the reactions illustrated in equations 1.01-1.03. In order that the results of steady-state kinetics have quantitative meaning, great care must be taken to assure that all possible errors have been eliminated. Unfortunately there are many examples in the literature where this care has not been exercised. An example of one such study was performed by Björkstén (1968) who reported, based on his steady-state kinetics, that the HRP-catalyzed oxidation of iodide was inhibited by iodide and acid. He further stated that his results indicated the formation of

a dead-end complex involving a proton and iodide atom bound to native HRP. We believe that a more reasonable explanation for Björkstén's observation can be obtained using the pH dependences of the rate constants for the reactions of HRP-I and HRP-II with iodide and the formation of HRP-I. The formation of HRP-I is a rapid reaction with a rate constant that is pH independent over the range 4-9 and decreases at higher and lower pH (Dolman and Dunford, 1972). The rate constants for the reactions of HRP-I and HRP-II with iodide increase with increasing acidity as illustrated in Figs. 2.02 and 2.05. Thus it is not surprising that the production of iodine becomes independent of iodide concentration at low pH since the rate of HRP-I formation is becoming the rate determining step.

The direct kinetic measurements in the present studies were all performed under experimental conditions where the change in the concentrations of HRP-I or HRP-II with time indicated that the reaction was first order in the enzyme species. This means that the concentration of the HRP compound is changing exponentially with time as described by the equation

$$-\frac{d[x]}{dt} = k_{\text{obs}}[x] \quad 1.06$$

where $[x]$ refers to the concentration of HRP-I or HRP-II (or some property that has a linear relation to concentration), k_{obs} is the first-order rate constant in units of sec^{-1} and t is time. The integrated relationship from

which the values of k_{obs} can be calculated takes the form

$$\ln \frac{([x]_0 - [x]_\infty)}{([x] - [x]_\infty)} = k_{\text{obs}} t \quad 1.07$$

where $[x]_0$, $[x]_\infty$ and $[x]$ refer to the concentrations of the compounds at time 0, ∞ and t respectively. The half time for the reaction, $t_{\frac{1}{2}}$, is given by

$$\ln \frac{([x]_0 - [x]_\infty)}{\frac{1}{2}([x]_0 - [x]_\infty)} = k_{\text{obs}} t_{\frac{1}{2}} = \ln 2 \quad 1.08$$

As shown by equation 1.08, k_{obs} is independent of the concentration of the enzyme compounds, thus the first-order rate constants may be obtained from the observed appearance or disappearance of HRP-I or HRP-II without knowledge of their absolute concentrations. This fact is of great practical importance with regard to the attainment of experimental results. For example, the labile nature of HRP-I and HRP-II make it difficult to estimate their concentrations even a few minutes after they have been prepared. However as long as first-order kinetics are observed a knowledge of these concentrations is not required and measurement of these rate constants becomes a routine task. In addition it is frequently observed that for very fast reactions, a significant extent of reaction occurs in the time required to mix the reactants, but as long as the observed kinetics are first order a plot of $\ln([x] - [x]_\infty)$ vs. time will yield a straight line with slope $-k_{\text{obs}}$.

For the reactions of HRP-I and HRP-II with iodide,

sulfite and nitrite the overall rate expression takes the form.

$$-\frac{d[x]}{dt} = k[x][s] \quad 1.09$$

where k is a second-order rate constant with units $M^{-1}sec^{-1}$ and $[s]$ is the substrate concentration. If $[s] \gg [x]$, then $[s]$ will remain relatively constant during the course of the reaction. Under such conditions the reaction is called pseudo first order and the rate constants k_{obs} and k are related by the expression

$$k_{obs} = k[s] \quad 1.10$$

In the present studies $[s]$ was always at least ten times larger than $[x]$, thus pseudo-first-order conditions were always maintained.

In the present study the values of k_{obs} were obtained from nonlinear least-squares analyses of the observed exponential traces. Graphical analysis of the form $\ln([x]-[x]_{\infty})$ vs. time were performed occasionally to give a visual interpretation of the errors in the experimental values and to assure that both graphical and computer analysis gave the same values for k_{obs} . The analysis of first-order kinetics using the computer had several advantages over the more commonly used graphical methods. First the computer is well suited to do repetitious calculations. For example, the study of the reaction between HRP-II and sulfite involved the analysis of almost 1000 experimental traces, a task that would have been most

tedious if graphical methods were used. Second the computer program has the facility to vary selected parameters, where desired, in order to optimize the fit to experimental results. Third, using the computer analyses, the individual experimental points could be weighted. In the analyses of first-order kinetics the points at the beginning of the reaction were weighted more heavily than the points near the end of the reaction since the term $([x]-[x]_{\infty})$ has a smaller relative error when $[x]$ is much different than $[x]_{\infty}$ (at the beginning of the reaction) than when $[x]$ and $[x]_{\infty}$ are very similar.

The equation used to analyze the first-order reactions was

$$V_t = (V_0 - V_{\infty})e^{-k_{\text{obs}}t} + V_{\infty} \quad 1.10$$

where V_t , V_{∞} and V_0 refer to the voltage or absorbance at times t , ∞ and an arbitrary time zero. In the equation V_0 , V_{∞} and k_{obs} were variable parameters that were adjusted to give the best fit to the experimental values V_t and t . Frost and Pearson (1961) lucidly illustrate that equations 1.06 to 1.08 are valid either for the concentration of x or some physical property that has a linear relation with the concentration of x , for example absorbance. In the stopped-flow apparatus, the reactions were observed as changes in voltage vs. time. The voltage is proportional to the intensity of the light reaching the photomultiplier and the relation is given by

$$\frac{V}{V_0} = \frac{I}{I_0} \quad 1.12$$

where I refers to light intensity through the sample and I_0 the light intensity in vacuum. The relation between intensity and absorbance is given by

$$\log\left(\frac{I_0}{I}\right) = \text{absorbance} \quad 1.13$$

The voltage and absorbance can be related by a series expansion of the type

$$\ln(1 + x) = x - \frac{x^2}{2} + \frac{x^3}{3} - \dots \quad 1.14$$

from which it can be shown that with a sufficiently small change in absorbance, voltage and absorbance are proportional. In the present work the concentration of HRP-I or HRP-II was such that the observed change in absorbance was less than 0.04 so there was at most a 5% error in the assumed proportionality between voltage and absorbance.

Oxidation of Iodide by Horseradish Peroxidase Compounds I and II

2.01 Introduction

The kinetic studies on the oxidation of iodide by HRP-I and HRP-II are part of a research program designed to elucidate the mechanism of HRP catalysis. In general the reactions of HRP-I and HRP-II, isolated from the overall reaction sequence described by equations 1.01-1.03, are studied over a range of pH. It is hoped that it will be possible to deduce a mechanism for HRP catalysis that is consistent with the kinetic pH dependences for these reactions as well as the known chemical properties of the different substrates studied. In this regard iodide is the second substrate for which the kinetic pH dependence of the HRP-I and HRP-II reactions have been studied, the first being ferrocyanide (Hasinoff and Dunford, 1970; Cotton and Dunford, 1972).

Iodide was chosen as a substrate for HRP-I and HRP-II for two reasons. First, iodide is a strong acid, thus there is no ambiguity with respect to the protonation of the reacting species as there is with ferrocyanide. Second, the HRP-catalyzed oxidation of iodide is a model for the reaction catalyzed by thyroid peroxidase. To date thyroid peroxidase has not been isolated in sufficient quantity to perform direct kinetic measurements of the type possible for HRP. The most recently reported preparation of thyroid peroxidase resulted in a yield of only 29 mg of enzyme, that the authors

estimated was at least 25% pure, from 23 kg of thyroid glands (Taurog et al., 1970). It is impossible to estimate how good a model HRP is for the oxidation of iodide in the thyroid gland, however the similarity observed for the oxidation of iodide by both HRP and lactoperoxidase compound II (Maguire and Dunford, 1972a) suggests that the analogy may be reasonably valid.

2.02 Experimental

Materials

Horseradish peroxidase was obtained from Boehringer-Mannheim either as a purified, lyophilized powder or as a highly purified ammonium sulfate suspension. The suspension was dialyzed against doubly distilled water and passed through a Millipore filter prior to use. The P.N. (the ratio of absorbance at 403 nm and 280 nm) of the resulting solution was always 3.0 or greater. The lyophilized powder, which had a P.N. of approximately 0.6, was purified by the method described in Appendix 1. The reaction between HRP-II and iodide was studied with both preparations of HRP and identical kinetic results were observed. Both enzyme preparations were sufficiently free from reducing impurities to give HRP-II a half life greater than 20 minutes. The fact that the observed reactions with both enzyme preparations were first order in HRP-II indicates that if more than one isozyme was present in detectable concentrations, these isozymes must react with similar rates.

The concentration of HRP was determined spectrophoto-

metrically at 403 nm using a molar absorptivity of $9.1 \times 10^4 \text{ M}^{-1}\text{cm}^{-1}$ (Keilin and Hartree, 1951). The value for the molar absorptivity of HRP has been the subject of considerable discrepancy in the recent literature and the determination of its precise value has been complicated by the existence of various isozymes of HRP. From the chromatography studies performed on the lyophilized HRP (Appendix 1), we believe that HRP used in the present studies is composed primarily of the B and C isozymes reported by Shannon *et al.* (1966), or isozyme III reported by Paul and Stigbrand (1970). We have chosen to use the quoted value for the molar absorptivity rather than that of Shannon *et al.* ($9.5 \times 10^4 \text{ M}^{-1}\text{cm}^{-1}$) or Paul and Stigbrand ($1.0 \times 10^5 \text{ M}^{-1}\text{cm}^{-1}$) to facilitate comparison with previously published work.

Potassium iodide was obtained from the McArthur Chemical Co. (stated purity 99.5%) and from Orion Research as a standard solution. The concentrations of these solutions were checked by titration with silver nitrate (Kolthoff and Sandell, 1963) or with an Orion specific ion electrode, and showed no detectable change during the storage period. Hydrogen peroxide, 30% by weight obtained from the Fisher Scientific Co., was stored in the dark as an approximately $5 \times 10^{-2} \text{ M}$ solution, and diluted before use; its concentration was determined spectrophotometrically by the molybdate-catalyzed oxidation of iodide (Ovenston and Rees, 1950; Ramette and Sandford, 1965). All solutions were prepared

from water that had been distilled from alkaline permanganate and twice redistilled. Reagent grade chemicals for the preparation of buffers and control of ionic strength were used without further purification.

Kinetic Experiments

Kinetic investigations were carried out using a stopped-flow apparatus and a Cary 14 recording spectrophotometer. The stopped-flow apparatus was a modification of the apparatus described previously (Hasinoff, 1970). Using this apparatus two solutions could be mixed and the reaction observed approximately 5 milliseconds after the beginning of the mixing process. The time interval of 5 milliseconds is defined as the dead time of the apparatus. One solution contained HRP-I or HRP-II in aqueous solution and the other contained a mixture of potassium nitrate, buffer and potassium iodide. In a typical experiment sufficient hydrogen peroxide was added from a Hamilton microliter syringe to convert 80 percent of a 2×10^{-6} M solution of HRP to HRP-I immediately before its addition to the stopped-flow apparatus. In the absence of added reducing agents and with reasonably pure preparations of HRP, the HRP-I is quite stable. The preparations of HRP used in the present study resulted in solutions of HRP-I that had half lives of 15 minutes or greater. The apparatus always contained some HRP-II from the spontaneous decay of HRP-I. To avoid the possible interference caused

by reaction of the HRP-II, the kinetics of the HRP-I reaction were monitored at 411 nm, the isosbestic point between HRP-II and HRP.

HRP-II was prepared from HRP-I by the addition of p-cresol to a concentration of 0.5 times that of the total concentration of HRP before transfer of the solution to the stopped-flow apparatus. HRP-I reacts with p-cresol more rapidly than it does with HRP-II (Critchlow and Dunford, 1972a) and with a stoichiometry that is believed to involve two moles of HRP-I for each mole of p-cresol. The slight excess concentration of added p-cresol over that of HRP-I, resulting from the addition of 0.5 moles of p-cresol to 0.8 moles of hydrogen peroxide, ensures that the resulting solution consists primarily of HRP-II and HRP. The HRP-II solutions were somewhat more stable than those of HRP-I with half lives ranging from 20 to 30 minutes. The reactions of HRP-II were monitored at 425 nm, close to the maximum difference in absorbance between HRP-II and HRP and in a region where the absorbances of HRP and HRP-I are similar. Thus every possible precaution was taken to ensure that the effect of HRP-I on the rate of the HRP-II reaction was minimized.

Care was taken in the formation of HRP-I and HRP-II not to add an excess of hydrogen peroxide over the total HRP concentration, since this could create a period at the beginning of the reaction where the HRP compounds could both react and form simultaneously, in other words, the

HRP reaction cycle would occur. This would lead to erroneous values for the observed rate constant. For this reason a small amount of HRP solution, sufficient to give a final concentration of about 10^{-8} M, was added to the solution containing potassium nitrate, buffer and potassium iodide. Any oxidizing impurity present in this solution that could form HRP-I would be consumed by the reaction between HRP-I, formed from the impurity, and iodide. Recent work in our laboratory has indicated that a variety of oxidizing agents, can oxidize HRP to HRP-I at a comparable rate to the hydrogen peroxide reaction (Cotton and Dunford, 1972).

The final mixture entering the observation chamber of the stopped-flow apparatus had a concentration of HRP-I or HRP-II (depending upon which reaction was being studied) of approximately 1×10^{-6} M and an ionic strength of 0.11 of which 0.01 was contributed by the buffer. Normally the potassium nitrate was 0.1 M, contributing the remaining portion of the ionic strength. However at high pH, where the observed reactions were very slow, concentrations of iodide high enough to affect the ionic strength were used and under these conditions the concentration of potassium nitrate was reduced to maintain a constant ionic strength. All reactions were carried out at a constant temperature of 25°.

The reactions of HRP-I and HRP-II were monitored by following the trace of photomultiplier voltage vs. time

on a 564 B Tektronix storage oscilloscope. Selected traces were photographed and voltage vs. time readings were taken from an enlargement of the negative. An average rate constant was obtained from 3-6 traces for each set of conditions. The observed reactions had half times from about 10 milliseconds to several seconds. After reaction the solutions were collected for pH measurement, which was carried out with an Orion digital pH meter in conjunction with a Fisher combination electrode.

For HRP-I reactions at pH values above 7 and for HRP-II reactions at pH values above 6.5, the reactions were performed on the Cary 14 spectrophotometer. The slowest reaction that can be conveniently measured on the stopped-flow apparatus has a first-order rate constant of approximately 0.1 sec^{-1} and the fastest reaction that can be measured on the Cary 14 has a first-order rate constant of approximately 0.2 sec^{-1} . Thus a small overlap was possible for the two instruments. In the alkaline region the reactions of both HRP-I and HRP-II with iodide became sufficiently slow that the spontaneous decay of these compounds began to contribute appreciably to the observed reaction, resulting in the alkaline limit of pH at which the reactions were studied.

On the Cary 14 the reactions of HRP-I were performed in two different fashions. In the first method, the rapid reaction between HRP and hydrogen peroxide was used to form

HRP-I in a cuvette containing potassium iodide, potassium nitrate and buffer. The formation of HRP-I took place within the mixing time on the Cary 14, thus only the reaction between HRP-I and iodide was observed. The HRP-I reactions were also performed by adding potassium iodide to a solution of HRP-I that had been formed in the presence of potassium nitrate and buffer. Both techniques resulted in the same rate constants for the HRP-I-iodide reaction, however, the former method was found to be more convenient.

The reactions of HRP-II were studied by first forming HRP-II in a cuvette by the addition of hydrogen peroxide and p-cresol, in the same relative concentrations as used for the stopped-flow experiments, to a solution of approximately 2×10^{-6} M HRP which also contained potassium nitrate and buffer. The potassium iodide was added following the formation of HRP-II. The addition of hydrogen peroxide, p-cresol and potassium iodide to the cuvette was routinely performed with a Hamilton microliter syringe. The total volume of the solutions, added by syringe, was usually less than 60 μ l and the resulting error in dilution (maximum of 3%) was neglected. When concentrations of iodide greater than 10^{-2} M were used, the potassium iodide was pipetted into the cuvette and compensation was made for the resulting change in volume. The voltage vs. time traces obtained from the stopped-flow apparatus and the absorbance vs. time traces obtained from the Cary 14 were analyzed using a least-squares computer program to equation 1.10.

The HRP-catalyzed oxidation of iodide by hydrogen peroxide was also studied using steady-state kinetics. The reactions were monitored by observing product formation at 353 nm, the maximum absorbance of triiodide ion. The reactions were studied at three values of pH from 4 to 7 and all experiments were performed on the Cary 14 spectrophotometer with the cell thermostatted at 25°. In a typical experiment, the reaction was initiated by the addition of hydrogen peroxide to 2.0 ml of solution in a cuvette containing buffer, potassium nitrate, potassium iodide and 9.2×10^{-9} M HRP. At pH values 4.01 and 5.41, the concentration of hydrogen peroxide was 6.5×10^{-5} M and the concentration of iodide was varied from 5×10^{-3} M to 5×10^{-4} M. At pH 6.99 the concentration of hydrogen peroxide was 3.2×10^{-5} M, the concentration of potassium iodide was 1×10^{-2} M and the concentration of HRP was varied from 9.2×10^{-9} M to 7.4×10^{-8} M. An experiment was also performed at pH 4.0 with an iodide concentration of 0.05 M, a hydrogen peroxide concentration of 6.5×10^{-6} M and an HRP concentration of 9.2×10^{-9} M.

The experiments were performed by starting the chart on the Cary 14 at the time of the hydrogen peroxide addition, thus marking the zero time of the reaction. The pen switch was closed at the same time that the cover was replaced on the cuvette compartment. The results were analyzed by extrapolating the initial observed rate (the average mixing time was 4-6 seconds) to zero time and measuring the initial rate of the reaction. For the experiment at pH 4.0 with

high iodide and low hydrogen peroxide concentrations, the whole curve was analyzed using an analysis for first-order reactions.

Steady-State Spectra

In order to determine the enzymatic species present in the steady-state for the HRP-catalyzed oxidation of iodide, experiments were performed using a sufficiently high concentration of HRP to ensure that an appreciable enzyme absorbance was observed. The reaction was initiated by the addition of 10 μ l of 6.0×10^{-3} M hydrogen peroxide to 2.0 ml of a solution containing 5.0×10^{-6} M HRP and 4.0×10^{-6} M potassium iodide in a pH 7.6 phosphate buffer of ionic strength 0.01. The spectrum of the resulting steady-state mixture was scanned on the Cary 14 from 350-450 nm at a rate of 2.5 nm/sec. An identical experiment was performed with the absorbance monitored at 411 nm to ensure that steady-state conditions did exist during the time taken to scan the spectrum and to determine the number of enzymatic cycles taking place during this time (six). A more accurate determination of the spectrum of the enzyme species present in the steady state was achieved by monitoring the absorbance changes at single wavelengths from 350 nm-450 nm and extrapolating the changes to zero time.

The nature of the enzymatic species present in the steady state under conditions where the enzyme is cycling about 100 times were determined by single wavelength measurements in a pH 8.4 borate buffer of ionic strength 0.01. The

reactions were monitored at 411 nm and 430 nm with an HRP concentration of 4.3×10^{-6} M. It was possible to observe the steady-state spectra of the enzyme intermediates without interference from iodine production in alkaline pH due to the rapid hydrolysis of iodine that takes place in such solutions. The absence of any appreciable absorbance by the product was verified by the experiments at 411 nm where the original absorbance of HRP was re-obtained when all the added hydrogen peroxide had been reacted.

Stoichiometric Experiments

The overall reaction stoichiometry for the HRP-catalyzed oxidation of iodide by hydrogen peroxide was determined at pH 7.24 by monitoring iodine production spectrophotometrically at 353 nm. The reaction was initiated by the addition of hydrogen peroxide from a microliter syringe to a cuvette containing a solution of 9.0×10^{-2} M potassium nitrate, 1.0×10^{-2} M potassium iodide, 4.4×10^{-6} M HRP and phosphate buffer of ionic strength 0.01. The concentrations of hydrogen peroxide used in the determination varied from 1.8×10^{-6} M to 1.2×10^{-5} M.

The stoichiometry of the reaction between HRP-I and iodide was determined by a titration of HRP-I monitored at 411 nm. Solutions of HRP-I were prepared by the addition of an equivalent concentration of hydrogen peroxide to a solution of 3.9×10^{-6} M HRP (the concentration of added hydrogen peroxide was determined from the known changes in absorbance

for HRP-I formation at 411 nm) in 0.1 M potassium nitrate and pH 5.95 phosphate buffer of ionic strength 0.01. The spontaneous decay of HRP-I was monitored until the rate of this reaction was much slower than the reaction with iodide, then solutions of potassium iodide were added from a micro-liter syringe and the changes in absorbance were measured. The concentration of HRP-I remaining when the iodide was added, was only 30% of the amount originally formed. The titration of HRP-II with iodide was performed in an analogous manner to the titration of HRP-I. The HRP-II was prepared by adding p-cresol, to a final concentration of 1.4×10^{-6} M, to a solution of 2.4×10^{-6} M HRP-I in a pH 4.03 citrate buffer of ionic strength 0.01. Again the spontaneous decay of the compound was monitored until its rate decreased appreciably, then solutions of potassium iodide were added and the changes in absorbance at 425 nm was measured.

2.03 Results

Kinetics of the HRP-I-Iodide Reaction

The kinetic behavior of the HRP-I-iodide system is consistent with a reaction that is first order in both HRP-I and iodide. All experiments were carried out with iodide concentrations at least ten times greater than the concentration of HRP-I; under these pseudo-first-order conditions the observed differential rate expression is

$$-\frac{d[\text{HRP-I}]}{dt} = k_{1,\text{obs}}[\text{HRP-I}] \quad 2.01$$

Equation 2.01 was verified by the linear nature of the semilogarithmic plots of the change in absorbance or voltage vs. time.

Values of the second-order rate constant, k_1 , were obtained from the equation

$$k_{1,obs} = k_1[I^-] \quad 2.02$$

Equation 2.02 was verified by measuring $k_{1,obs}$ over a range of iodide concentrations at a given pH. Plots of $k_{1,obs}$ vs. $[I^-]$ were linear as illustrated in Figure 2.01 for the reaction at pH 4.99. Similar studies were carried out at pH values of 2.70, 3.30, 3.99, 4.39, 7.37, 8.33, 9.18 and 9.87. At pH values below 3.5 and above 7.0 positive intercepts in the plots of $k_{1,obs}$ vs. $[I^-]$ were observed. These positive intercepts can be explained by the reaction of HRP-I with small concentrations of reactive impurities in the buffer, potassium nitrate or HRP solutions. Thus the general relation between $k_{1,obs}$ and $[I^-]$ is

$$k_{1,obs} = k_1[I^-] + k_{spont} \quad 2.03$$

where k_{spont} represents the rate of HRP-I decay that is independent of iodide concentration. It is clear from equation 2.03 that even under conditions where k_{spont} is significant, that it has no effect on the value of k_1 obtained from linear plots of $k_{1,obs}$ vs. $[I^-]$. The magnitudes of the k_{spont} terms expressed as percentages of the

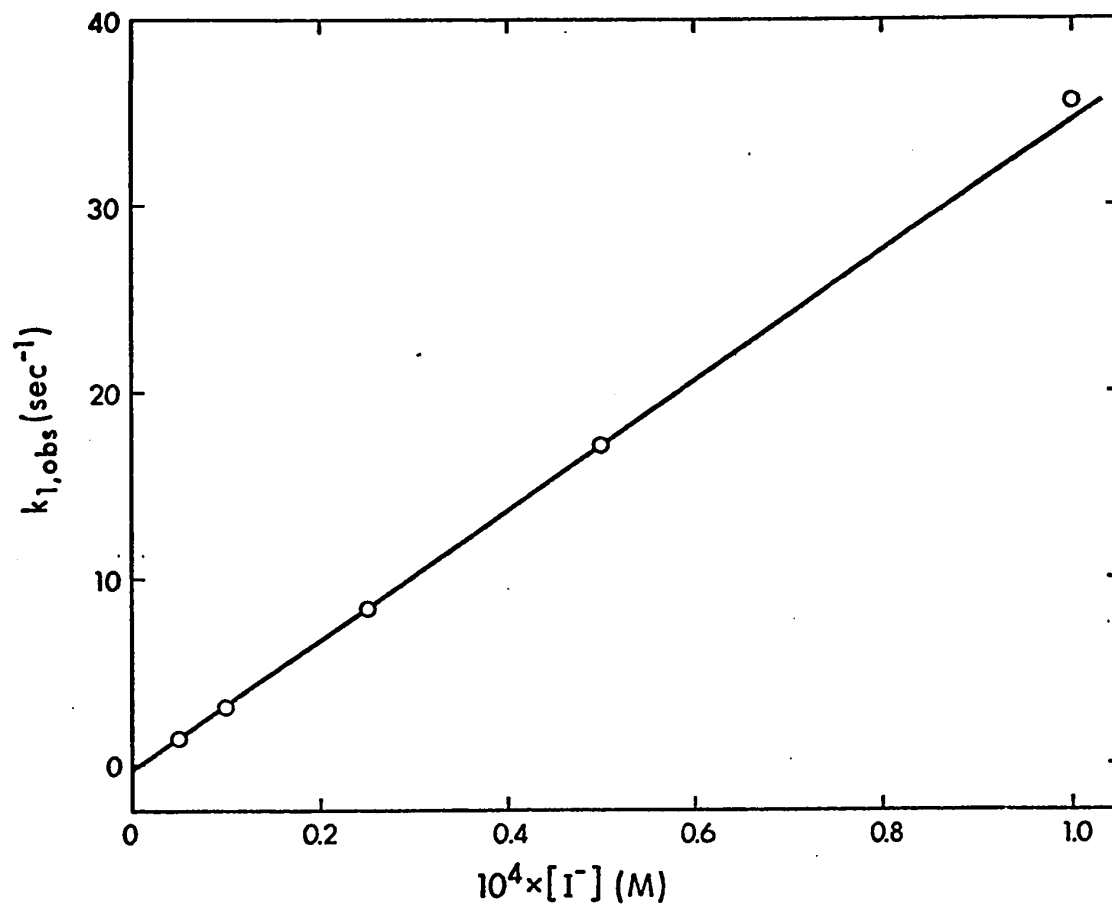


Fig. 2.01: Plot of $k_{1,obs}$ vs. $[I^-]$ for the HRP-I-iodide reaction at pH 4.99. The solid line was calculated by a weighted linear least-squares analysis. The slope, k_1 , with its standard error is $(3.5 \pm 0.04) \times 10^5 \text{ M}^{-1} \text{ sec}^{-1}$.

largest values of $k_{1,obs}$ obtained at any given pH are recorded in Table 2.01. If only a single determination of $k_{1,obs}$ were made at a given pH a large concentration of iodide was used to minimize the error in calculating k_1 , since under these conditions the value of k_{spont} is assumed to be zero. For those values of k_1 determined from a range of iodide concentrations the error in k_1 was equated to the standard deviation calculated from the linear analysis of the $k_{1,obs}$ vs. $[I^-]$ data. The error in k_1 at the other pH values was estimated at $\pm 10\%$. The values of k_1 as a function of pH are listed in Table 2.01 along with the ranges of iodide concentrations and buffers used at each pH. Different buffers used at the same pH yielded identical kinetic results within the experimental error, indicating that there were no detectable buffer effects.

It is possible to demonstrate that iodide and not hydriodic acid is the reacting species in the reaction with HRP-I. The pK_a of hydriodic acid has been reported to be approximately -9 (Bell, 1959). If we take the observed value for k_1 at any given pH, for example, $5.7 \times 10^3 M^{-1} sec^{-1}$ at pH 6.97, we can calculate the concentration of hydriodic acid present at the same pH. At pH 6.97 the $[HI]$ is approximately $10^{-16} [I^-]$. With an iodide concentration of $10^{-3} M$ the value of $k_{1,obs}$ would be 5.7 and the relationship would be

$$k_{1,obs} = k_1' [HI] \quad 2.04$$

Table 2.01

Second-Order Rate Constants for the HRP-I-Iodide
Reaction at 25°.

pH	k_1 ($M^{-1}sec^{-1}$)	$\frac{k_{spont}}{k_{1,obs}} \times 100$	[I ⁻]	Buffer ^a
			$10^5 \times$ Range of [I ⁻] (M)	
2.70	$(2.1 \pm 0.1) \times 10^6$	10	2 - 5	Pt
2.90	1.9×10^6		1 - 5	Pt
3.15	1.6×10^6		1 - 2	Pt
3.30	$(1.5 \pm 0.1) \times 10^6$	3	1 - 4	Ci
3.58	1.4×10^6		1 - 2	Pt
3.79	1.1×10^6		5	A
3.99	$(9.9 \pm 0.2) \times 10^5$	<1	0.5 - 5	A
4.01	9.6×10^5		5	Ci
4.39	$(7.8 \pm 0.5) \times 10^5$	<1	1 - 4	A
4.78	5.7×10^5		2	A
4.95	4.0×10^5		5	Ci
4.99	$(3.5 \pm 0.04) \times 10^5$	<1	0.5 - 10	A
5.39	2.0×10^5		5	Ca
5.44	1.8×10^5		5	A
5.99	5.6×10^4		2.5×10	P
6.97	5.7×10^3		0.5 - 1	P
7.27	$(2.6 \pm 0.1) \times 10^3$	2	0.5 - 8	P
8.33	$(2.4 \pm 0.1) \times 10^2$	3	1 - 5×10	T
9.18	$(3.3 \pm 0.3) \times 10$	11	2.5 - 20×10	C
9.87	7.7×0.3	9	2.5 - 10×10^2	C

^aBuffer key: A, acetic acid-sodium acetate; C, sodium bicarbonate-sodium carbonate; Ca, cacodylic acid-sodium cacodylate; Ci, citric acid-sodium citrate, P, potassium dihydrogen phosphate-disodium hydrogen phosphate; Pt, phthalic acid-sodium phthalate; T, tris (hydroxymethyl)-aminomethane hydrochloride-tris (hydroxymethyl)aminomethane.

where k_1' represents the second-order rate constant for the reaction if hydriodic acid is the reacting species. Under the present conditions k_1' would have a value of approximately $5 \times 10^{19} \text{ M}^{-1} \text{ sec}^{-1}$. The largest possible value for a second-order rate constant would be the diffusion controlled limit which is approximately $10^{11} \text{ M}^{-1} \text{ sec}^{-1}$ for small reactant molecules. However, when one of the reacting species is a macromolecule like HRP, the limiting value for the diffusion controlled limit is lower and has been estimated to be from $10^8 \text{ M}^{-1} \text{ sec}^{-1}$ to $10^{10} \text{ M}^{-1} \text{ sec}^{-1}$ (Alberty and Hammes, 1958). Clearly the value of k_1' is far greater than the diffusion controlled limit, thus providing unequivocal evidence that iodide ion is the reacting species. A similar calculation at the lowest pH where the reaction was studied also resulted in a value of k_1' orders of magnitude greater than the diffusion controlled limit.

The pH dependence of k_1 is illustrated in Fig. 2.02. The analysis of the kinetic pH dependence that results in the computed solid line shown in Fig. 2.02 can be performed in two different fashions. The more traditional of these two methods involves the prediction of a reaction scheme which includes all of the possible reactions between the various protonated forms of the enzyme and the various protonated forms of the substrate. It is assumed in this scheme that the proton transfers for the ionizable groups on the enzyme and substrate are much faster than reactions between the enzyme and substrate (Alberty and Bloomfield,

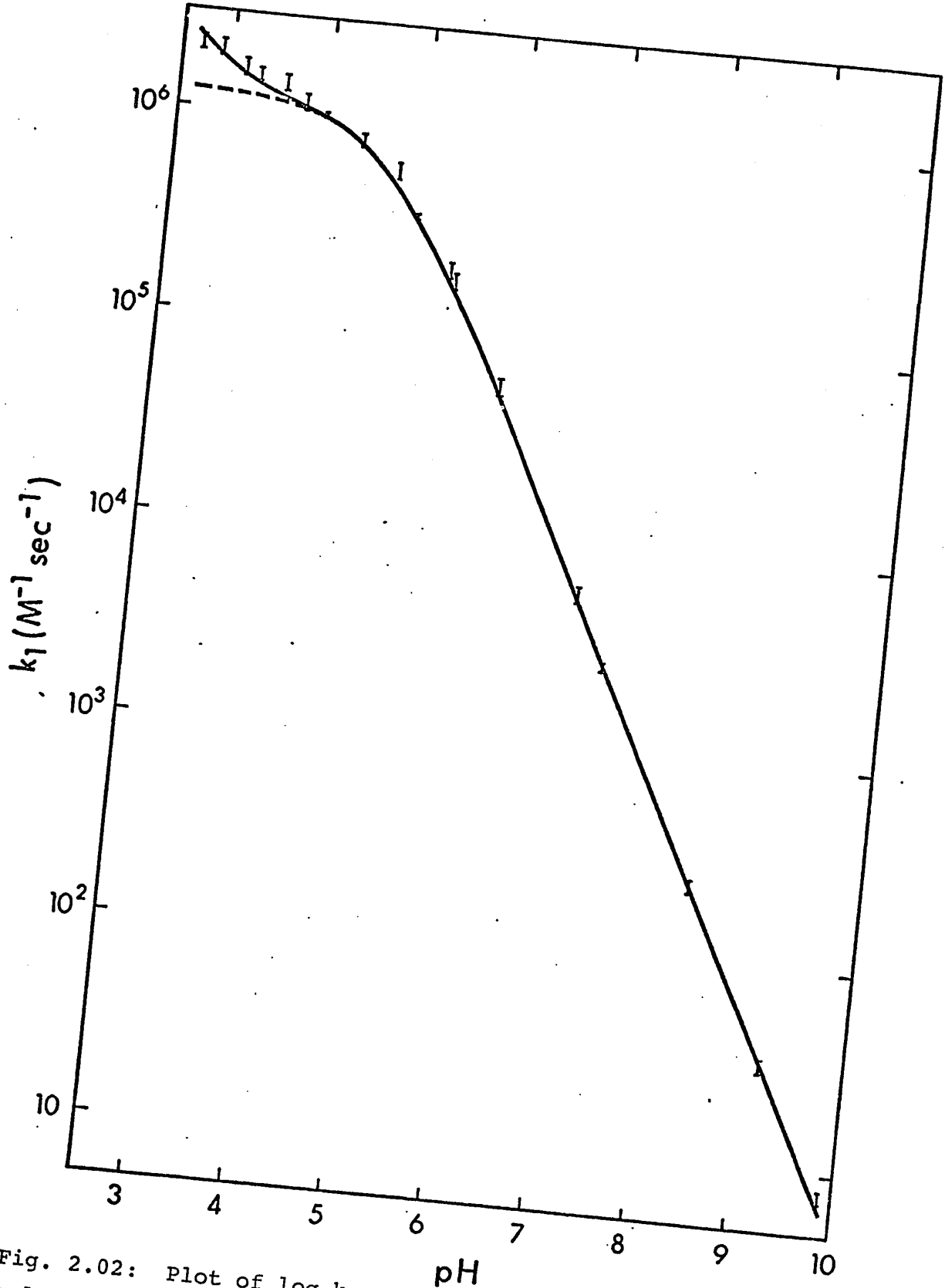


Fig. 2.02: Plot of $\log k_1$ vs. pH. The solid line was calculated by a weighted nonlinear-least squares analysis using equation 2.17 and the broken line was calculated using equation 2.18.

1963). An expression can then be derived for the pH dependence of the experimentally determined rate constant in terms of the rate and equilibrium expressions for the various possible reactions. The denominator of this expression contains a term for every enzyme or substrate dissociation constant and these values can be obtained unambiguously (in principle) from an analysis of the pH dependence of the observed reaction. The numerator of the expression contains complex terms involving all of the rate and dissociation constants. Since the rate constants are included as parts of more complex terms, in general all of the rate constants cannot be determined unambiguously. An example of an analysis of this type is found in the study of Hasinoff and Dunford (1970) on the reactions of HRP-I and HRP-II with ferrocyanide.

The second method for the analysis of the kinetic pH dependence involves the association of the inflections in the log rate constant vs. pH profile to ground state and transition state ionizations (Critchlow and Dunford, 1972c). The expression for the pH dependence of the rate constant derived from this approach has the same denominator terms as the expression derived by the previous method. The complex terms in the numerator resulting from the previous derivation, however, are replaced by terms involving acid dissociation constants for the transition state. Analysis of the expression for the kinetic pH dependence obtained from

the latter derivation results in unambiguous values for both ground state and transition state dissociation constants.

To illustrate the difference between the two methods as applied to the HRP-I-iodide reaction, let us consider the minimum hypothetical pH profile that would be obtained if the reaction could be studied to very high and low pH. Such a pH profile is illustrated in Fig. 2.03 where the solid line represents the experimental points and the broken line the hypothetical one. The pH profile in Fig. 2.03 is shown to be pH independent at high and low pH. This must be the case because of the limitations imposed on the reaction rate by the diffusion controlled limit. Thus at sufficiently low pH the concentration of any reactive unprotonated species will be so low that its contribution to the observed rate will be negligible. Therefore the observed rate will be invariant at any lower value of pH, since it will either be diffusion controlled or composed of the rates for protonated species the concentration of which do not change at lower pH. The converse argument applies to the rate at high pH.

The plot of log rate constant vs. pH can be considered to consist of straight line sections of integral slope connected by short curved regions (Dixon and Webb, 1964). Curved areas where slope change is negative are attributed to ionizations on either the enzyme or substrate using both the traditional and transition state approaches. In the traditional approach the regions where the slope change

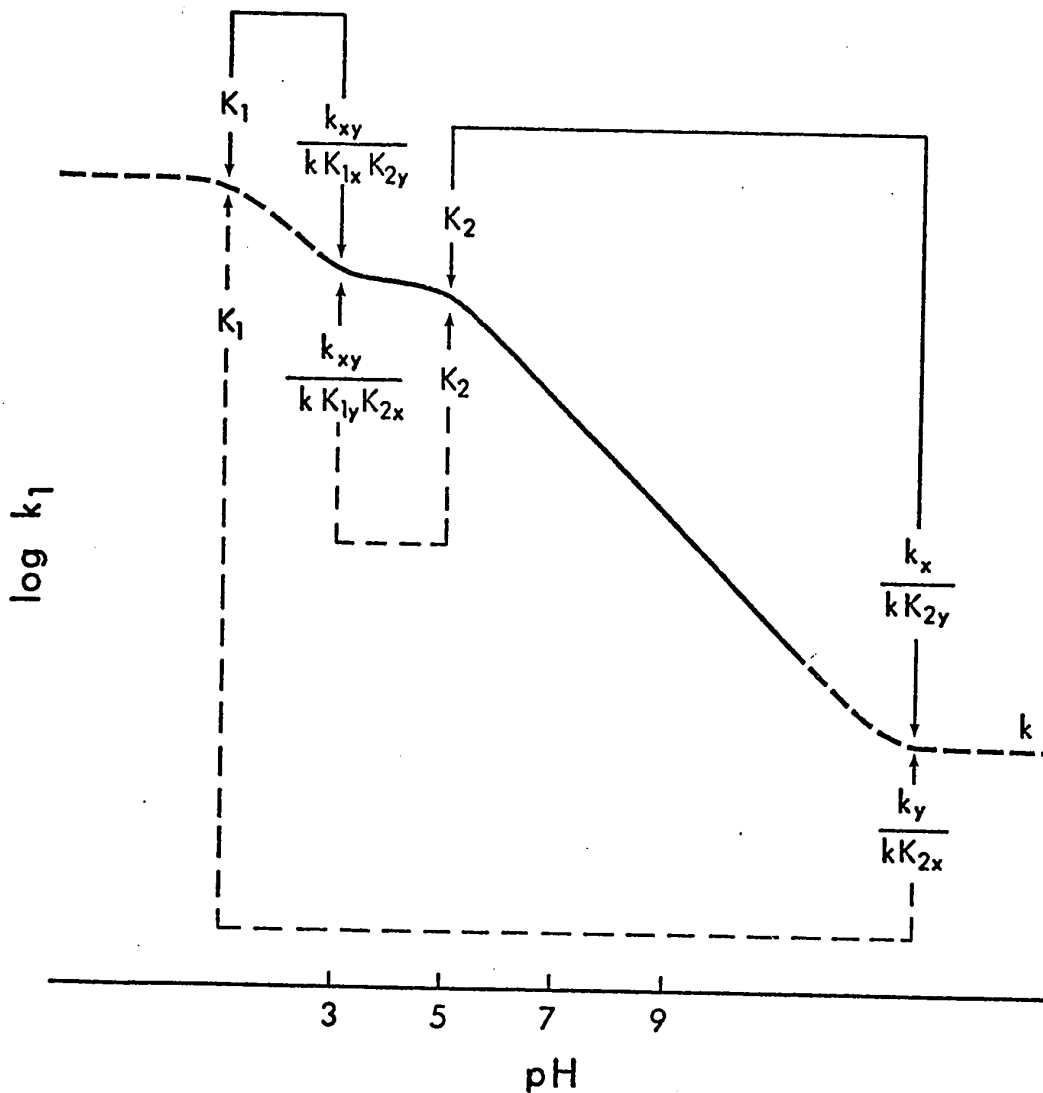
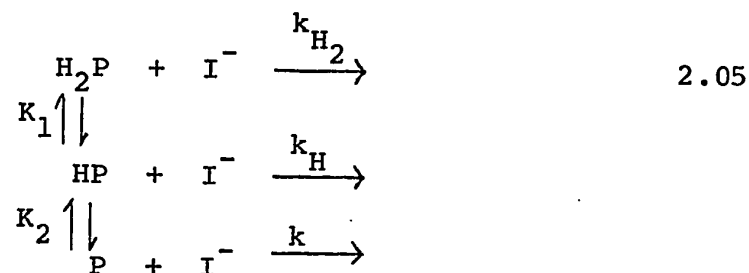


Fig. 2.03: Plot of $\log k_1$ vs. pH. The solid line represents the experimental curve illustrated in Fig. 2.02 and the broken line represents the hypothetical curve at high and low pH. The values of $\log k_1$ for the hypothetical curve are arbitrary. The broken arrows below the curve and the solid arrows above the curve represent the pairing schemes for the two possible reaction mechanisms.

is positive result from the complex terms in the numerator of the expression for the pH dependence of the rate constant. In the transition state approach these regions of positive curvature are attributed to transition state dissociation constants. Since the kinetic pH profile must be pH independent at sufficiently high and low pH, this means that there must be a region of positive curvature for every enzyme or substrate ionization, that is, corresponding to every region of negative curvature.

Let us now consider in detail the analysis of the kinetic pH dependence illustrated in Fig. 2.03, using the traditional approach. Using the formalism employed by Hasinoff and Dunford (1970), the pH dependence for the HRP-I-iodide reaction may be expressed as



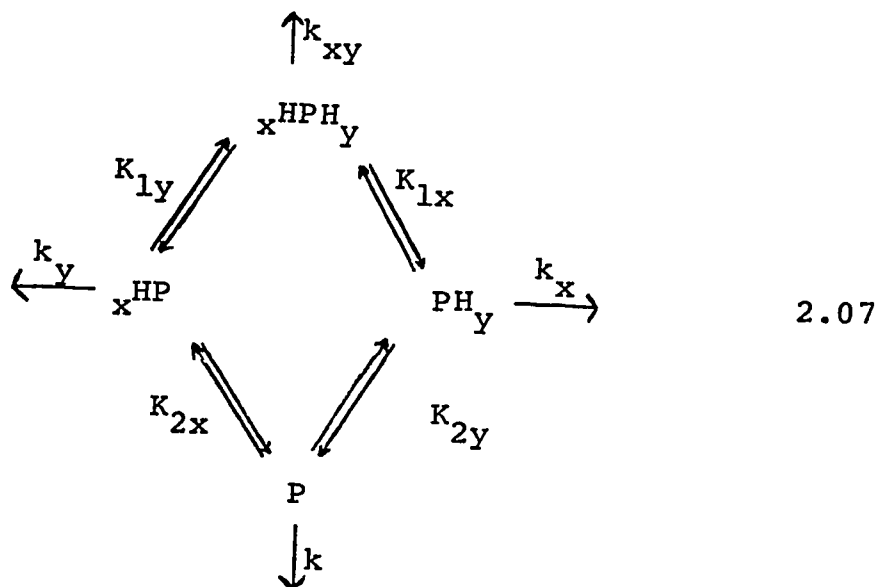
where H_2P , HP and P represent the various protonated forms of HRP-I, k_{H_2} , k_H and k represent the second-order rate constants for the reactions of the various protonated species; and K_1 and K_2 represent the two ionizations on HRP-I illustrated in Fig. 2.03. The expression for the pH dependence of k_1 derived from equation 2.05 is

$$k_1 = \frac{k \left(1 + \frac{k_H [H^+]}{k K_2} + \frac{k_{H_2} [H^+]^2}{k K_1 K_2} \right)}{1 + \frac{[H^+]}{K_2} + \frac{[H^+]^2}{K_1 K_2}} \quad 2.06$$

where k is the pH independent rate constant measured at high pH. The analysis of equation 2.06 would result in values for K_1 and K_2 .

Although the reaction illustrated in equation 2.05 is adequate for calculating the values of K_1 and K_2 , it is not completely satisfactory for the discussion of all possibilities for the mechanism of the HRP-I-iodide reaction. In order to define all possible mechanisms for the reaction one must consider every protonated species that could be kinetically important. Dixon and Webb (1964) have pointed out that when an enzyme possesses two or more ionizations, both molecular and group ionization constants must be considered. The molecular ionization constants refer to the various stages of ionization for the enzyme that can be distinguished by titration, in the present case K_1 and K_2 . The group ionization constants, of which the molecular ionization constants are composed, represent the ionization of particular groups on the enzyme. The authors point out that knowledge of the group ionization constants is desirable, since it is possible that only one of the intermediate forms of the enzyme may be active.

A reaction scheme which illustrates all the possible enzyme forms when two molecular ionizations are observed is



where P represents the unprotonated HRP-I, PH_y and $\text{}^x\text{HP}$ the two singly protonated forms of HRP-I, $\text{}^x\text{HPH}_y$ the doubly protonated form of HRP-I; K_{1x} , K_{1y} , K_{2x} and K_{2y} represent the group ionization constants relating the various protonated forms of HRP-I, and k , k_x , k_y and k_{xy} are the second-order rate constants for the reactions of the various protonated species with iodide. The subscripts on the group ionization constants are the same as those used by Dixon and Webb (1964) for the ionization of an unsymmetrical dibasic acid. The molecular ionization constants K_1 and K_2 are related to the group ionization constants by the equations

$$K_1 = K_{1x} + K_{1y} \tag{2.08}$$

and

$$K_2 = \frac{1}{\frac{1}{K_{2x}} + \frac{1}{K_{2y}}} \tag{2.09}$$

The pH dependence for the experimental second-order rate constant k_1 using the mechanism illustrated in equation 2.07 is derived in Appendix 2 and is

$$k_1 = \frac{k \left(1 + \frac{k_y [H^+]}{k K_{2x}} + \frac{k_x [H^+]}{k K_{2y}} + \frac{k_{xy} [H^+]^2}{k K_{1x} K_{2y}} \right)}{1 + \frac{[H^+]}{K_{2x}} + \frac{[H^+]}{K_{2y}} + \frac{[H^+]^2}{K_{1x} K_{2y}}} \quad 2.10$$

where k has the same meaning as in equation 2.06.

Using the relationship between the group ionization constants

$$K_{1y} K_{2x} = K_{1x} K_{2y} \quad 2.11$$

and equations 2.08 and 2.09 the large difference between K_1 and K_2 shown in Fig. 2.03 indicates that both pairs of constants K_{2x} and K_{2y} , and K_{1x} and K_{1y} must also be well separated. If we make the arbitrary assumption that $K_{2x} \gg K_{2y}$, which from equation 2.11 implies that $K_{1x} \gg K_{1y}$, then equations 2.08 and 2.09 reduce to

$$K_1 \approx K_{1x} \quad 2.12$$

$$K_2 \approx K_{2y} \quad 2.13$$

Returning now to equation 2.10, there are two possible interpretations for the pH dependence of the HRP-I-iodide reaction. According to one mechanism the term $\frac{k_x [H^+]}{k K_{2y}}$ in the numerator is responsible for the region of positive curvature at high pH, that is, as $[H^+]$ increases this term

becomes significant compared to one, resulting in an increase in k_1 with decreasing pH. The region of negative curvature at pH 5 is due to the effect of the term $\frac{[H^+]}{K_{2y}}$ in the denominator. The second region of positive curvature at pH 3 results from the contribution from the term $\frac{k_{xy}[H^+]^2}{k K_1 K_{2y}}$ in the numerator and the final negative curvature occurs when the term $\frac{[H^+]^2}{K_{1x} K_{2y}}$ becomes appreciable. Thus equation 2.10 reduces to

$$k_1 = \frac{k \left(1 + \frac{k_x [H^+]}{k K_{2y}} + \frac{k_{xy} [H^+]^2}{k K_{1x} K_{2y}} \right)}{1 + \frac{[H^+]}{K_{2y}} + \frac{[H^+]^2}{K_{1x} K_{2y}}} \quad 2.14$$

where the term $\frac{[H^+]}{K_{2x}}$ in the denominator has been dropped since $K_{2x} \gg K_{2y}$. In this interpretation it is assumed that $\frac{k_x [H^+]}{k K_{2y}} > \frac{k_y [H^+]}{k K_{2x}}$ and hence the latter term can be neglected. However if $k_y \gg k_x$ the latter assumption is not necessarily valid and a second interpretation of the pH dependence of k_1 is possible in which the region of positive curvature at high pH is due to the term $\frac{k_y [H^+]}{k K_{2x}}$ in the numerator with the remaining inflections having the same meaning as in the previous interpretation. Thus even though $\frac{[H^+]}{K_{2y}} > \frac{[H^+]}{K_{2x}}$ the greater inequality $k_y \gg k_x$ could result in a second equally reasonable interpretation of the kinetic pH dependence for the HRP-I-iodide reaction, for which equation 2.10 reduces to

$$k_1 = \frac{k \left(1 + \frac{k_y [H^+]}{k K_{2x}} + \frac{k_{xy} [H^+]^2}{k K_{1y} K_{2x}} \right)}{1 + \frac{[H^+]}{K_{2y}} + \frac{[H^+]^2}{K_{1x} K_{2y}}} \quad 2.15$$

The term $\frac{k_{xy} [H^+]^2}{k K_{1x} K_{2y}}$ from equation 2.10 has been rewritten as $\frac{k_{xy} [H^+]^2}{k K_{1y} K_{2x}}$ in equation 2.15, using the equality in equation 2.11, in order to correspond to the term $\frac{k_y [H^+]}{k K_{2x}}$.

The two possibilities for the regions of positive curvature in the $\log k_1$ vs. pH plot, if K_{2x} is assumed to be greater than K_{2y} , are illustrated in Fig. 2.03.

If the values for K_{1x} and K_{2y} in equation 2.14 are substituted using equations 2.12 and 2.13, equation 2.14 becomes equivalent to equation 2.06 (derived using only molecular ionization constants). Thus, the use of molecular ionization constants in the derivation of an expression for the pH dependence of k_1 results in only one of the two possible mechanisms for the reaction. For a more complicated pH profile than the one illustrated in Fig. 2.03, with more than two ionizations, the number of possible mechanisms increases rapidly; however analysis of these results in terms of molecular ionization constants still results in only one possible mechanism.

Although the equations 2.14 and 2.15 representing the

two possible interpretations for the kinetic pH dependence have an identical form, the differences between the mechanisms corresponding to the two equations are significant. The mechanism represented by equation 2.14 (or 2.06) has the terms $[H^+]/K_{2y}$ and $[H^+]^2/K_{1x}K_{2y}$ in both numerator and denominator. Thus both the positive and negative inflections at high pH are associated with the term containing K_{2y} in the numerator and denominator. In other words, the positive inflection at high pH can be thought of as arising from the reaction of a reactive protonated form of the enzyme whose concentration is determined by the ionization constant K_{2y} . As the pH approaches the value of pK_{2y} , the concentration of the protonated species approaches its maximum concentration and the rate becomes pH independent. Similarly the positive and negative inflections at low pH are associated with the term containing K_{1x} in both the numerator and denominator. Thus the rate can be thought of increasing in steps with decreasing pH, where the second step influences the rate only after the first step has had its influence. The use of molecular ionization constants to derive the expression for the kinetic pH dependence will always result in this type of mechanism, where successive positive and negative inflections in the pH profile can be considered to be paired together (as in equation 2.06 or 2.14). The association of the positive and negative inflection corresponding to this mechanism are illustrated by the two solid arrows in Fig.2.03.

The mechanism represented by equation 2.15 differs from the previous mechanism in that the terms in the numerator that result in the positive inflections in the pH profile contain different ionization constants than the terms in the denominator that result in the adjacent regions of negative curvature. In equation 2.15 the positive inflection at high pH can be seen to result from the term involving K_{2x} , while the negative inflection at high pH results from the term involving K_{2y} . That is, the increase in rate with increasing acidity at high pH can be thought of as resulting from a very reactive protonated form of the enzyme whose concentration is controlled by an ionization constant, K_{2x} , that is associated with the negative curvature at low pH. The influence of the other enzyme ionization, K_{1y} , on the rate can be thought of as a smaller effect that is superimposed on the larger effect resulting from the other ionization. Since the protonation of the enzyme group whose ionization constant is K_{2x} accelerates the rate, the protonation of the group whose ionization constant is K_{1y} must decelerate the rate in order to produce the kinetic pH profile illustrated in Fig. 2.03. The association of positive and negative inflections corresponding to this mechanism are illustrated by the broken set of arrows in Fig. 2.03.

Although the two possible mechanisms were illustrated with the assumption that $K_{2x} \gg K_{2y}$, the reverse assumption could also have been made without affecting the interpretation

of equation 2.10. An important conclusion concerning the two mechanisms is that no matter which mechanism is used, the analysis of the appropriate pH dependent expression will result in identical values for K_1 and K_2 . This must be the case since the reaction of two species with the same extent of protonation, for example PH_y and ${}_x\text{HP}$, are kinetically indistinguishable. The corollary of this conclusion is that the value of specific parameters determined for the analysis of a particular mechanism, for example k_x or k_y , will only be meaningful if the mechanism is correct.

The alternative method for the analysis of the pH dependence of the rate constants equates the regions of negative curvature in the plots of log rate constant vs. pH to transition state ionization constants. The rigorous derivation of a transition state approach that is applicable to the present systems has been described in detail elsewhere and will not be repeated here (Critchlow and Dunford, 1972c). There has been some controversy as to whether information on the nature of the transition state can be gained from such an analysis. However, in the present context this problem is of no concern since the theory will only be used to give a systematic approach to the determination of the simplest form of the expressions which will fit the experimental pH-rate profile.

For the purposes of the present discussions, the transition state approach can be fairly simply summarized. As mentioned previously positive curvatures in the kinetic

pH profile are assumed to result from transition state ionizations and negative curvatures from ground state ionizations. The expression for the pH dependence of the rate constant takes the form

$$k_1 = \frac{k_1^{\circ} \left(\dots + \frac{K_i^{\ddagger}}{[H^+]} + 1 + \frac{[H^+]}{K_{i+1}^{\ddagger}} + \frac{[H^+]^2}{K_{i+1}^{\ddagger} K_{i+2}^{\ddagger}} + \dots \right)}{\left(\dots + \frac{K_i^E}{[H^+]} + 1 + \frac{[H^+]}{K_{i+1}^E} + \dots \right) \left(\dots + \frac{K_i^S}{[H^+]} + 1 + \frac{[H^+]}{K_{i+1}^S} + \dots \right)} \quad 2.16$$

where k_1° is a pH independent rate constant with the same units as k_1 , the terms in the numerator refer to the various observed transition state ionization constants and the terms in denominator refer to the observed enzyme and substrate ionizations with superscripts E and S respectively. When applied to the $\log k_1$ vs. pH profile illustrated in Figs. 2.03 or 2.04, the transition state approach leads to

$$k_1 = \frac{k \left(1 + \frac{[H^+]}{K_2^{\ddagger}} + \frac{[H^+]^2}{K_1^{\ddagger} K_2^{\ddagger}} \right)}{\left(1 + \frac{[H^+]}{K_2} + \frac{[H^+]^2}{K_1 K_2} \right)} \quad 2.17$$

where k has the same meaning as in equation 2.10. K_1^{\ddagger} , K_2^{\ddagger} and K_1 and K_2 from equation 2.17 are illustrated on the $\log k_1$ vs. pH profile in Fig. 2.04. The various possible mechanisms,

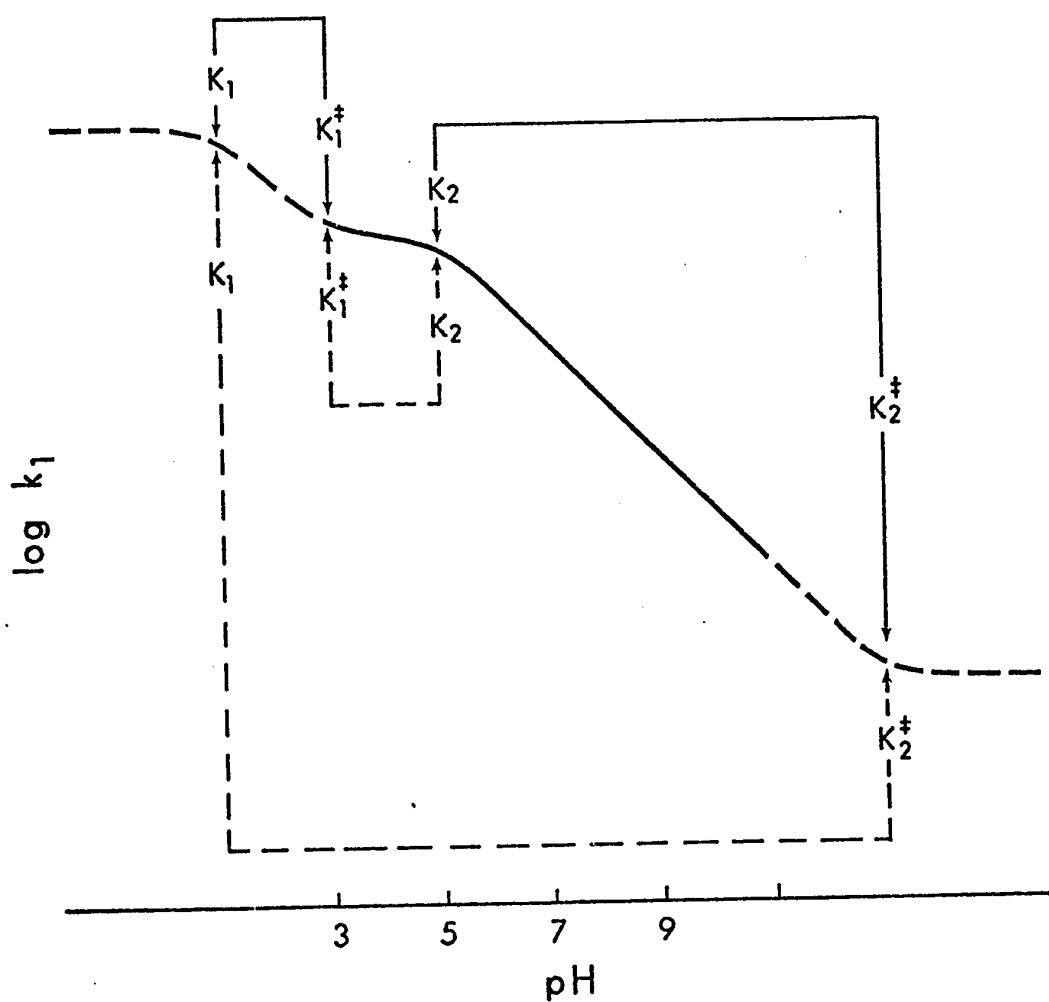


Fig. 2.04: Plot of $\log k_1$ vs. pH. The solid line represents the experimental curve illustrated in Fig. 2.02 and the broken line represents the hypothetical curve at high and low pH. The values of $\log k_1$ for the hypothetical curve are arbitrary. The broken arrows below the curve and the solid arrows above the curve represent the pairing schemes for the two possible reaction mechanisms.

from the point of view of the transition state approach, are simply illustrated in Fig. 2.04 by all the possible combinations of pK_a 's and pK_a^\ddagger 's. In the present example, with two ground state pK_a 's and two transition state pK_a^\ddagger 's, only two pairing schemes are possible. The difference $pK_a^\ddagger - pK_a$ indicates the sensitivity of the reaction to the particular ionization. If the $pK_a^\ddagger - pK_a$ difference is positive the protonation increases the rate of reaction, and if the difference is negative the protonation decreases the rate. The mechanism illustrated by the solid arrows indicates that both ground state ionizations are rate accelerating, whereas the mechanism illustrated by the broken arrows indicates that the rate has a large sensitivity to a rate accelerating protonation at low pH and a smaller sensitivity to a rate decelerating protonation at pH 5. Thus the mechanistic conclusions of the traditional approach, with the inclusion of group ionization constants and the transition state approach are identical, however in the latter case these conclusions may be reached by simply inspecting the observed pH profile.

A major advantage of the transition state approach for complex reaction schemes is that there are only as many constants in the analysis of the pH profile of the reaction rate as there are independently obtainable parameters. The reason for this fact is that all the kinetically indistinguishable steps in the reaction sequence, for example the

reaction between a singly protonated enzyme species and unprotonated substrate contrasted to the reaction between the unprotonated enzyme species and the singly protonated substrate, are associated with a single term in the numerator of the pH dependent rate expression. In the present example both equation 2.06 derived using molecular ionization constants and equation 2.17 derived from the transition state approach have five constants. The reason is that the reaction scheme illustrated in equation 2.05 has no kinetic ambiguity since iodide ion has been assumed to be the only reacting species. Such a simplification is not possible for every substrate. For example in the reaction between HRP-I and ferrocyanide (Hasinoff and Dunford, 1970) two protonated forms of the substrate were considered and the pH dependence was analyzed in terms of six rate and equilibrium constants even though only four independent parameters could be obtained from the analysis. The use of the transition state approach for the analysis would require only four constants, all of which could be determined. Thus the traditional approach can result, at best, in an expression for the kinetic pH dependence that is as simple as that derived from the transition state approach.

A further advantage of the transition state approach is that all possible mechanisms can be obtained from the various pairing schemes for the pK_a^\ddagger and pK_a values, without recourse to any mathematics other than computing the total

number of possible permutations of pairs. Although in the present case, with only two possible mechanisms, the simplification resulting from the use of the transition state approach is not great, with the more complicated pH profiles observed for other substrates the use of the transition state approach becomes a virtual necessity. For example, the pH profile for the HRP-I-sulfite reaction was analyzed in terms of three ground state pK_a values and one transition state pK_a^\ddagger value. This means that there are six possible pairing schemes using the transition state approach. A reaction sequence involving the ground state group ionization constants necessary to define all six mechanisms would be unwieldy at best, and a solution of this type has not been attempted. In general there will be $n!$ possible pairing schemes, where $n!$ is the number of observed ground state or transition state ionizations, whichever is greater. This means that if four ground state or transition state ionization are observed, there will be twenty-four possible mechanisms. Such a situation has been observed for the reaction of HRP-II (Critchlow and Dunford, 1972a) and lactoperoxidase compound II (Maguire and Dunford, 1972b) with p-cresol. Consideration of all the group ionization constants for these kinetic pH profiles is impractical and without the transition state approach the only practical alternative is to analyze the pH dependence in terms of a single mechanism using molecular ionization constants. We feel the transition state approach is sufficiently advantageous

to have used it exclusively for the analysis of the kinetic pH dependence of the other substrates discussed later in this thesis.

Returning now to the experimental plot of $\log k_1$ vs. pH illustrated in Fig. 2.02: since the plot maintains a slope of -1 in the alkaline region, no estimate can be made for the value of k in equation 2.17. A value of $\frac{k}{K_2^\ddagger}$ can be obtained, however, from any value of k_1 in the alkaline region and the equation for the pH dependence of k_1 can be written

$$k_1 = \frac{k' [H^+] \left(1 + \frac{[H^+]}{K_1^\ddagger} \right)}{1 + [H^+]/K_2} \quad 2.18$$

where k' is $\frac{k}{K_2^\ddagger}$ and the term $\frac{[H^+]^2}{K_1^\ddagger K_2}$ has been dropped from the denominator since there is no evidence for the second ground state pK_a at low pH. The broken line in Fig. 2.02 illustrates the line calculated from the equation

$$k_1 = \frac{k' [H^+]}{1 + [H^+]/K_2} \quad 2.19$$

which does not involve a transition state pK_a^\ddagger at low pH. The systematic deviation between calculated and experimental points at low pH indicates that equation 2.19 does not satisfactorily describe the data, thus the more complicated equation 2.18 must be used. Both the solid and broken

lines in Fig. 2.02 represent the best fit to equations 2.18 and 2.19 calculated with a weighted nonlinear least-squares program. The use of a similar program, without weighting, has been described with regard to the analysis of the pH dependence of the reactions of HRP-I and HRP-II with ferrocyanide (Hasinoff and Dunford, 1970). The values of the parameters calculated from equations 2.18 and 2.19 are listed in Table 2.02.

Table 2.02
Ground State and Transition State Ionization
Constants Obtained by the Nonlinear Least-Squares
Analyses of Equations 2.18 and 2.19.

	Equation 2.18	Equation 2.19
$k' \text{ (M}^{-2} \text{sec}^{-1})$	$(5.0 \pm 0.1) \times 10^{10}$	$(4.9 \pm 0.2) \times 10^{10}$
$K_2 \text{ (M)}$	$(2.3 \pm 0.1) \times 10^{-5}$	$(2.6 \pm 0.2) \times 10^{-5}$
$K_1^\ddagger \text{ (M)}$	$(2.1 \pm 0.35) \times 10^{-3}$	

Kinetics of the HRP-II-Iodide Reaction

The kinetic behavior of the HRP-II-iodide system, like that of the HRP-I-iodide system, is consistent with a reaction that is first order in both HRP-II and iodide. Under pseudo-first-order conditions a differential rate expression

$$-\frac{d[\text{HRP-II}]}{dt} = k_{2,\text{obs}}[\text{HRP-II}] \quad 2.20$$

was observed. The linearity of the semilogarithmic plots of the change in voltage or absorbance vs. time indicated the validity of equation 2.20. Values of the second-order rate constant, k_2 , were obtained from the equation

$$k_{2,\text{obs}} = k_2[\text{I}^-] \quad 2.21$$

Plots of $k_{2,\text{obs}}$ vs. $[\text{I}^-]$ were linear as illustrated in Fig. 2.05 for the reaction at pH 3.41. Similar studies were carried out at pH values of 2.71, 2.99, 6.00, 8.66 and 9.05. At pH values below 3.4 and above 8.5 the plots of $k_{2,\text{obs}}$ vs. $[\text{I}^-]$ have a positive intercept indicating an appreciable spontaneous rate of disappearance of HRP-II. The values of these intercepts are found never to be greater than 15% of the largest measured value of $k_{2,\text{obs}}$. For values of k_2 obtained from plots of $k_{2,\text{obs}}$ vs. $[\text{I}^-]$, the error was equated to the standard deviation calculated from the linear analysis. The other values of k_2 were assumed to have an error of $\pm 10\%$. As for the reaction between HRP-I and iodide no buffer effects were observed.

The values of k_2 are listed in Table 2.03 along with the ranges of iodide concentrations and buffers used at each pH. The logarithm of k_2 is plotted vs. pH in Fig. 2.06. Since the slope of the plot is -1 within experimental error the value of k_2 is proportional to hydrogen ion concentration

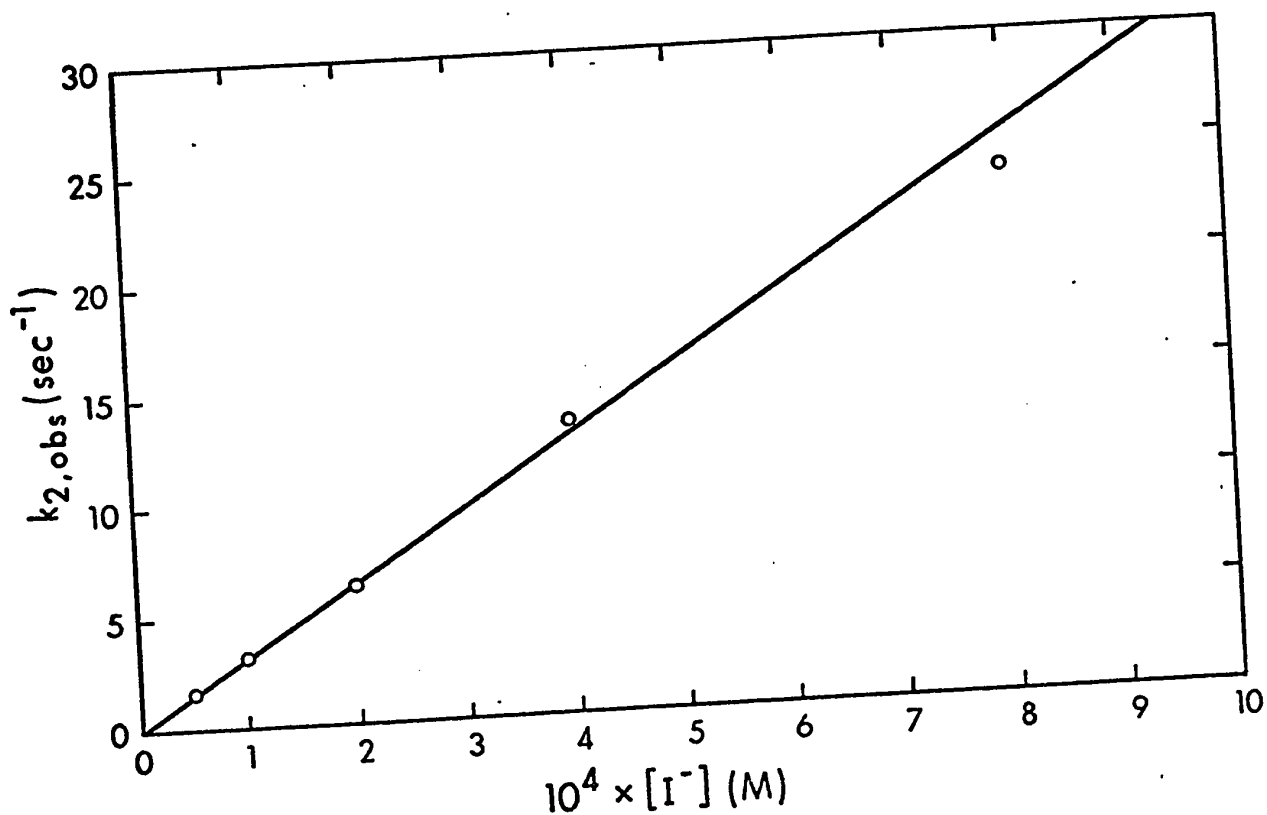


Fig. 2.05: Plot of $k_{2,obs}$ vs. $[I^-]$ for the HRP-II-iodide reaction at pH 3.41. The solid line was calculated by a weighted linear least-squares analysis. The slope, k_2 , with its standard error is $(3.2 \pm 0.1) \times 10^4 \text{ M}^{-1} \text{ sec}^{-1}$.

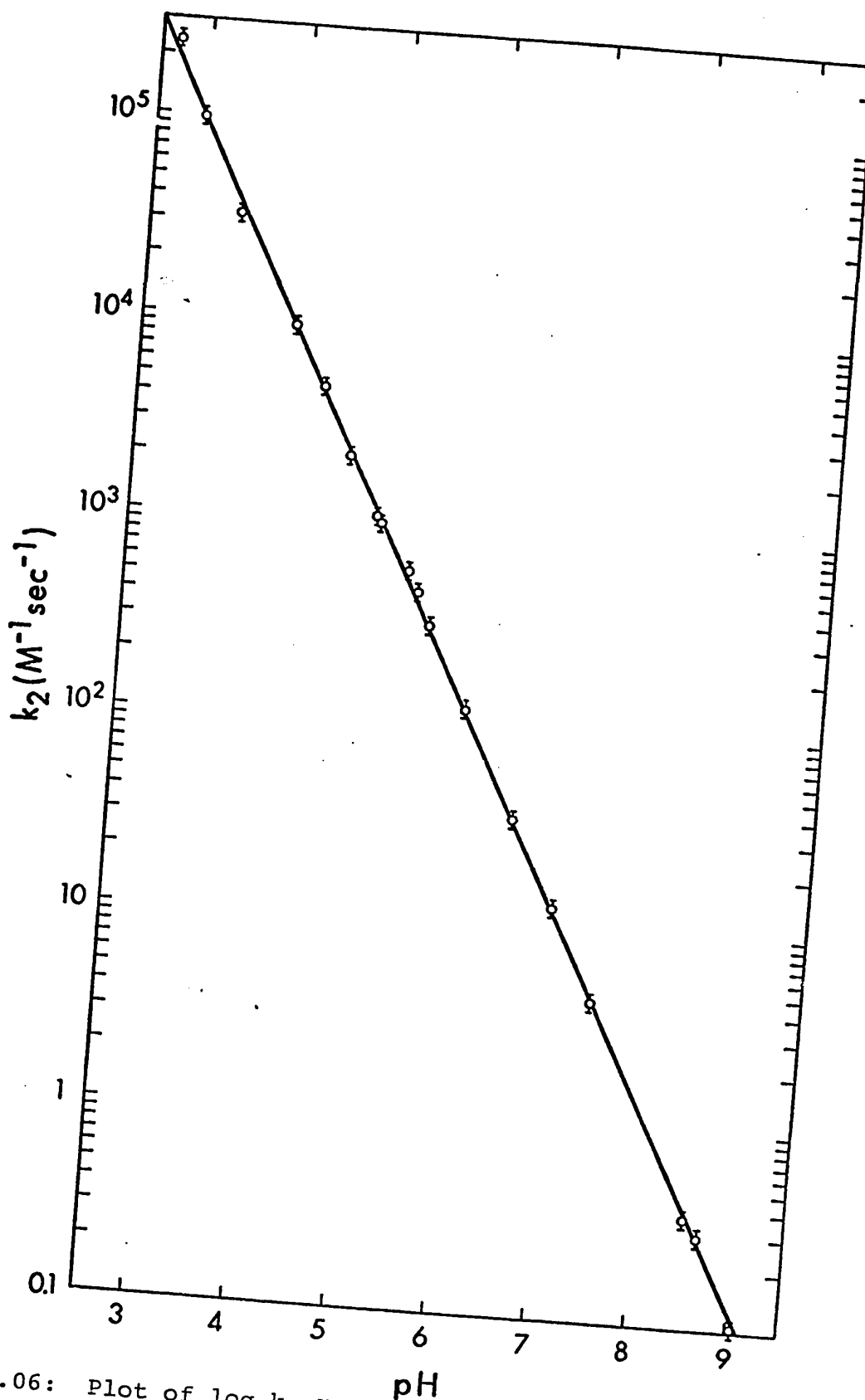


Fig. 2.06: Plot of $\log k_2$ vs. pH for the HRP-II-iodide reaction. The solid line was calculated by a weighted linear least-squares analysis and has a slope of -0.99 ± 0.006 .

Table 2.03
 Second-Order Rate Constants for the HRP-II-Iodide
 Reaction at 25°

pH	k_2 ($M^{-1}sec^{-1}$)	$[I^-]$ (M)	Buffer ^a
2.71	$(2.3 \pm 0.15) \times 10^5$	$0.5 - 2 \times 10^{-4}$	G
2.99	$(8.8 \pm 0.3) \times 10^4$	$0.5 - 3 \times 10^{-4}$	G
3.41	$(3.2 \pm 0.08) \times 10^4$	$0.5 - 8 \times 10^{-4}$	G
4.03	9.1×10^3	1.0×10^{-3}	A
4.38	4.6×10^3	1.0×10^{-3}	A
4.68	2.1×10^3	2.5×10^{-3}	A
4.98	1.1×10^3	1.0×10^{-2}	A
5.01	9.7×10^2	5.0×10^{-3}	A
5.31	5.8×10^2	1.0×10^{-2}	Ca
5.44	4.5×10^2	2.5×10^{-3}	A
5.58	3.1×10^2	1.0×10^{-2}	Ca
6.00	$(1.2 \pm 0.04) \times 10^2$	$0.1 - 1.0 \times 10^{-2}$	P
6.53	3.4×10	3.3×10^{-4}	P
6.99	1.2×10	1.6×10^{-3}	T
7.46	4.3	9.1×10^{-3}	T
8.51	0.37	3.3×10^{-2}	B
8.66	$(2.9 \pm 0.11) \times 10^{-1}$	$1.05 - 5.0 \times 10^{-2}$	T
9.05	$(1.0 \pm 0.03) \times 10^{-1}$	$0.3 - 1.0 \times 10^{-1}$	C

^aBuffer key: A, C, Ca, P and T are the same as in Table 2.01; B, sodium tetraborate - HNO₃; G, glycine hydrochloride-glycine.

over the entire pH range of the study. This behavior can be most simply explained by the presence of a kinetically important ionization on the enzyme which is outside the pH range covered in the study. In a manner analogous to that used for the reaction of HRP-I and iodide it can be shown that iodide and not hydriodic acid must be the reacting species since, over the range of pH and iodide concentrations used in our study, the reaction of hydriodic acid would require a rate constant that exceeded the diffusion controlled limit by a factor of 10^7 .

In a recent publication, Björkstén (1970) reported a value of the second-order rate constant, for the reaction of HRP-II and iodide, of $1.8 \times 10^2 \text{ M}^{-1} \text{ sec}^{-1}$ at pH 6.19. Considering the different techniques employed in the two studies (Björkstén measured the reaction directly but used initial velocity measurements instead of analyzing the whole trace as was done in the present study) the agreement is reasonable with our value for the rate constant, $7.1 \times 10 \text{ M}^{-1} \text{ sec}^{-1}$, at the same pH. We feel that our value for the rate constant is more accurate, since it does not depend on the concentration of HRP-II or knowledge of the molar absorptivity differences between HRP and HRP-II.

Reaction Sequence for the HRP-I-Iodide Reaction

The commonly accepted mechanism for reactions of HRP-I involves the transfer of a single electron from an oxidizable substrate to HRP-I forming HRP-II (Brill, 1966). If

this mechanism were applicable to the reaction between HRP-I and iodide, excess hydrogen peroxide in the HRP-I solution would not affect the reaction, since HRP-II reacts much more slowly than HRP-I. It was observed, however, that if an excess of hydrogen peroxide were added to that required for complete conversion of HRP to HRP-I, the recording of absorbance vs. time at 411 nm exhibited an initial constant absorbance followed by an exponential decay. Increasing the concentration of hydrogen peroxide extended the duration of the linear section, but left the exponential section unchanged. Analysis of the exponential section, with and without an excess of hydrogen peroxide, resulted in the same value for the first-order rate constant. An example of such an experiment is illustrated in Fig. 2.07 for the reaction of HRP-I at pH 8.4. Fig. 2.07a shows a typical experiment performed on the Cary 14 spectrophotometer. In this experiment 2.2×10^{-6} M hydrogen peroxide is added to a 2.7×10^{-6} M solution of HRP in buffer, potassium nitrate and 2.5×10^{-4} M potassium iodide. The initial drop in absorbance is due to HRP-I formation and the exponential trace to the reaction between HRP-I and iodide. In Fig. 2.07b the conditions are the same except that the concentration of hydrogen peroxide has been increased to 4.4×10^{-6} M; in 2.07c this concentration was further increased to 8.8×10^{-6} M. The observed first-order rate constants in the three cases were: $5.5 \times 10^{-2} \text{ sec}^{-1}$, $5.3 \times 10^{-2} \text{ sec}^{-1}$ and $4.9 \times 10^{-2} \text{ sec}^{-1}$ respectively.

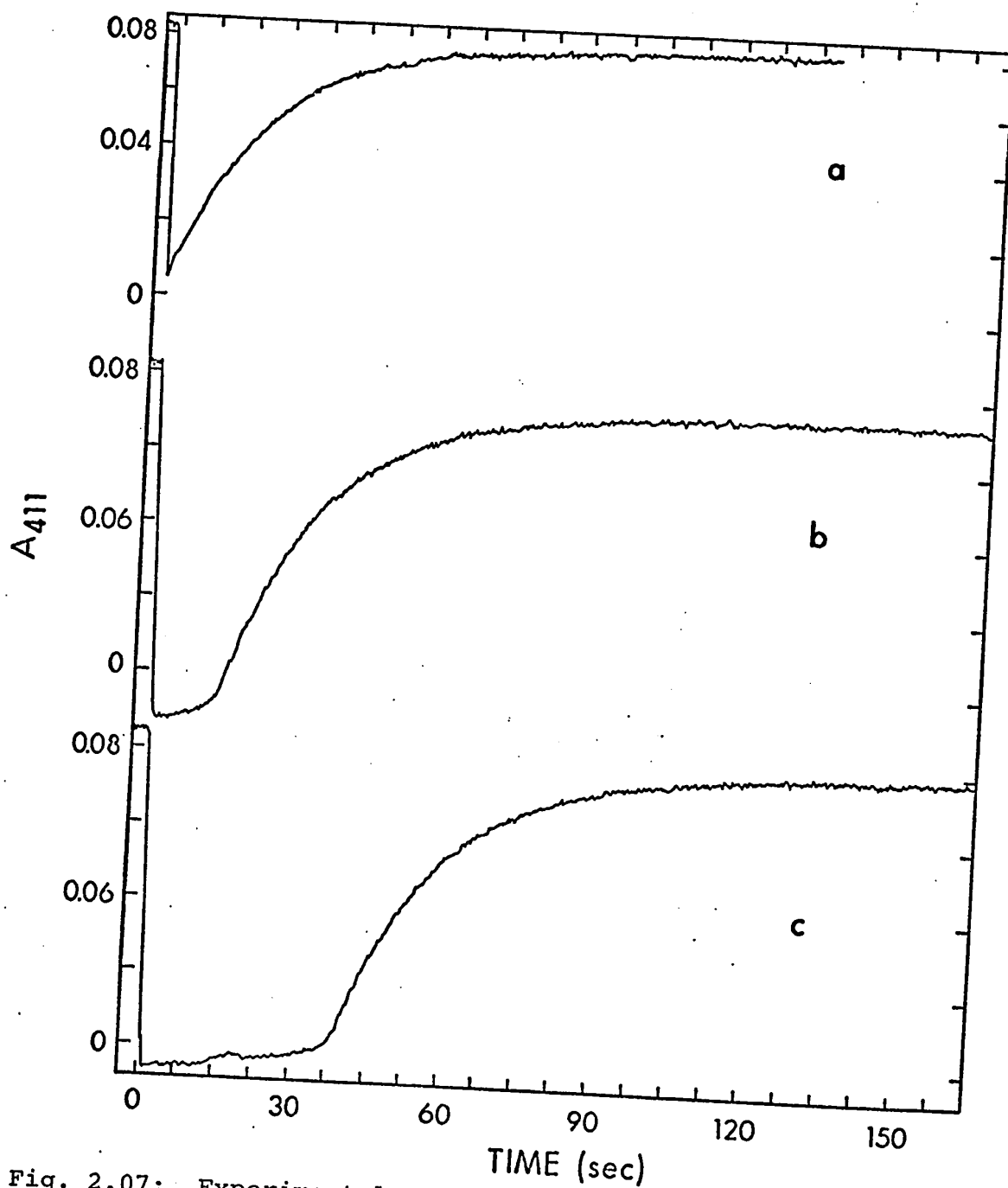


Fig. 2.07: Experimental traces of absorbance at 411 nm vs. time for the HRP-I-iodide reaction. The reaction in (a) was performed with an excess of HRP compared to hydrogen peroxide. The reactions in (b) and (c) were performed with varying excesses of hydrogen peroxide compared to HRP.

One explanation for the kinetic behavior of the reaction in the presence of excess hydrogen peroxide is that HRP and not HRP-II is produced directly from HRP-I. This behavior would result in the formation of a large steady-state concentration of HRP-I, which would exist until the hydrogen peroxide had been consumed. Negligible amounts of HRP and HRP-II would be present. To check this hypothesis the absorbance difference between HRP-I and the enzymatic reaction product was measured at 395, 403, 411, 427 and 430 nm. The experimental values for the total change in absorbance at the various wavelengths were converted to molar absorptivity values using the absorbance difference at 411 nm (the isosbestic point between HRP and HRP-II) as a reference. Fig. 2.08 illustrates the molar absorptivity difference spectra calculated for the conversion of HRP-I to HRP and HRP-II. The solid line represents the molar absorptivity difference between HRP and HRP-I and the broken line represents the difference between HRP-II and HRP-I. The experimental points are the total change in absorbance observed for the reaction of 2.7×10^{-6} M HRP-I with 2.5×10^{-4} M potassium iodide in 0.1 M potassium nitrate and pH 8.4 tris buffer. The HRP : HRP-I difference spectrum was calculated from values interpolated from Fig. 2.13; the HRP-II : HRP-I spectrum was calculated from the spectrum of HRP-I in Fig. 2.13 and the spectrum of HRP-II published by Chance et al. (1967). The experimental points clearly indicate that the spectrum of the enzymatic product of the

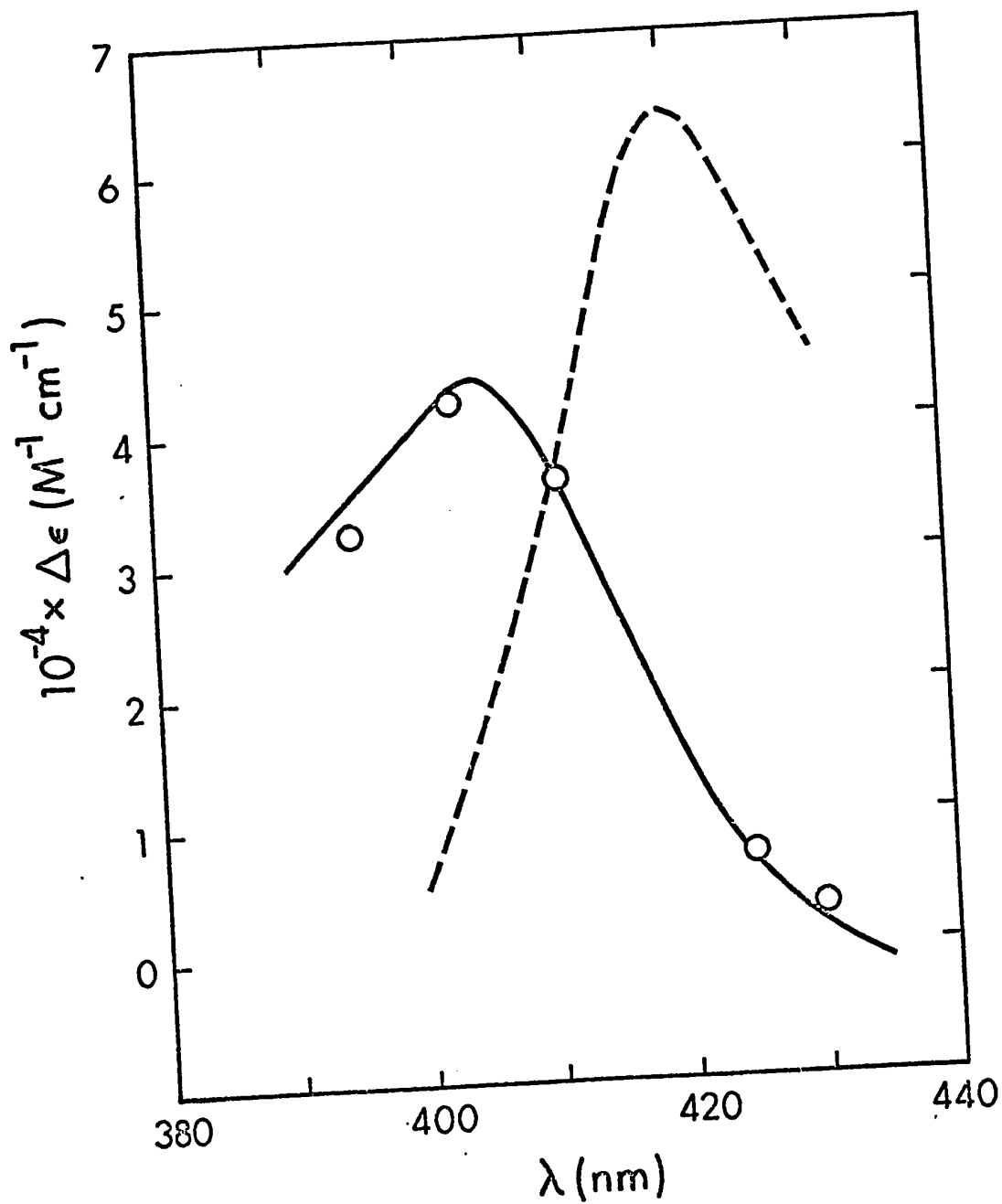
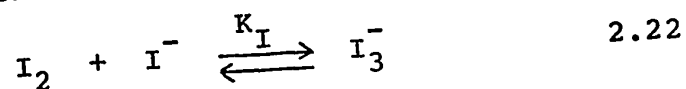


Fig. 2.08: Plot of the molar absorptivity difference between HRP:HRP-I and HRP-II:HRP-I vs. wavelength. The solid line represents the molar absorptivity difference between HRP and HRP-I and the broken line represents the difference between HRP-II and HRP-I.

reaction between HRP-I and iodide resembles HRP.

A further test as to whether HRP-II is produced from the reaction of HRP-I was performed by making successive additions of hydrogen peroxide to a solution of 2.4×10^{-6} M HRP in 1.5×10^{-4} M potassium iodide, 0.1 M potassium nitrate and pH 8.4 tris buffer. As illustrated in Fig. 2.09, the addition of hydrogen peroxide causes the rapid formation of HRP-I which then reacts more slowly with iodide. When the reaction trace at 411 nm reached its asymptotic value a second equivalent of hydrogen peroxide was added and a reaction trace identical to the first was observed. From the known rate constant for the reaction between HRP-II and iodide, the latter reaction would be less than 5% complete at the time of the second peroxide addition. The observed first-order rate constants were $3.6 \times 10^{-2} \text{ sec}^{-1}$ for the first addition and $3.8 \times 10^{-2} \text{ sec}^{-1}$ for the second addition of peroxide. The experiment was repeated at 420 nm, a wavelength that is more sensitive to the production of HRP-II, and similar results were observed.

The participation of a long-lived enzymatic intermediate in the reaction of HRP-I can also be checked by monitoring the reaction products. In iodide solutions the iodine produced is in equilibrium with triiodide ion as described by the equation



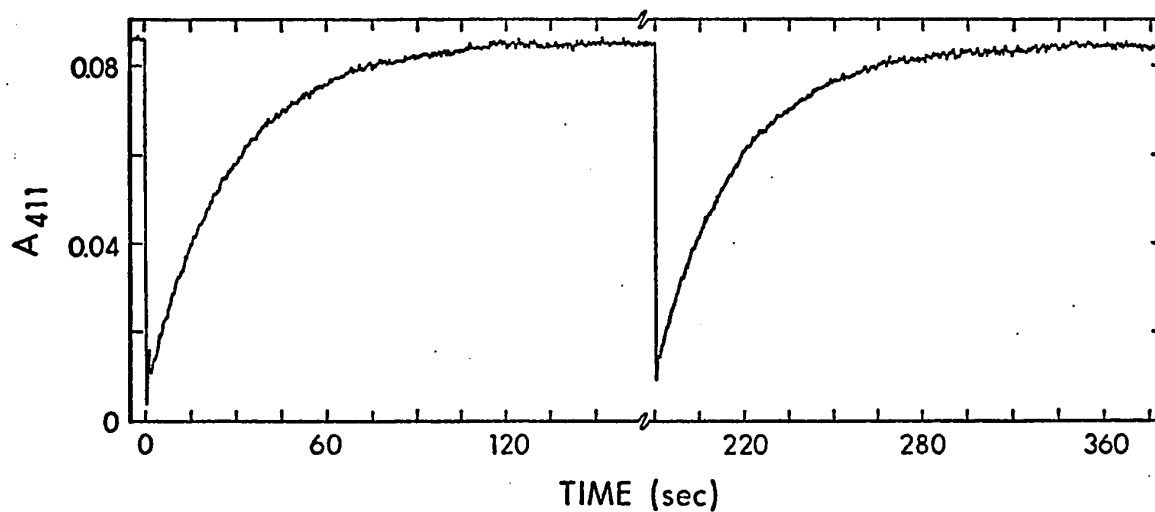
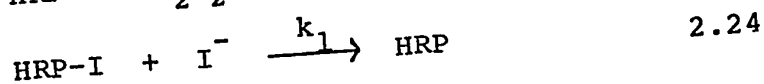
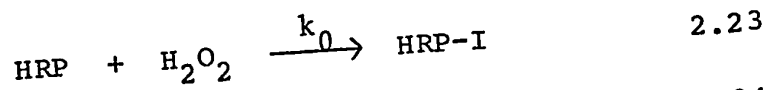


Fig. 2.09: Experimental trace of absorbance at 411 nm vs. time resulting from the successive addition of equivalent concentrations of hydrogen peroxide to a solution of HRP and iodide. The time taken for the second addition of hydrogen peroxide was 10 sec.

where K_I is 721 M^{-1} at 25° and the triiodide ion has a molar absorptivity (ϵ_{353}) of $2.62 \times 10^4 \text{ M}^{-1} \text{ cm}^{-1}$ at 353 nm (Ramette and Sandford, 1965). At pH 7.0 and iodide concentration of 10^{-3} M , a single reaction was observed at 353 nm on the stopped-flow apparatus. These results clearly indicate that there is no kinetic evidence for the participation of HRP-II or other enzymatic intermediate in the reaction of HRP-I with iodide. The total change in absorbance indicated that one mole of iodine was produced for every mole of HRP-I which reacted providing clear evidence that, within the time scale of the experiment, iodine does not react with the enzyme at a detectable rate.

These results indicate that, for the HRP-catalyzed oxidation of iodide by hydrogen peroxide, the rate determining step at high concentrations of hydrogen peroxide should be the reaction between HRP-I and iodide. To test this hypothesis the steady-state kinetics of the HRP-catalyzed reaction were studied using the technique of Björkstén (1968). If the catalytic action of HRP can be described by the equations



then

$$\frac{[\text{HRP}]_0}{v} = \frac{1}{k_0[\text{H}_2\text{O}_2]} + \frac{1}{k_1[\text{I}^-]} \quad 2.25$$

where

$$v = \frac{dA_{353}/dt}{\epsilon_{353}} \left(1 + \frac{1}{K_I [I^-]_0} \right) \quad 2.26$$

From equation 2.24, where v is the initial velocity, $[HRP]_0$ is the initial concentration of HRP and $[I^-]_0$ is the initial iodide concentration, a plot of $[HRP]_0/v$ vs. $1/[I^-]$ should have a slope of $1/k_1$. The rate constants obtained from the steady-state experiments are compared to the second-order rate constants measured for the reactions of HRP-I and HRP-II in Table 2.04. At every pH the value of k_1 obtained from the steady-state measurements is much larger than the rate constant for the reaction of HRP-II, but a factor of 3 or 4 smaller than the rate constant for the reaction of HRP-I. We believe that the rate measured by the steady-state technique is smaller than that measured directly for the reaction of HRP-I with iodide because of the spontaneous decomposition of HRP-I to HRP-II that is occurring during the reaction cycle described by equations 2.23 and 2.24. The reaction of HRP-II with iodide is sufficiently slow that an accumulation of HRP-II occurs, effectively reducing the concentration of HRP available to maintain the enzymatic cycle and thus reducing the apparent value of k_1 . From analogous reasoning the rate constant for HRP-I formation would be expected to be low under the same experimental conditions. Fig. 2.10 illustrates the Lineweaver-Burk plot obtained at pH 4.0. The intercept of

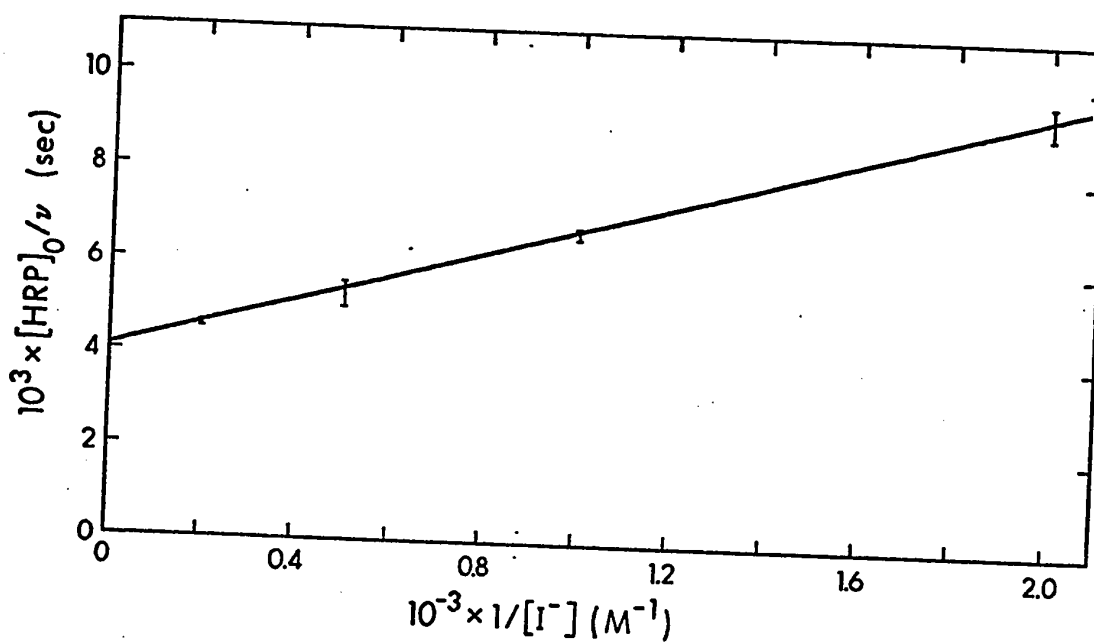


Fig. 2.10: Plot of $[\text{HRP}]_0/v$ vs. $1/[\text{I}^-]$ at pH 4.0. The concentration of hydrogen peroxide was 6.5×10^{-5} M and $[\text{HRP}]_0$ was 9.2×10^{-9} M. The solid line was calculated by a weighted linear least-squares analysis. The slope with its standard error is $(2.6 \pm 0.1) \times 10^{-6}$ M-sec with an intercept of $(4.1 \pm 0.2) \times 10^{-3}$ sec.

Table 2.04

Comparison of Rate Constants Measured Directly and by
the Steady-State Method for the HRP-Catalyzed
Oxidation of Iodide

pH	Second-Order Rate Constants		
	HRP-I + I ⁻ ^a (M ⁻¹ sec ⁻¹)	HRP-II + I ⁻ ^b (M ⁻¹ sec ⁻¹)	Steady State (M ⁻¹ sec ⁻¹)
4.01	9.9×10^5	1.0×10^4	3.8×10^5
5.41	1.7×10^5	4.4×10^2	5.1×10^4
6.99	5.1×10^3	1.2×10	1.2×10^3

^aRate constants interpolated from Fig. 2.02.

^bRate constants interpolated from Fig. 2.06.

this plot can be used to calculate a value for k_0 of $3.8 \times 10^6 \text{ M}^{-1}\text{sec}^{-1}$, which is a factor of 3 or 4 lower than the value of k_0 measured directly at this pH (Dolman and Dunford, 1972). To check that the low values of k_0 and k_1 were not due to a systematic error in the calculations, the steady-state experiments were repeated at pH 4.0 with a high concentration of iodide and a low concentration of hydrogen peroxide. Under these conditions equation 2.25 takes the form

$$\frac{[\text{HRP}]_0}{v} = \frac{1}{k_0 [\text{H}_2\text{O}_2]} \quad 2.27$$

which can be rearranged to give

$$v = - \frac{d[\text{H}_2\text{O}_2]}{dt} = k_0 [\text{H}_2\text{O}_2] [\text{HRP}]_0 \quad 2.28$$

Equation 2.28 predicts that the observed reaction will be first order in hydrogen peroxide. This prediction was borne out by the linear plot of the change in absorbance at 353 nm vs. time. The value of k_0 calculated from the slope of this line, for an iodide concentration of 0.1 M, an HRP concentration of 9.2×10^{-9} M and a hydrogen peroxide concentration of 6.5×10^{-6} M, was $3.8 \times 10^6 \text{ M}^{-1}\text{sec}^{-1}$ in exact agreement with the value obtained from the intercept.

The fact that the value of k_0 agrees using the two different calculations indicates that the only possibility for a systematic deviation in the calculation of k_0 and k_1 must be related to $[\text{HRP}]_0$. It is possible with the low

concentration of HRP used in the steady-state studies that a portion of the enzyme could be deactivated resulting in the observed values for k_0 and k_1 . To check this possibility, the steady-state kinetics were studied as a function of $[\text{HRP}]_0$ at pH 7.0. The plot of the change in absorbance at 353 nm vs. $[\text{HRP}]_0$, illustrated in Fig. 2.11, is a straight line with a zero intercept, indicating that the reaction is first order in HRP at the concentrations used for the steady-state studies.

There appears to be reasonable evidence to indicate that the values of k_0 and k_1 are low due to the formation of a small concentration of some HRP-II under steady-state conditions. The HRP-II could be formed by the spontaneous decay of HRP-I to HRP-II which is observed under non-steady-state conditions, or it could also be formed through a reaction with HRP-I as indicated in equation 1.02. If the HRP-II is formed from such a reaction, it must be a secondary pathway for the reaction of HRP-I with iodide since the majority of the HRP-I goes directly to HRP. The latter possibility was suggested by Björkstén (1970) as an explanation for results he obtained from a study of the HRP-catalyzed oxidation of iodide. In order to test which of these two possibilities was more reasonable as a source of HRP-II, a sufficiently high initial concentration of HRP was employed to ensure that the spectra of the enzymatic species present in the steady state could be observed.

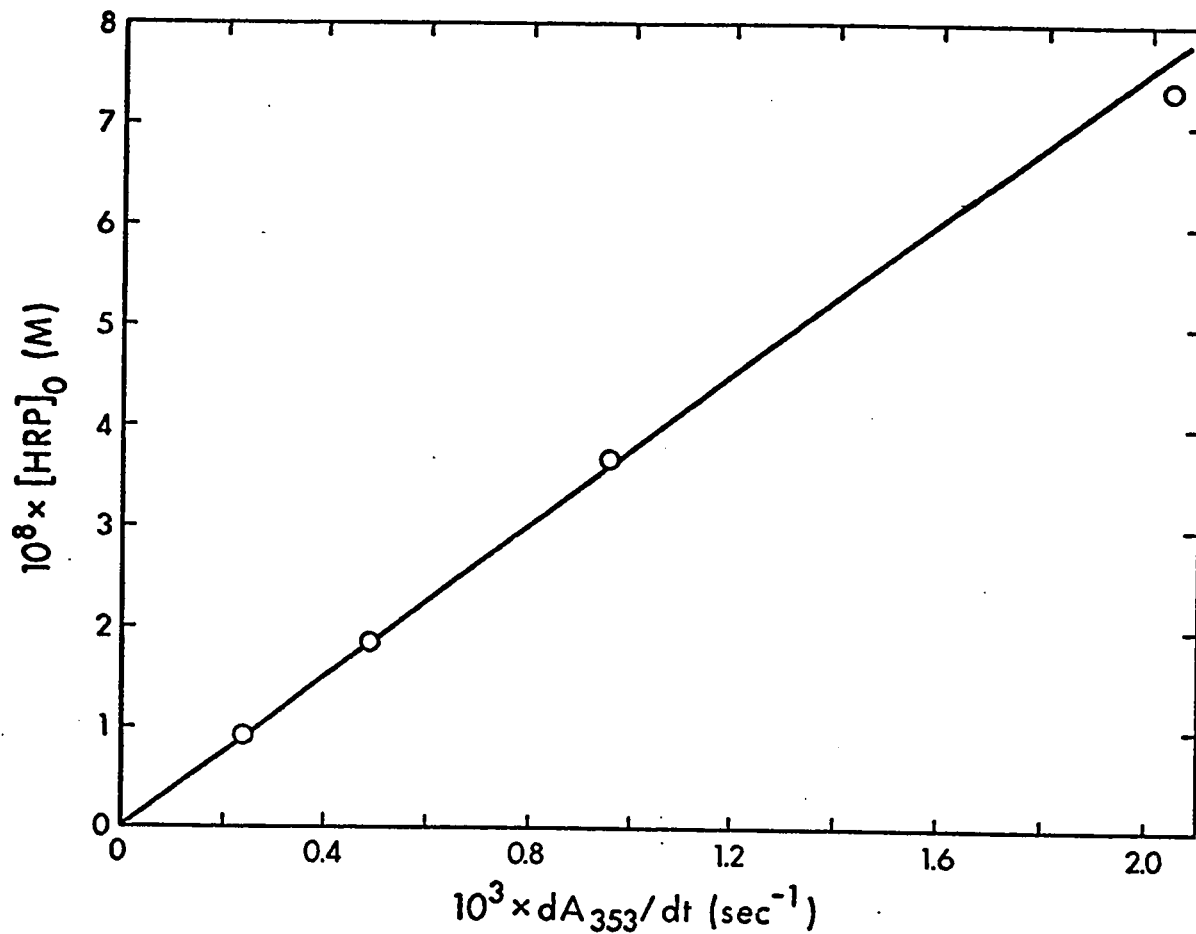


Fig. 2.11: Plot of $[\text{HRP}]_0$ vs. $\frac{dA_{353}}{dt}$ at pH 7.0. The concentration of hydrogen peroxide was 3.2×10^{-5} M and the concentration of potassium iodide was 1.0×10^{-2} M.

These reactions were performed at pH 8.4 so that there would be no interference from the production of iodine. Fig. 2.12 illustrates three such experiments; in all three cases the reaction was initiated by the addition of hydrogen peroxide to a final concentration of 6.5×10^{-4} M to a solution of 4.3×10^{-6} M HRP, iodide and buffer. In Fig. 2.12a the reaction was monitored at 411 nm, the isosbestic point between HRP-II and HRP, thus changes in absorbance observed at this wavelength should reflect changes only in the concentration of HRP-I. The rapid drop in absorbance at time zero in Fig. 2.12a represents the conversion of HRP to HRP-I. The slow increase in absorbance that levels off after about two minutes is most probably due to the formation of HRP-II. The level section from two to eight minutes indicates that the concentrations of HRP-I and HRP-II are relatively invariant during this period. The rapid increase in absorbance after eight minutes, to an absorbance approaching that of the original HRP solution is due to the reaction of HRP-I with iodide when all the hydrogen peroxide present in solution has been consumed. The absorbance after eight minutes is constant, as would be expected for a mixture of HRP and HRP-II monitored at 411 nm. Fig. 2.12b illustrates the same reaction monitored at 430 nm. The absorbances of HRP-I and HRP-II are very similar at 430 nm, thus there will be only a slight contribution from these species and the majority of the absorbance change can be attributed to HRP-II. From time zero, the absorbance in

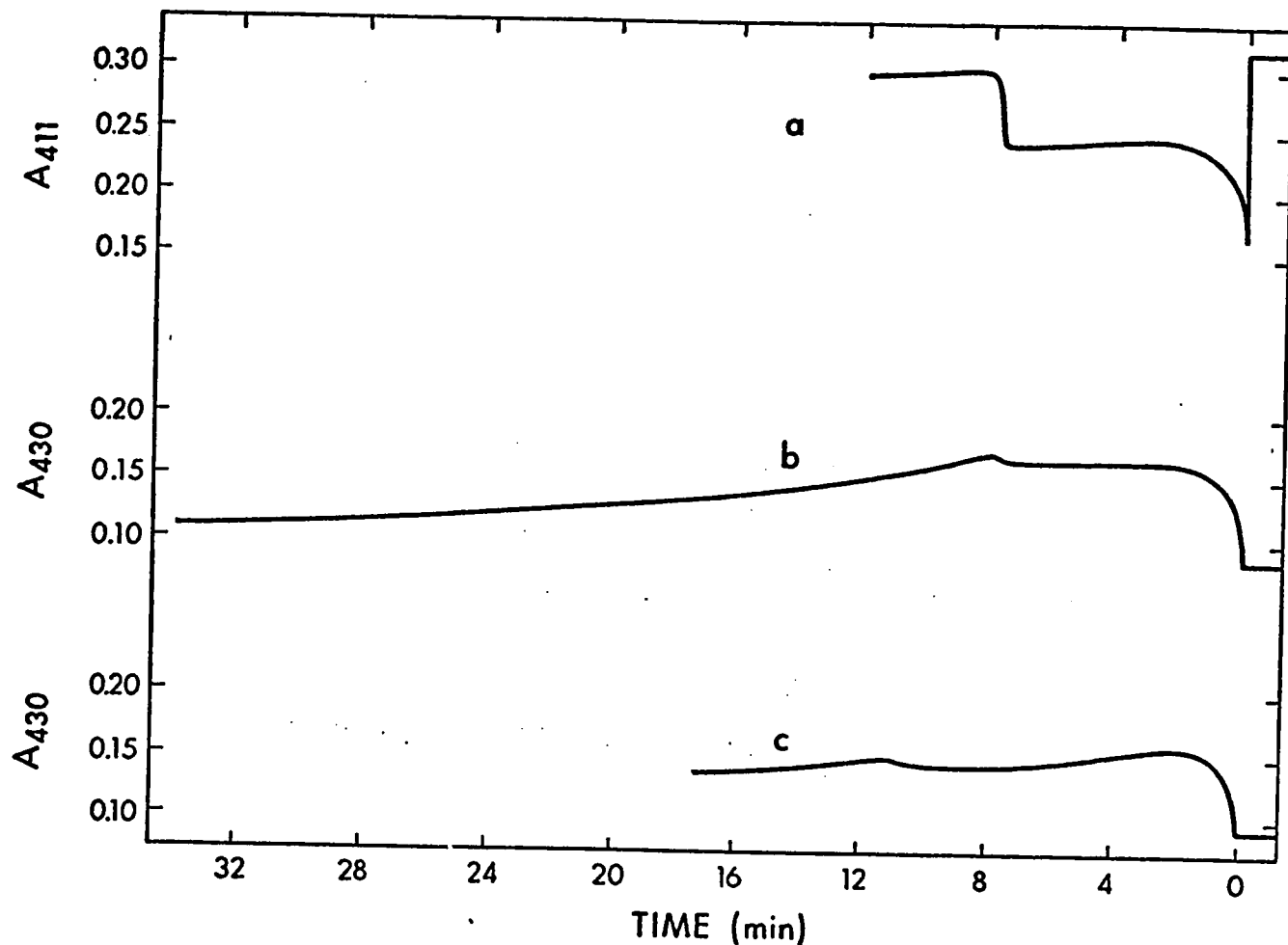
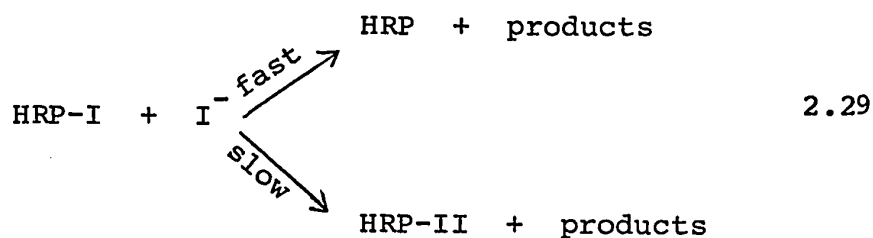


Fig. 2.12: Experimental traces of absorbance vs. time resulting from the addition of hydrogen peroxide to a solution of HRP and iodide at pH 8.4. In the three cases hydrogen peroxide was added to a final concentration of 6.5×10^{-4} M. In (a) the reaction was monitored at 411 nm with an iodide concentration of 1.0×10^{-3} M. In (b) and (c) the reaction was monitored at 430 nm with iodide concentrations of 1.0×10^{-3} M and 2.5×10^{-4} M respectively.

Fig. 2.12b increases at a similar rate to the increase at 411 nm confirming the production of HRP-II. The mixture of HRP-I and HRP-II existing from two to eight minutes is also shown by the level section in Fig. 2.12b. The small increase in absorbance at eight minutes corresponds to the reaction of HRP-I when the excess hydrogen peroxide is consumed as observed in Fig. 2.12a. The exponential decrease in absorbance from 8 to 32 minutes observed in Fig. 2.12b represents the slow reaction between HRP-II and iodide. At this pH the rate constant for the reaction of HRP-I with iodide is 500 times that for the reaction of HRP-II. Although Fig. 2.12a and 2.12b confirm the slow transition from HRP-I to HRP-II in the steady state, they do not distinguish between the two possible modes of formation of HRP-II. If the formation of HRP-II were due to a competing reaction between HRP-I and iodide as illustrated by the mechanism



then the concentration of HRP-II produced in the steady state would be independent of the concentration of iodide and hydrogen peroxide. Fig. 2.12c illustrates that this is not the case; by lowering the concentration of iodide or increasing the concentration of hydrogen peroxide the

amount of HRP-II, as measured by the increase in absorbance at 430 nm, is decreased. Thus the contribution of a competing reaction of HRP-I with iodide for the formation of HRP-II is negligible compared to the spontaneous decay of HRP-I.

The possibility of observing the spectra of enzymatic intermediates in steady-state concentrations provides a novel method for obtaining accurate spectra of these compounds. Fig. 2.13 illustrates what we believe is a more accurate spectrum of HRP-I than those previously reported in the literature. The spectrum in Fig. 2.13 was scanned over a period of time during which the HRP had completed six reaction cycles.

Since the spectrum was scanned under conditions where the spontaneous decay is significant, some HRP-II was formed during the time required to obtain the spectrum. The effect of this HRP-II formation was minimized in two ways (1) by scanning the spectrum rapidly, producing the spectrum shown by the solid line in Fig. 2.13 and (2) by observing the absorbance changes with time at single wavelengths and extrapolating to zero time. The spectrum of HRP-I obtained in the latter fashion is shown by the broken line in Fig. 2.13. The molar absorptivity values for the spectrum of HRP-I obtained by extrapolation of the steady-state results to zero reaction time are recorded in Table 2.05. Brill and Sandberg (1968) have published the molar absorptivity

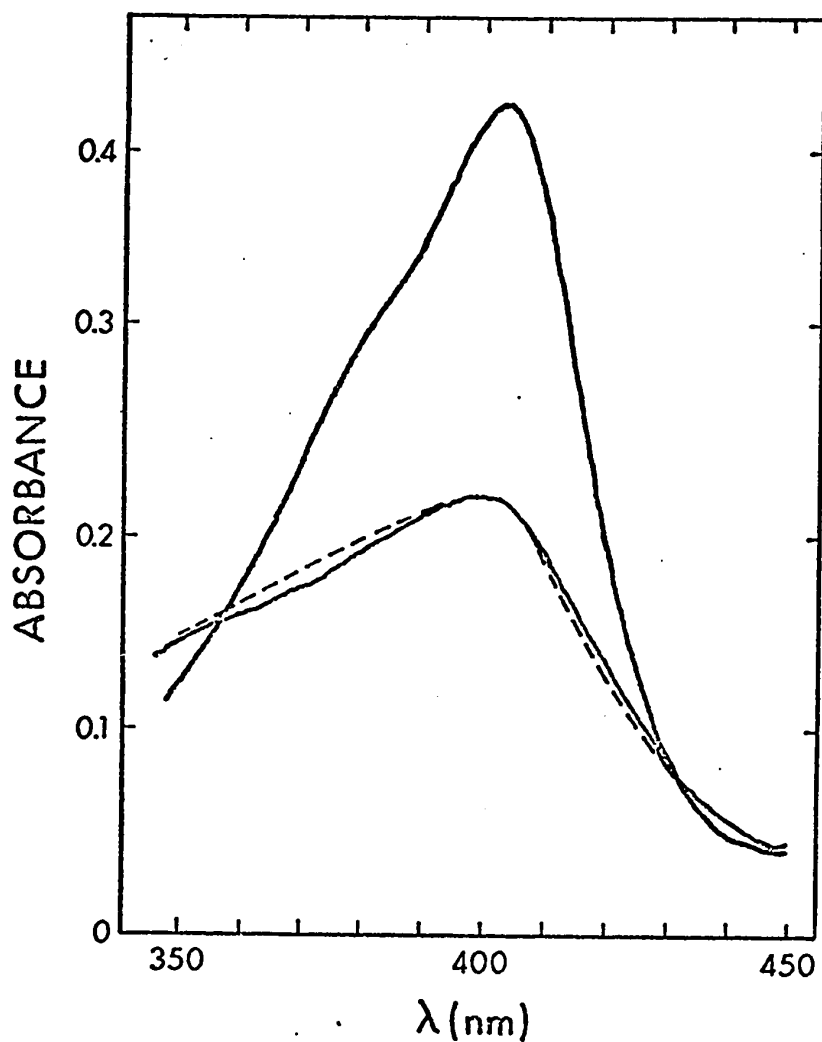


Fig. 2.13: Spectrum of HRP-I compared to the spectrum of HRP. The solid line represents the spectrum scanned over a period of 40 seconds following the addition of hydrogen peroxide to a solution of HRP and iodide. The broken line illustrates the corrected spectrum of HRP-I obtained by monitoring the reaction at each wavelength and extrapolating to zero time.

Table 2.05
Molar Absorptivity Values for the Spectrum of HRP-I^a

λ (nm)	$10^4 \times \epsilon$ (M ⁻¹ cm ⁻¹)
440	1.31
432	1.74
430	1.86
420	2.83
410	4.12
400	4.80
390	4.62
380	4.30
370	4.00
360	3.60
350	3.28

^aCalculated using a molar absorptivity value of 9.1×10^4 M⁻¹cm⁻¹ for HRP at 403 nm.

and wavelength of the Soret maximum which they use as criteria for the purity of HRP-I. The present value for the Soret maximum of 400 nm with molar absorptivity of $4.8 \times 10^4 \text{ M}^{-1} \text{ cm}^{-1}$ indicates that our HRP-I is slightly more pure than their sample. In addition the present study shows the existence of the isosbestic points between HRP-I and HRP at 432 and 357 nm which are more sensitive to small concentrations of HRP-II than is the Soret maximum.

Stoichiometry Measurements

It has been established that the overall stoichiometry of the HRP-catalyzed reaction between hydrogen peroxide and iodide is described by the equation



under conditions where the hydrogen peroxide concentration is much larger than the concentration of HRP (Björkstén, 1968). The validity of equation 2.30, under conditions where the concentrations of HRP and hydrogen peroxide are similar, was verified by measuring the iodine production at 353 nm on the Cary 14 spectrophotometer; the results are illustrated in Fig. 2.14. The solid line in Fig. 2.14 was calculated assuming a 1:1 equivalence between hydrogen peroxide and iodine using the formula

$$\Delta A_{353} = \frac{[\text{H}_2\text{O}_2]}{\epsilon_{353}} \left(1 + \frac{1}{K_I [\text{I}^-]} \right) \quad 2.31$$

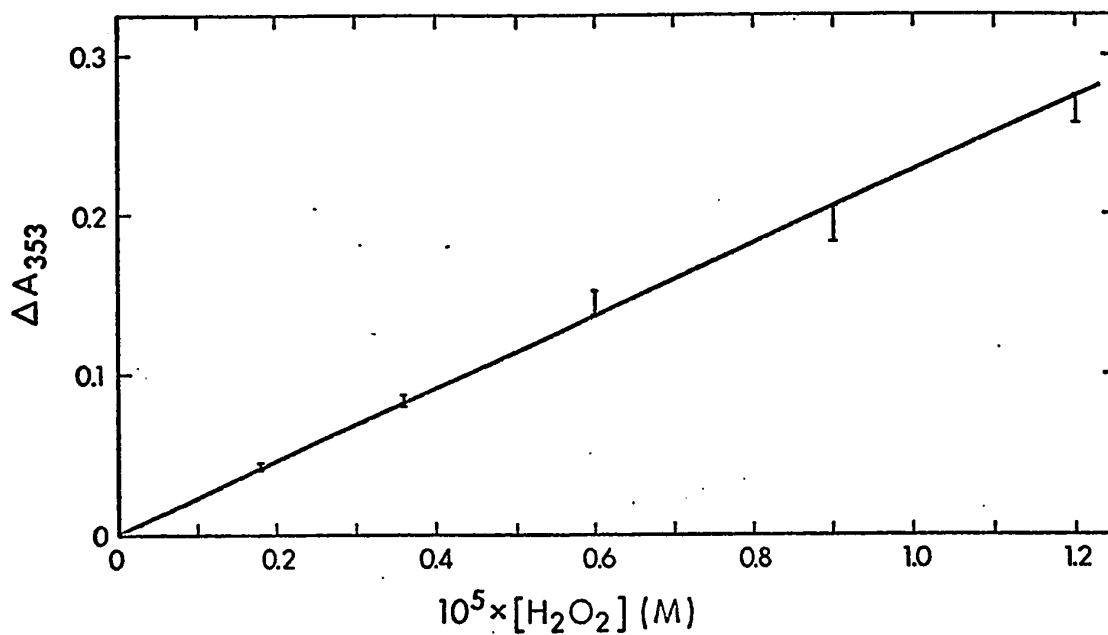


Fig. 2.14: Plot of the change in absorbance at 353 nm vs. the concentration of hydrogen peroxide. The solid line was calculated assuming a 1:1 equivalence between hydrogen peroxide and iodine using the formula

$$\Delta A_{353} = \frac{[\text{H}_2\text{O}_2]}{\epsilon_{353}} \left(1 + \frac{1}{K_I [\text{I}^-]} \right)$$

The linear relation in Fig. 2.14 offers conclusive proof that iodine is not incorporated into the enzyme on the time scale of our experiments, even when the enzyme is present in large excess compared to the concentration of iodine produced.

A titration of HRP-I with iodide was performed by monitoring the absorbance changes at 411 nm resulting from the addition of various concentrations of iodide to a solution of HRP-I. The results of the titration are illustrated in Fig. 2.15. The solid line was calculated assuming a 1:1 equivalence between HRP-I and iodide using a difference in molar absorptivity of $3.6 \times 10^4 \text{ M}^{-1} \text{ cm}^{-1}$ interpolated from Fig. 2.13. The results of the titration of HRP-I with iodide indicate that the reaction



requires a 1:1 ratio of the two reactants.

A titration of HRP-II with iodide was also performed. The results of the titration, as illustrated in Fig. 2.16, had a larger error than those for HRP-I because the HRP-II-iodide reaction was much slower than the reaction of HRP-I. The solid line in Fig. 2.16 was calculated assuming a 1:1 equivalence between HRP-II and iodide using a difference in molar absorptivity of $5.5 \times 10^4 \text{ M}^{-1} \text{ cm}^{-1}$ interpolated from the spectrum of HRP-II measured at pH 4.2 (Critchlow and Dunford, 1972b). The results of the titration indicate that the reaction

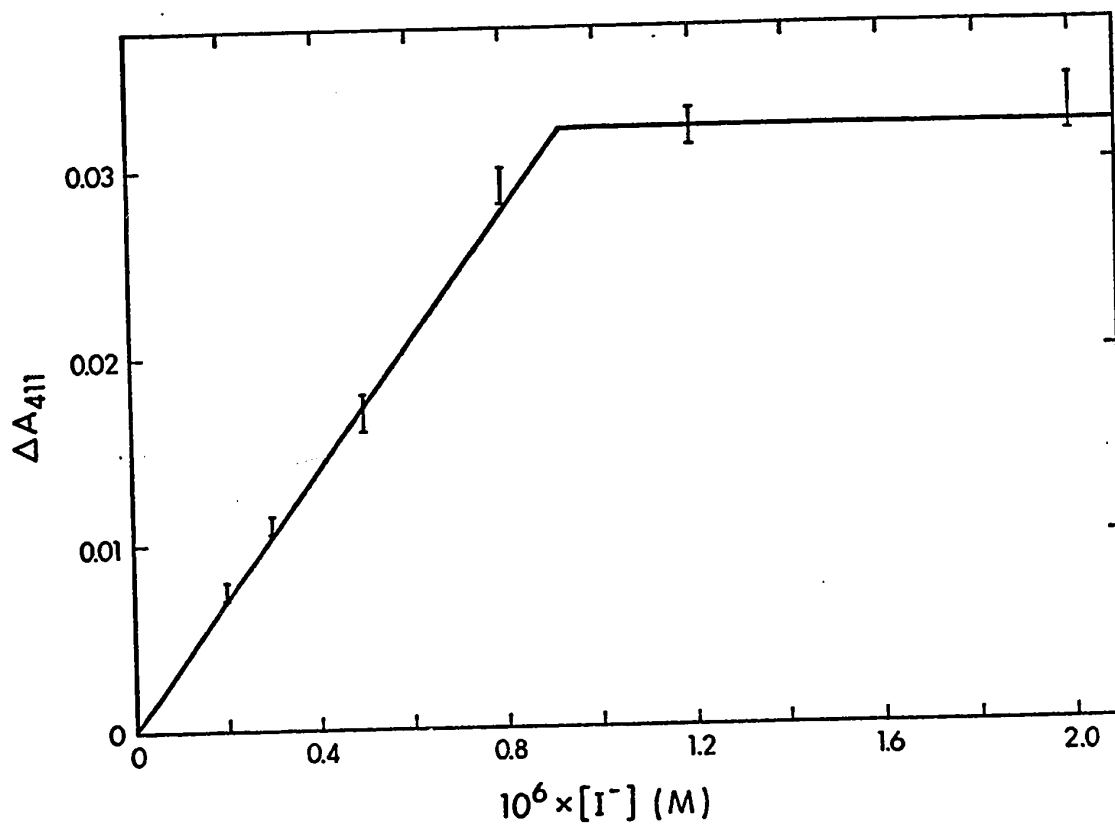


Fig. 2.15: Plot of the change in absorbance at 411 nm vs. the concentration of iodide for the titration of HRP-I with iodide. The solid line was calculated assuming a 1:1 equivalence between HRP-I and iodide using a difference in molar absorptivity of $3.6 \times 10^4 \text{ M}^{-1} \text{ cm}^{-1}$ interpolated from Fig. 2.13.

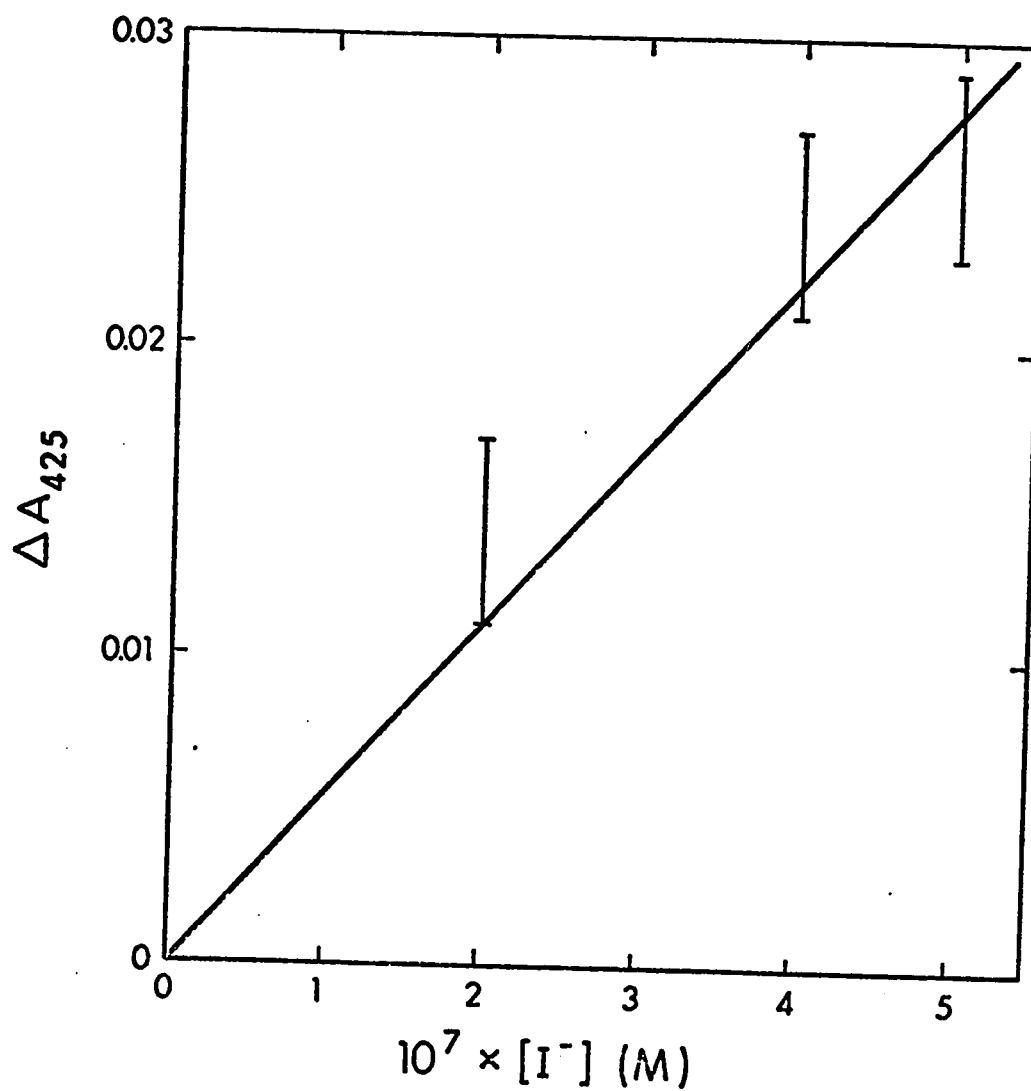
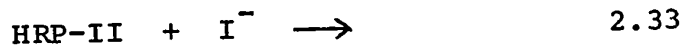


Fig. 2.16: Plot of the change in absorbance at 425 nm vs. the concentration of iodide for the titration of HRP-II with iodide. The solid line was calculated assuming a 1:1 equivalence between HRP-II and iodide using a difference in molar absorptivity of $5.5 \times 10^4 \text{ M}^{-1} \text{ cm}^{-1}$ interpolated from the spectrum of HRP-II measured at pH 4.2 (Critchlow and Dunford, 1972b).

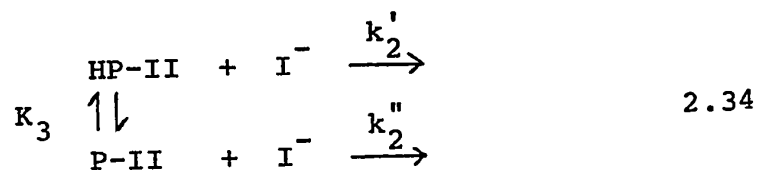


also proceeds with a 1:1 ratio of the two reactants.

2.04 Discussion

Kinetics

Since the pH dependence of the reaction between HRP-II and iodide is simpler than the reaction with HRP-I it will be discussed first. It has been shown that a protonation of iodide could not be responsible for the slope of -1 on the plot of $\log k_2$ vs. pH. The kinetic results can therefore be explained if HRP-II exists in two forms with the protonated form reacting much more rapidly than the unprotonated form with iodide. This reaction mechanism can be written in general terms as



where P-II and HP-II represent the two protonated forms of HRP-II related by the ionization constant K_3 and

$$k_2 = \frac{k_2'}{1 + \frac{K_3}{[\text{H}^+]}} + \frac{k_2''}{1 + \frac{[\text{H}^+]}{K_3}} \quad 2.35$$

Since the $\log k_2$ vs. pH plot has a slope of -1 over the pH range of the study, we can conclude that (1) the term involving k_2'' is negligible and (2) $\frac{K_3}{[\text{H}^+]} \gg 1$. The latter condition provides an estimate of the lower limit for K_3 ;

the lowest pH of the study is 2.7 which means that K_3 must be greater than 10^{-2} M. The maximum value of K_3 must be such that k_2' does not exceed the diffusion controlled limit. The combined effect of the above two conditions is to reduce equation 2.35 to

$$k_2' = \frac{k_2 [H^+]}{K_3} \quad 2.36$$

from which any point on the $\log k_2$ vs. pH plot can be used to calculate that $k_2' = 10^8 K_3$. Using the maximum value for the diffusion controlled limit of $10^{10} \text{ M}^{-1} \text{ sec}^{-1}$, the largest possible value for K_3 would be 10^2 . The minimum difference between k_2' and k_2'' can be estimated at the highest pH on the $\log k_2$ vs. pH plot. Assuming the minimum value for K_3 of 10^{-2} , the relative concentrations of P-II and HP-II at pH 9.0 indicate that k_2' must be at least 10^7 times greater than k_2'' .

As an explanation for the large difference between k_2' and k_2'' we postulate that the ionization characterized by K_3 must be that of a group that is bonded to the heme. We reason that a kinetic difference of this magnitude can only be explained in terms of a major electronic rearrangement in the environment of the iron upon ionization and that only a group that is bonded to the heme could cause this rearrangement. There appear to be three reasonable possibilities for ionizations which could exhibit this large kinetic effect. One is that an ionizable amino acid from the protein moiety, either a terminal or side chain group,

binds in one of the co-ordination positions of the iron. The large observed value of K_3 cannot define the nature of such a group since any ionizable amino acid bound to the iron would experience a substantial diminution in its pK_a value. A second possibility is the binding of a molecule that is not derived from the enzyme in a co-ordination position of the iron. This would most likely be a fragment of the peroxide or a hydroxide group from the aqueous solution. The final explanation is an ionization of a portion of the porphyrin ring. Such an ionization would most probably involve protonation of the nitrogen atoms in the pyrrole rings. It seems unlikely that the ionization of the propionic acid groups on the heme could produce large kinetic effects since these groups are not conjugated to the aromatic ring.

An important feature of the $\log k_2$ vs. pH plot is the absence of the kinetically important ionization at pH 8.6 that was observed for HRP-II in a similar study with ferrocyanide as a substrate (Cotton and Dunford, 1972). This recent study on the ferrocyanide reaction showed that the small effects attributed to two other ionizations on HRP-II in the oxidation of ferrocyanide (Hasinoff and Dunford, 1970) are within the error limits of the experiments. The plot of the logarithm of the second-order rate constant vs. pH for the reaction of HRP-II with ferrocyanide has a slope of -1 from pH 10.8 to 9.0, a ground state pK_a at 8.6, a transition state pK_a^\ddagger at 6.0 and a slope of -1 from pH 5.5 to pH 3.8.

If the rate determining steps for the reactions of HRP-II with iodide and ferrocyanide are the same, the different pH dependences for the two reactions cannot result from the ionization of a group at pH 8.6 that is bonded to the heme. A heme-bonded group would be a major factor in determining the electronic environment of the heme, thus its ionization would be expected to have a similar effect in all the reactions of HRP-II. We propose that the ionization of a heme-bonded group in the reaction between HRP-II and ferrocyanide, in analogy to the bonded group ionization proposed for the iodide reaction, results in the overall acid catalysis observed for the reaction, while the difference in the pH dependence for the two reactions results from a different sensitivity to the ionization of a group with pK_a 8.6 that is not bonded to the heme.

Because ferrocyanide is such a highly charged ion, it might appear that the difference between the kinetic pH dependences for the reactions of iodide and ferrocyanide could result from different electrostatic interactions for the two ions. There are three lines of evidence, however, to indicate that this is not the case. First, ferrocyanide being a more highly charged anion than iodide would be expected to be more sensitive than iodide to the ionization of groups on HRP-II capable of participating in electrostatic interactions, in accord with observation. However, the complete insensitivity of the iodide reaction to these ionizations must be considered evidence against

electrostatic interactions which exert their effect over large internuclear distances. Second, the second-order rate constant for the reaction of HRP-II with ferrocyanide is larger than the rate constant for the iodide reaction over the pH range of the two studies. The Hammond postulate predicts, for one step mechanisms, that there is a relation between the rates of analogous reactions and the position of the transition state along the reaction co-ordinate (Hammond, 1955). That is, for faster reactions the transition state more closely resembles the starting materials and thus occurs earlier along the reaction co-ordinate. In the present case, since the ferrocyanide reaction is more than 10^4 times faster than the iodide reaction at pH 9, the ferrocyanide-HRP-II transition state would be expected to be formed earlier along the reaction co-ordinate than the iodide-HRP-II transition state. Thus the HRP-II-ferrocyanide reaction would be expected to be less sensitive to any general electrostatic interactions than the HRP-II-iodide reaction, contrary to the observed results.

The third factor against the involvement of electrostatic interactions is a consequence of the interpretation of the pH dependence of the reaction of HRP-II with ferrocyanide that is possible when the inflections in the plot of the logarithm of the second-order rate constant vs. pH are considered to reflect either ground state or

transition state ionizations. Using the transition state treatment the reaction of HRP-II and iodide would be interpreted in terms of a transition state pK_a^\ddagger the value of which is higher than that of the highest pH of the study and a ground state pK_a that is lower than the lowest pH. Thus for the iodide reaction, the value of $pK_a^\ddagger - pK_a$ is large and positive indicating that the reaction is very sensitive to a rate accelerating protonation. If the reactions of HRP-II with ferrocyanide and iodide proceed via the same mechanism then a kinetically important ionization of a heme-bonded group in the reaction of HRP with iodide must also be important for the ferrocyanide reaction. Thus the overall acid catalysis observed for the HRP-II-ferrocyanide reaction would be the result of a large position value for a $pK_a^\ddagger - pK_a$ difference like that observed for iodide with both the ground and transition state pK_a values outside the pH range of the study. The ground state pK_a observed at 8.6 and transition state pK_a at 6.0 observed for the ferrocyanide reaction can be thought of as being superimposed on the overall acid catalysis resulting from a large positive $pK_a^\ddagger - pK_a$ difference. With this interpretation for the overall acid catalysis the pK_a at 8.6 would be paired with the pK_a^\ddagger at 6.0, that is the protonation of the group of pK_a 8.6 would be rate inhibiting since the $pK_a^\ddagger - pK_a$ difference is negative. Even if the group at pH 8.6 were paired to an unobserved pK_a^\ddagger at high pH, consideration of all

the possible pairing schemes for the new pK_a 's and pK_a^\ddagger 's indicate that at least one pairing must result in a value for the $pK_a^\ddagger - pK_a$ that is negative with a minimum value of -2.6. An electrostatic interpretation would predict that the protonation of any group would increase the rate of reaction since the added positive charge would tend to make the enzyme a better oxidizing agent in addition to increasing its affinity for a highly charged anion. Thus the fact that at least one ionization observed in the HRP-II-ferrocyanide reaction must be rate inhibiting indicates that simple electrostatic interactions do not offer a sufficient explanation for the difference in the kinetic pH dependences for the reactions of HRP-II with iodide and ferrocyanide.

The difference between the two pH profiles must be the result of a specific interaction between an ionizable group on the enzyme with a pK_a value of 8.6 and the particular substrate. We believe that there are two possible explanations for the kinetic effects resulting from the ionization of this non-heme-bonded group that are based on the fact that iodide is a smaller more weakly hydrated anion than ferrocyanide. The first possibility is that ferrocyanide could participate in hydrogen bond formation to the group of pK_a 8.6 whereas iodide does not. Thus ionization of this group would alter the rate for the ferrocyanide reaction but not that for iodide. The alternative possibility is that the ionization of the non-heme-bonded group could cause

small conformational changes in the tertiary structure of the active site of HRP-II that could result in a steric interaction with ferrocyanide but not with iodide. These explanations for the difference in the kinetic pH profiles for the two reactions are based on the premise that both reactions have the same mechanisms over the entire pH ranges of the two studies, a reasonable assumption considering the similarity in the overall acid catalysis for the two reactions. Another explanation for this difference has been proposed by Critchlow and Dunford (1972b) based on the assumption that the HRP-II-ferrocyanide reaction undergoes a change in mechanism from alkaline to acidic pH. This mechanism has been extensively discussed in relation to the reaction of HRP-II with p-cresol and will not be repeated here.

In alkaline solution the plot of $\log k_1$ vs. pH for the HRP-I-iodide reaction has a slope of -1, the same behavior observed for the HRP-II-iodide reaction. The difference between the kinetic pH profiles for the two reactions is that HRP-I exhibits a rate influencing ionization with a pK_a value of 4.6 that has no observable effect on the rate of the HRP-II reaction. Otherwise the pH profiles are similar and this similarity suggests that a mechanism of the type proposed for the HRP-II-iodide reaction involving a large positive $pK_a^\ddagger - pK_a$ might also be operative for the HRP-I-iodide reaction. It would be of great interest to determine whether the group of pK_a 4.6 is a heme-bound group or a non-heme-bonded group with a small inhibiting effect on the overall acid catalysis.

This problem amounts to distinguishing between the two possible mechanisms for the HRP-I-iodide reaction described previously. On the basis of kinetic evidence only, a choice between the two mechanisms can be accomplished only if one of the mechanisms can be shown to require a rate constant that exceeds the diffusion controlled limit.

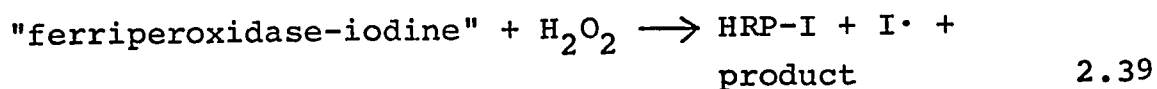
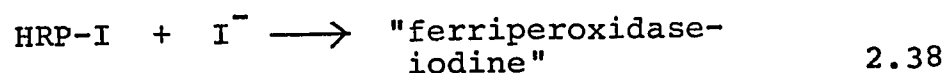
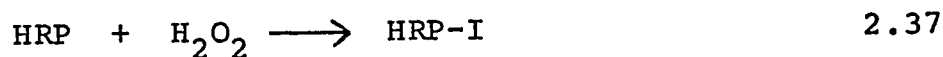
If the ionization corresponding to the pK_a value of 4.6 is not that of the heme bound group, then the heme-bound group must have a smaller pK_a value. The analysis of the pH dependence for the HRP-I-iodide reaction illustrated by the solid line in Fig. 2.02 was calculated assuming that any enzyme pK_a less than 4 did not influence the observed reaction. That is, extrapolation of the solid line to lower pH than indicated in Fig. 2.02 would result in a slope of -1 on the $\log k_1$ vs. pH plot, as is observed in the alkaline region. The low pH region could have been analyzed with an additional ground state pK_a , however the experimental data did not warrant the inclusion of an additional parameter. Such a pK_a value at low pH would indicate the minimum value possible for the dissociation constant of a heme-bound group. From the experimental points illustrated in Fig. 2.02, the minimum pK_a for such a group would be approximately 3.

Using a method similar to that used to define k_2' and k_2'' for the HRP-II-iodide reaction, a pK_a value of 3 for the heme-bound group would only require a rate constant of approximately $5 \times 10^7 \text{ M}^{-1} \text{ sec}^{-1}$, thus the diffusion controlled limit cannot aid in distinguishing the two mechanisms.

If the heme-bound group had a pK_a value which was within the pH range accessible for kinetic studies, its ionization would be expected to influence the observed kinetic pH profile for every substrate in its reaction with HRP-I. Thus the absence of a kinetic effect at pH 4.6 for any substrate would be a good indication that this group was not the heme-bound group. This fact increased the importance of the comparison of the pH dependence of the HRP-I iodide reaction to that previously observed for ferrocyanide. The plot of the logarithm of the second-order rate constant for the HRP-I-ferrocyanide reaction is pH independent from pH 11.3 to 7.5, has a transition state pK_a^\ddagger of 6.4, a ground state pK_a of 5.3 and a second transition state pK_a of 4.4. As will be described in more detail later, the pK_a of 5.3 for the ferrocyanide reaction and 4.6 for the iodide reaction agree within the experimental error of the two studies, thus comparison of the kinetic pH dependences for these two substrates cannot further elucidate the nature of this group. The fact that the second-order rate constant for the HRP-I-ferrocyanide reaction is pH independent in the alkaline region while the plot of $\log k_1$ vs. pH in the same pH region has a slope of -1 for the HRP-I-iodide reaction indicates that whatever the pK_a value of the heme-bound group, the acceleration in rate resulting from its protonation is much less for ferrocyanide than for iodide.

Reaction Sequence of the HRP-I-Iodide Reaction

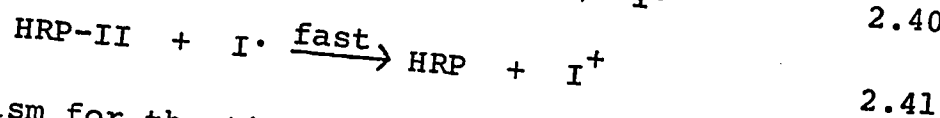
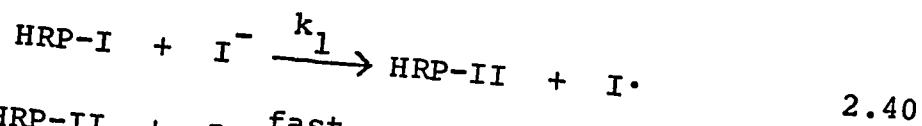
Substantial evidence has been presented to indicate that the reaction of HRP-I with iodide forms HRP without the intermediate formation of HRP-II. Iodide is the first substrate of HRP that has been shown to deviate from the reaction mechanism illustrated in equations 1.01 - 1.04, although it has been reported that compound I of catalase can oxidize various substrates including alcohols, formic acid and nitrite without the involvement of catalase compound II (Brill, 1966). This observation of the unique nature of the HRP-I-iodide reaction was first suggested by Björkstén (1970) who reported that the HRP-catalyzed oxidation of iodide proceeds primarily via HRP-I, with HRP-II contributing at most 2% of the oxidized iodide. Björkstén considered that the HRP-II was formed from a secondary reaction between HRP-I and iodide. We have presented evidence, however, to indicate the formation of HRP-II is more likely due to the spontaneous decay of HRP-I. The mechanism Björkstén proposes for the reaction of the main pathway is



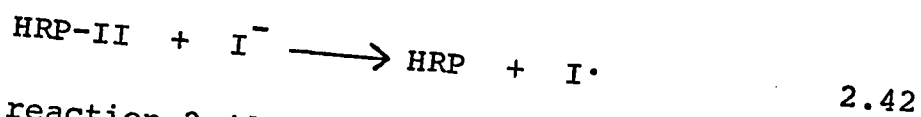
Björkstén observed the spectrum of the "ferriperoxidase-iodine" complex at an iodide concentration equal to the concentration of HRP-I. Under conditions of high iodide concentration we have never observed such a complex. Fig. 2.14 illustrates that the concentration of iodine produced is the same as the concentration of hydrogen peroxide used to form HRP-I, even when the iodine concentration is considerably less than the concentration of HRP. This provides clear evidence that under conditions of high iodide concentration there can be no incorporation of any form of iodine into HRP. In addition, since the "ferriperoxidase-iodine" complex is formed slowly compared to the reaction of HRP-I with iodide, the complex may not play an important role in the catalytic cycle. For example at pH 6.2 under conditions where Björkstén observed the "ferriperoxidase-iodine" spectrum, the reaction between HRP-I and iodide is 88% complete in 10 seconds (calculated using a rate constant interpolated from Fig. 2.02) while measurements of the absorbance of the complex spectrum were made after six minutes.

Björkstén included atomic iodine in the reaction mechanism as a result of an attempted correlation with evidence involving the oxidation of oxalate ion. From our results the 1:1 ratio between H_2O_2 and I_2 in the stoichiometry of the overall reaction, the 1:1 ratio between HRP-I and iodide in reaction 2.32 and the direct conversion of HRP-I to HRP indicate that if the reaction between HRP-I

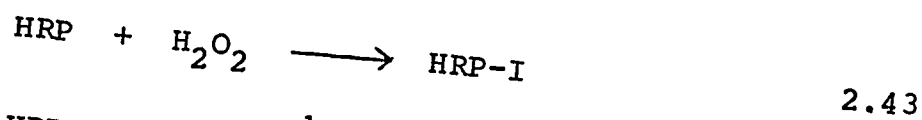
and iodide produces atomic iodine, then the reaction must proceed via a mechanism



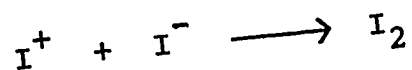
The mechanism for the titration of HRP-II with iodide would then become



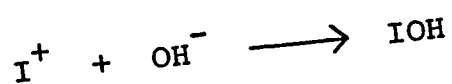
followed by reaction 2.41, which predicts that HRP-II and iodide would react in a 2:1 ratio. This is contrary to the results observed for the titration of HRP-II with iodide illustrated in Fig. 2.16. A reaction mechanism that is consistent with our results is



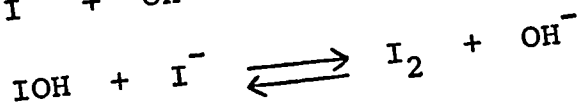
where I^+ does not necessarily exist in solution. As pointed out by Brill (1966), a distinction cannot be made between a simultaneous two-electron transfer and the formation of a transient enzyme-free-radical complex unless the decomposition of such a complex can be shown to be rate limiting under conditions of high substrate concentration. If excess iodide is present in the solution, the production of iodine can formally be accounted for by the rapid reactions



2.45



2.46



2.47

(Cotton and Wilkinson, 1966). If iodide is not present in excess the IOH or its degradation products could account for the slow reaction to form the "ferriperoxidase-iodine" complex.

The oxidation of oxalate observed by Björkstén could be explained if the reaction between HRP-I and iodide proceeds via the formation of an I^+ -iron complex which is a sufficiently powerful oxidizing agent to react with oxalate. Such a complex could provide a rationale for the involvement of peroxidases in the catalysis of iodination reactions.

CHAPTER 3

Oxidation of Sulfite by Horseradish
Peroxidase Compounds I and II

3.01 Introduction

HRP has been observed to have both peroxidatic (Yang, 1970) and oxidatic (Klebanoff, 1961) activity in the oxidation of sulfite. An appreciable oxidase activity for HRP is only observed in the presence of both Mn^{++} ions and phenolic compounds. The reaction between sulfite and oxygen is initiated by free radicals (Abel, 1951), and Yang has suggested that the production of a phenolic radical by a HRP- Mn^{++} system is the basis for the oxidase activity. The HRP-catalyzed reaction between hydrogen peroxide and sulfite was also accelerated by the addition of phenols (Fridovich and Handler, 1961), in agreement with Yang's proposal since the oxidation of phenols under these conditions has been shown to produce free radicals (Caldwell and Steelink, 1969). A detailed study of the kinetics of the HRP-catalyzed reaction between hydrogen peroxide and sulfite has not been reported in the literature.

The oxidation of sulfite by a variety of inorganic oxidizing agents has been studied. For oxidizing agents capable of accepting two electrons, such as hydrogen peroxide, chlorine and bromine, the sulfite oxidation proceeds via a two electron transfer with the formation of

one equivalent of sulfate for every equivalent of oxidizing agent (Higginson and Marshall, 1957). The products resulting from one-electron oxidizing agents are mixtures of dithionate formed by radical combination and sulfate formed by radical disproportionation or further radical oxidation. In the reaction between hydrogen peroxide and sulfite, sulfite has been shown to accept both oxygen atoms from oxygen-18 labelled hydrogen peroxide (Halperin and Taube, 1952). This surprising result lead the authors to postulate a persulfurous acid intermediate for the reaction.

The reaction between HRP-I and iodide was the first reaction observed which involved a direct two electron transfer from substrate to HRP-I with the resulting formation of HRP. Since this phenomenon is of potential relevance to the mechanism of iodide oxidation in the thyroid gland, it was felt that the investigation of a second substrate reacting with the same mechanism might more completely define the nature of this reaction. Sulfite was chosen as a substrate because it was thought that HRP-I, in analogy to the inorganic oxidizing agents, might also oxidize sulfite via a direct two electron transfer.

3.02 Experimental

Materials

Horseradish peroxidase was obtained from Boehringer-Mannheim as a highly purified suspension in aqueous ammonium sulfate and was dialyzed and passed through a Millipore

filter prior to use. The concentration of the enzyme was determined as described previously.

Anhydrous sodium sulfite, with stated purity of 99.0%, was obtained from Fisher Scientific Co. Stock solutions of 0.1 M or greater were prepared fresh daily and were routinely analyzed by the method of Seo and Sawyer (1964). These authors observed that SO_2 has a molar absorptivity of $3.88 \times 10^2 \text{ M}^{-1} \text{ cm}^{-1}$ at 276 nm in solutions of 0.1 M sulfuric acid. The wavelength maximum and molar absorptivity vary with changing concentrations of sulfuric acid, thus care must be taken in this analysis to duplicate accurately the experimental conditions of these authors. Seo and Sawyer were able to analyze solutions with concentrations as high as $2 \times 10^{-3} \text{ M}$ to an accuracy of 1% without special precautions to prevent the loss of SO_2 . The value of the molar absorptivity calculated from the present sulfite solutions prepared by weight agreed with the value reported by Seo and Sawyer to within 2%. These sulfite solutions were found to decompose less than 1% over a period of eight hours. The effect of sodium sulfite on the final pH of the reacting solutions was minimized by bringing the sulfite solutions to the approximate pH of the buffer with sulfuric or nitric acid.

Hydrogen peroxide was obtained and stored as described previously. The concentration was determined by the HRP-catalyzed oxidation of iodide. Using this technique, hydrogen peroxide to a final concentration of approximately $6 \times 10^{-6} \text{ M}$

was added from a microliter syringe to 2.0 ml of solution containing 0.05 M potassium iodide, pH 4.0 acetate buffer of ionic strength 0.01 and approximately 10^{-8} M HRP. Several successive additions of hydrogen peroxide were performed and the resulting changes in absorbance due to triiodide ion formation were monitored at 353 nm. The absorbance changes were converted to concentrations using the molar absorptivity determined by Ramette and Sandford (1965). The concentration of hydrogen peroxide determined using the HRP-catalyzed oxidation of iodide was shown to be the same as that observed for the molybdate-catalyzed reaction (Ovenston and Rees, 1950) using the same experimental conditions.

Kinetic Experiments

The majority of the kinetic experiments for the reactions of both HRP-I and HRP-II were carried out on the stopped-flow apparatus using similar techniques and conditions to those described for the reaction of HRP-I and HRP-II with iodide. Because of the similarity in the rates for the reactions of HRP-I and HRP-II with sulfite, the HRP-II reaction was monitored at 427 nm, close to the isosbestic point between HRP and HRP-I. The HRP-I reaction was monitored at 411 nm, the same wavelength used to monitor the HRP-I-iodide reaction. The stopped-flow data were recorded in the form of a four figure digital print-out of the amplified photomultiplier voltage at 30 equally spaced

intervals of time. The details of this analog-to-digital converter are given in Appendix 4. The rate constants measured using the digital device and the photographic method described previously were shown to agree within experimental error (Critchlow and Dunford, 1972a). Kinetic experiments on the HRP-I-sulfite reaction at pH values greater than 5.5 were performed by monitoring the reaction, at 411 nm on the Cary 14 spectrophotometer, resulting from the addition of sodium sulfite to solutions of HRP-I prepared in the same fashion as those described for the HRP-I-iodide reaction also studied on the Cary 14. After reaction the solutions were collected for pH measurement, which was carried out with an Orion digital pH meter in conjunction with a Fisher combination electrode.

The rate of the air oxidation of sulfite was measured by monitoring the decrease in the sulfite absorbance at 212.5 nm on a Gilford spectrophotometer. A solution of 4×10^{-4} M sodium sulfite in pH 6.92 phosphate buffer of ionic strength 0.01 was left open to the atmosphere. The absorbance at 212.5 nm was reduced to half its initial value in approximately eight hours. The experiment was repeated on a solution containing 2×10^{-6} M HRP in addition to the sulfite. The decay of sulfite in the presence of HRP was almost the same as in its absence.

The kinetics of the reaction of HRP-II with sulfite were complicated by the presence of two additional reactions. When the HRP-II-sulfite reaction was monitored at 427 nm

the observed absorbance change was as expected for the conversion of HRP-II to HRP. However when the reaction was monitored at 411 nm, where no reaction of HRP-II should have been observable if HRP were the only product, a pronounced decrease in absorbance to a value about half that for native HRP was observed. The rate of decrease in absorbance at 411 nm corresponded to the decay rate of HRP-II observed at 427 nm. Monitoring the HRP-II-sulfite reaction at 411 nm also revealed a slower absorbance increase resulting in a final absorbance approaching that of native HRP. This second change in absorbance could not be detected at 427 nm. A reasonable explanation for these absorbance changes at different wavelengths is that the reaction of HRP-II and sulfite produces an intermediate enzyme species which decays to products more slowly than it is formed. The spectrum of this transient enzyme species must resemble that for HRP-I since a large decrease in absorbance is observed when its formation is monitored at 411 nm but not at 427 nm. Similarly the decay of the species can be observed at 411 nm but not at 427 nm. This decay was independent of sulfite concentration and pH over the range of conditions where it was observed. When the rate of formation of the species was sufficiently rapid that it could be considered part of the mixing, its decay proved to be a first-order reaction as judged by the linear plots of the change in absorbance vs. time. Because of

the transient nature of this species, its accurate spectrum could not be obtained.

The second reaction complicating the HRP-II-sulfite kinetics was very slow and could only be detected on the Cary 14 spectrophotometer as a slow decrease in absorbance at 427 nm. This reaction was also independent of sulfite concentration, since at sulfite concentrations high enough to observe the HRP-II-sulfite reaction on the stopped-flow apparatus no interference from this source could be detected. As a result of this fact, the kinetics of the HRP-II-sulfite reaction were studied exclusively on the stopped-flow apparatus. The total change in absorbance at 427 nm for this slow reaction was small, about 10% of that observed for the HRP-II-sulfite reaction at pH 7. However this change in absorbance resulting from the slow reaction was dependent on the concentration of native HRP. When HRP-II was formed with an excess of HRP present, so that a mixture of HRP and HRP-II with an approximate ratio of 1:1 existed, the total change in absorbance for this reaction at pH 7 increased by 80%.

Steady-State Spectra

The spectrum of the enzymatic species present in the steady state for the HRP-catalyzed oxidation of sulfite was determined using a technique similar to that used for the

HRP-catalyzed oxidation of iodide. For the HRP-sulfite system, the reaction was initiated by the addition of 1 μ l of 6.6×10^{-2} M hydrogen peroxide to 2.0 ml of a solution containing 5.1×10^{-6} M HRP and 5.0×10^{-6} M sodium sulfite in a pH 6.01 phosphate buffer of ionic strength 0.01. The spectrum of the resulting steady-state mixture was scanned on a Cary 14 spectrophotometer from 350-450 nm at a rate of 2.5 nm/sec. An identical experiment was performed with the absorbance monitored at 411 nm to ensure that steady-state conditions did exist during the time taken to scan the spectrum. The experiment monitored at 411 nm also indicated that the reaction had completed five reaction cycles during the time taken to scan the spectrum.

Second Ionization Constant of Sulfurous Acid

The second ionization constant of sulfurous acid at an ionic strength of 0.01 was measured spectrophotometrically using a Gilford spectrophotometer with the cell block maintained at 25.0°. The pH was maintained with six potassium dihydrogen phosphate-disodium hydrogen phosphate buffers over the range 6.12-7.50 and three sodium tetraborate buffers over the pH range 8.09-9.64. The buffers were also added to the reference solution. Absorbance measurements were made at 212.5 nm, close to the maximum absorbance for the sulfite ion.

3.03 Results

Second Ionization Constant of Sulfurous Acid

The second ionization constant of sulfurous acid, K_s , under conditions of the present work may be defined in terms of concentrations and the operational pH scale by the relation

$$pK_s = \log \frac{[\text{HSO}_3^-]}{[\text{SO}_3^{=}] } + \text{pH} \quad 3.01$$

The value of pK_s obtained from equation 3.01 was 6.92 ± 0.02 . Using the present spectroscopic method for measuring pK_s it was not possible to determine the value at an ionic strength of 0.11. Potassium nitrate, which was used to control ionic strength in the kinetic experiments, has an intense absorbance at 212 nm and, as a result, could not be used. Experiments were attempted using potassium chloride to maintain the ionic strength, however under these conditions the spontaneous decay of sulfite was sufficiently rapid to interfere with the determination of the ionization constant. This spontaneous decay of sulfite was likely due to the presence of a small amount of oxidizing agent in the chloride solution. Assuming the applicability of the Debye-Hückel limiting law, the value of pK_s calculated at an ionic strength of 0.11 is 6.70.

Kinetics of the HRP-I-Sulfite Reaction

The kinetic behavior of the HRP-I-sulfite system is consistent with a reaction that is first order in both

HRP-I and sulfite. Under pseudo-first-order conditions the observed differential rate expression is

$$-\frac{d[\text{HRP-I}]}{dt} = k_{3,\text{obs}}[\text{HRP-I}] \quad 3.02$$

The validity of equation 3.02 was verified by semilogarithmic plots of the change in voltage or absorbance vs. time. Values of the second-order rate constant, k_3 , were obtained from the equation

$$k_{3,\text{obs}} = k_3[\text{sulfite}] \quad 3.03$$

where [sulfite] refers to the total concentration of sodium sulfite without regard to its state of protonation. Equation 3.03 was verified by measuring $k_{3,\text{obs}}$ over a range of sulfite concentrations at a given pH. Plots of $k_{3,\text{obs}}$ vs. [sulfite] were linear as illustrated in Fig. 3.01 for the reaction at pH 3.81. At those values of pH where the reaction was studied over a range of sulfite concentrations, the error in k_3 was equated to the standard deviation calculated from the linear analysis of $k_{3,\text{obs}}$ vs. [sulfite] data. The error in k_3 at the other pH values was estimated at $\pm 10\%$. Different buffers used at the same pH yielded the same kinetic results within experimental error, indicating that there were no detectable buffer effects.

The values of k_3 as a function of pH are listed in Table 3.01 along with the ranges of sulfite concentrations

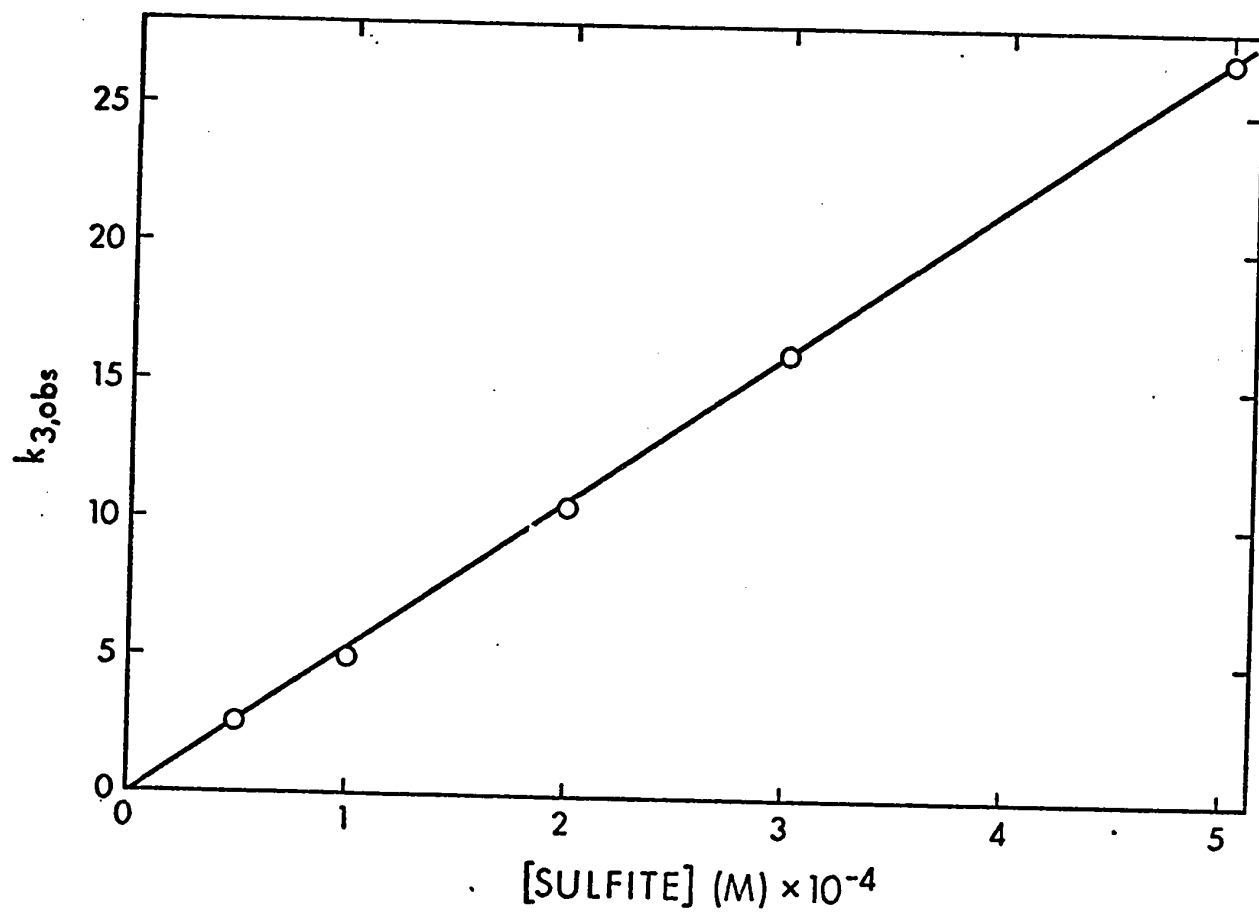


Fig. 3.01: Plot of $k_{3,obs}$ vs. [sulfite] for the HRP-I-sulfite reaction at pH 3.81. The solid line was calculated by a weighted linear least-squares analysis. The slope, k_3 , with its standard error is $(5.4 \pm 0.1) \times 10^4 \text{ M}^{-1}\text{sec}^{-1}$.

Table 3.01

Second-Order Rate Constants for the HRP-I-Sulfite
Reaction at 25°

pH	k_3 ($M^{-1} \text{sec}^{-1}$)	Range of [sulfite] (M)	Buffer*
2.28	1.3×10^5		
2.42	1.2×10^5	$(1-5) \times 10^{-4}$	C
2.45	1.2×10^5	$(1-5) \times 10^{-4}$	C
2.60	1.2×10^5	5×10^{-4}	G
2.69	$(1.2 \pm 0.03) \times 10^5$	$(1.5) \times 10^{-4}$	C
2.81	1.1×10^5	$(0.5-7.5) \times 10^{-4}$	G
2.85	1.1×10^5	5×10^{-4}	G
2.96	1.0×10^5	$(1-5) \times 10^{-4}$	C
3.14	9.2×10^4	5×10^{-4}	G
3.31	$8.8 \pm 0.06) \times 10^4$	5×10^{-4}	G
3.36	7.8×10^4	$(0.5-5) \times 10^{-4}$	C
3.53	6.7×10^4	$(1-5) \times 10^{-4}$	C
3.81	$(5.4 \pm 0.1) \times 10^4$	$(1-5) \times 10^{-4}$	C
3.99	$(4.7 \pm 0.04) \times 10^4$	$(0.5-5) \times 10^{-4}$	A
4.41	$(3.0 \pm 0.08) \times 10^4$	$(1-7.5) \times 10^{-4}$	A
4.65	$(2.3 \pm 0.04) \times 10^4$	$(0.2-2) \times 10^{-3}$	A
4.98	$(1.8 \pm 0.06) \times 10^4$	$(0.4-2) \times 10^{-3}$	A
5.45	$(9.5 \pm 0.5) \times 10^3$	$(0.25-2) \times 10^{-3}$	A
5.97	$(3.2 \pm 0.1) \times 10^3$	$(0.25-2) \times 10^{-3}$	A
6.33	$(1.3 \pm 0.03) \times 10^3$	$(1-5) \times 10^{-5}$	P
6.63	$(4.9 \pm 0.2) \times 10^2$	$(1-10) \times 10^{-5}$	P
6.89	$(2.4 \pm 0.04) \times 10^2$	$(0.25-25) \times 10^{-4}$	P
7.22	$(7.6 \pm 0.8) \times 10$	$(0.503.5) \times 10^{-4}$	P
		$(0.1-1.5) \times 10^{-3}$	P

* A, acetic acid-sodium acetate; C, citric acid-sodium citrate; G, glycine HNO₃-glycine; P, potassium dihydrogen phosphate-disodium-hydrogen phosphate.

and buffers used at each pH. The logarithm of k_3 is plotted vs. pH in Fig. 3.02. The pH dependence of k_3 was analyzed using the transition state approach described previously. The solid line in Fig.3.02 illustrates the best fit to the phenomenological equation

$$k_3 = \frac{k'_3 \left(1 + \frac{K_3^\ddagger}{[H^+]} \right)}{\left(1 + \frac{K_4}{[H^+]} + \frac{K_4 K_5}{[H^+]^2} \right) \left(1 + \frac{K_S}{[H^+]} \right)} \quad 3.04$$

where K_3^\ddagger is a transition state dissociation constant associated with the positive curvature at pH 4, K_4 and K_5 are the ground state dissociation constants for the acid groups of HRP-I associated with the negative curvatures at pH 2 and pH 5. K_S is the sulfite dissociation constant associated with the negative curvature at pH 7 and k'_3 is the pH independent second-order rate constant at low pH. The values of the parameters calculated from equation 3.04 are listed in Table 3.02. The broken line in Fig. 3.02 represents the best fit to the equation

$$k_3 = \frac{k'_3}{\left(1 + \frac{K_4}{[H^+]} \right) \left(1 + \frac{K_S}{[H^+]} \right)} \quad 3.05$$

which represents a simpler interpretation than equation 3.04, involving only one ground state dissociation constant and no transition state dissociation constants. The substantial deviation between the calculated and experimental points

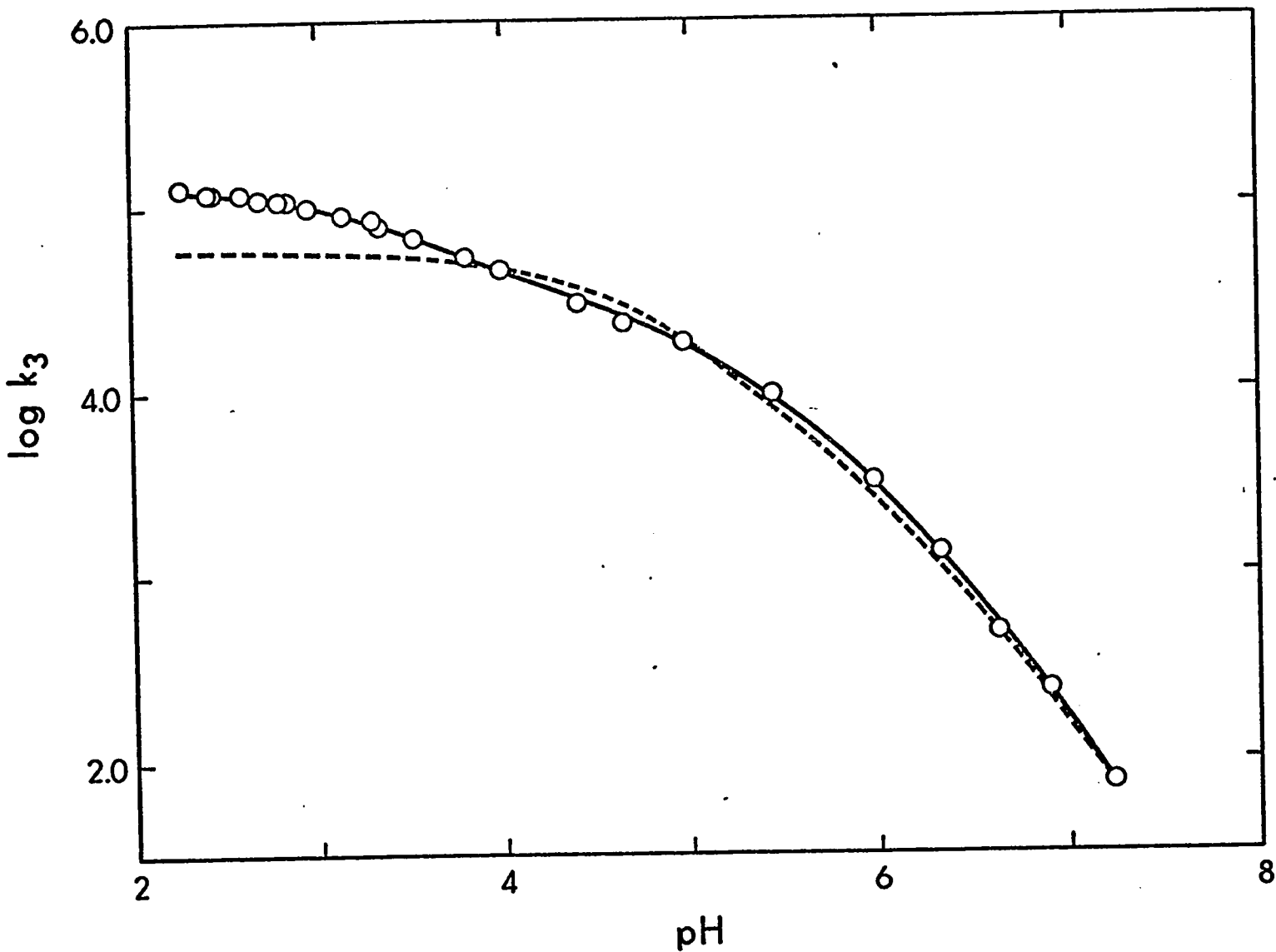


Fig. 3.02: Plot of $\log k_3$ vs. pH for the HRP-I-sulfite reaction. The solid line was calculated by a weighted nonlinear least-squares analysis of equation 3.04 and the broken line by the analysis of equation 3.05.

at low pH indicates that equation 3.05 does not offer a satisfactory interpretation of the pH dependence of the reaction.

Table 3.02

Ground State and Transition State Ionization Constants
Obtained by the Nonlinear Least-Squares Analysis of
Equation 3.04 for the HRP-I-Sulfite Reaction

	Equation 3.04	pK _a values
K ₄ (M)	4.6 × 10 ⁻⁴	3.3
K ₅ (M)	8.5 × 10 ⁻⁶	5.1
K _S (M)	1.2 × 10 ⁻⁷	6.9
K ₃ [‡] (M)	1.1 × 10 ⁻⁴	4.0
k ₃ ' (M ⁻¹ sec ⁻¹)	1.3 × 10 ⁵	

Kinetics of the HRP-II-Sulfite Reaction

The kinetic behavior of the HRP-II-sulfite system, like that of the HRP-I-sulfite system, is consistent with a reaction that is first order in both HRP-II and sulfite. Under pseudo-first-order conditions a differential rate expression

$$-\frac{d[\text{HRP-II}]}{dt} = k_{4,\text{obs}}[\text{HRP-II}] \quad 3.06$$

analogous to equation 3.02 was observed. The plots of the change in voltage vs. time were linear indicating the

validity of equation 3.06. Values of the second-order rate constant, k_4 , were obtained from the equation

$$k_{4,obs} = k_4[\text{sulfite}] \quad 3.07$$

Plots of $k_{4,obs}$ vs. [sulfite] were linear as illustrated in Fig. 3.03 for the reaction at pH 5.38. Similar studies were performed at all values of pH. The error in k_4 was equated to the standard deviation calculated from the linear analysis of the $k_{4,obs}$ vs. [sulfite] data. No buffer effects were observed.

The values of k_4 with their standard deviations are listed in Table 3.03 along with the ranges of sulfite concentrations and buffers used at each pH. The logarithm of k_4 is plotted vs. pH in Fig. 3.04. The pH profile for the HRP-II reaction closely resembles that for HRP-I. At high pH the HRP-II rate is slightly smaller than that of HRP-I, the two rates are the same at pH 6 and at lower pH the HRP-II rate becomes substantially larger than that of HRP-I. The solid line in Fig. 3.04 illustrates the best fit to the equation

$$k_4 = \frac{k_4' \left(1 + \frac{[H^+]}{K_4^\ddagger} \right)}{\left(1 + \frac{K_6}{[H^+]} \right) \left(1 + \frac{K_s}{[H^+]} \right)} \quad 3.08$$

where K_4^\ddagger is a transition state dissociation constant associated with the positive curvature at pH 2, K_6 is a ground state dissociation constant associated with the

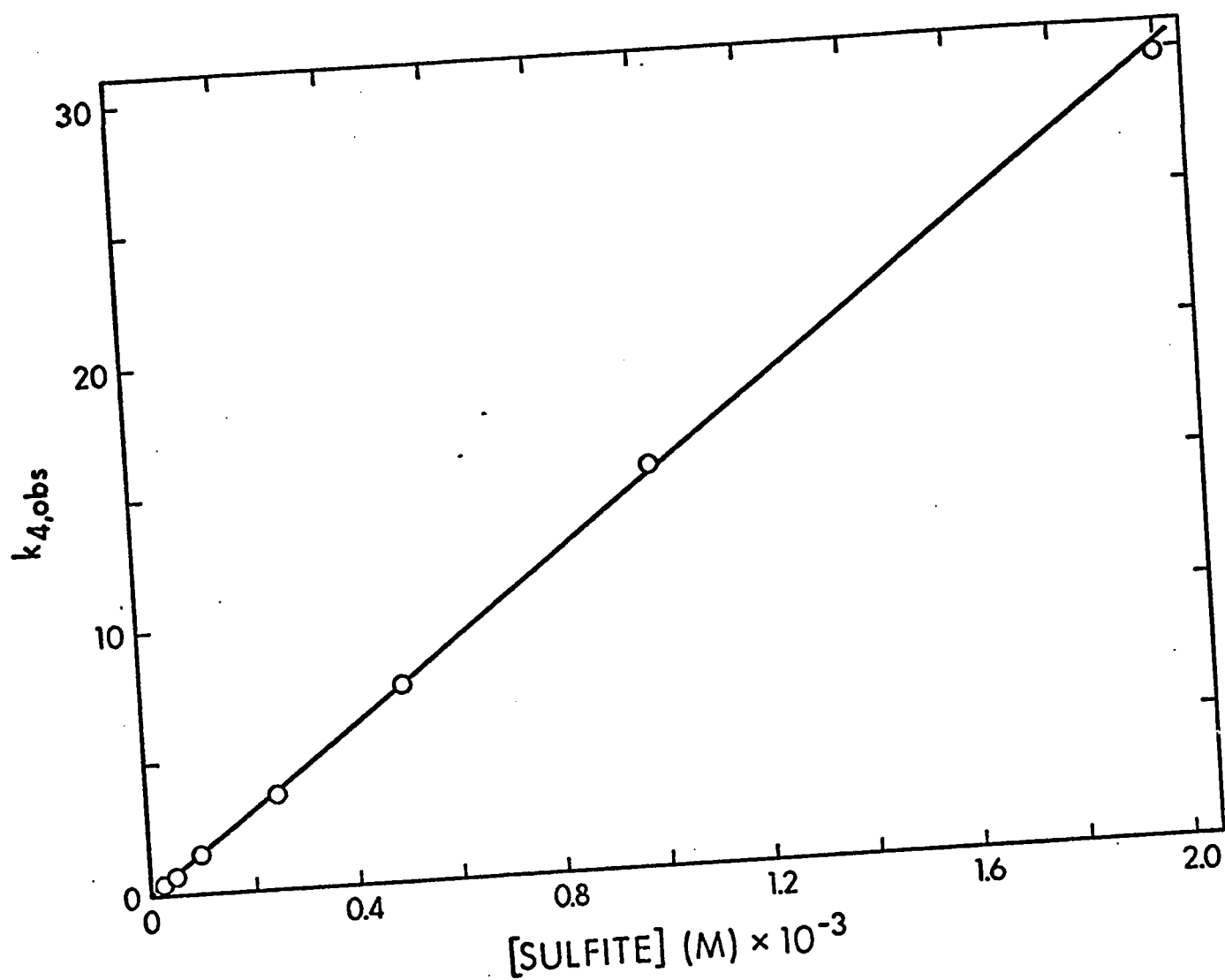


Fig. 3.03: Plot of $k_{4,obs}$ vs. [sulfite] for the HRP-II-sulfite reaction at pH 5.38. The solid line was calculated by a weighted linear least-squares analysis. The slope, k_4 , with its standard error is $(1.5 \pm 0.02) \times 10^4 \text{ M}^{-1} \text{ sec}^{-1}$.

Table 3.03

Second-Order Rate Constants for the HRP-II Sulfite
Reaction at 25°

pH	k_4	Range of [sulfite] (M)	Buffer*
2.43	$(6.8 \pm 0.4) \times 10^5$	$(2-6) \times 10^{-5}$	C
2.62	$(5.9 \pm 0.03) \times 10^5$	$(2-8) \times 10^{-5}$	C
2.86	$(5.3 \pm 0.3) \times 10^5$	$(0.2-1) \times 10^{-4}$	C
3.13	$(4.5 \pm 0.02) \times 10^5$	$(0.2-1.2) \times 10^{-4}$	C
3.39	$(3.7 \pm 0.1) \times 10^5$	$(0.2-1) \times 10^{-4}$	C
3.53	$(3.0 \pm 0.1) \times 10^5$	$(0.2-1.5) \times 10^{-4}$	C
3.81	$(2.5 \pm 0.08) \times 10^5$	$(0.1-2) \times 10^{-4}$	A
4.02	$(2.0 \pm 0.2) \times 10^5$	$(0.25-2) \times 10^{-4}$	A
4.03	$(1.9 \pm 0.06) \times 10^5$	$(0.25-2.5) \times 10^{-4}$	C
4.41	$(1.1 \pm 0.04) \times 10^5$	$(0.25-3) \times 10^{-4}$	A
4.66	$(6.2 \pm 0.2) \times 10^4$	$(0.25-3) \times 10^{-4}$	A
4.99	$(3.0 \pm 0.1) \times 10^4$	$(0.375-5) \times 10^{-4}$	C
5.38	$(1.5 \pm 0.02) \times 10^4$	$(0.025-2) \times 10^{-3}$	Ca
5.43	$(1.3 \pm 0.03) \times 10^4$	$(0.1-1) \times 10^{-3}$	A
5.45	$(1.1 \pm 0.03) \times 10^4$	$(0.05-1) \times 10^{-3}$	A
6.06	$(2.4 \pm 0.08) \times 10^3$	$(0.15-2.5) \times 10^{-3}$	P
6.33	$(1.2 \pm 0.01) \times 10^3$	$(0.1-1.5) \times 10^{-3}$	P
6.65	$(4.6 \pm 0.5) \times 10^2$	$(0.5-1) \times 10^{-3}$	P
6.92	$(1.8 \pm 0.06) \times 10^2$	$(0.5-4) \times 10^{-3}$	P

*A, acetic acid-sodium acetate; C, citric acid-sodium citrate; Ca, cacodylic acid-sodium cacodylate; P, potassium dihydrogen phosphate-disodium hydrogen phosphate.

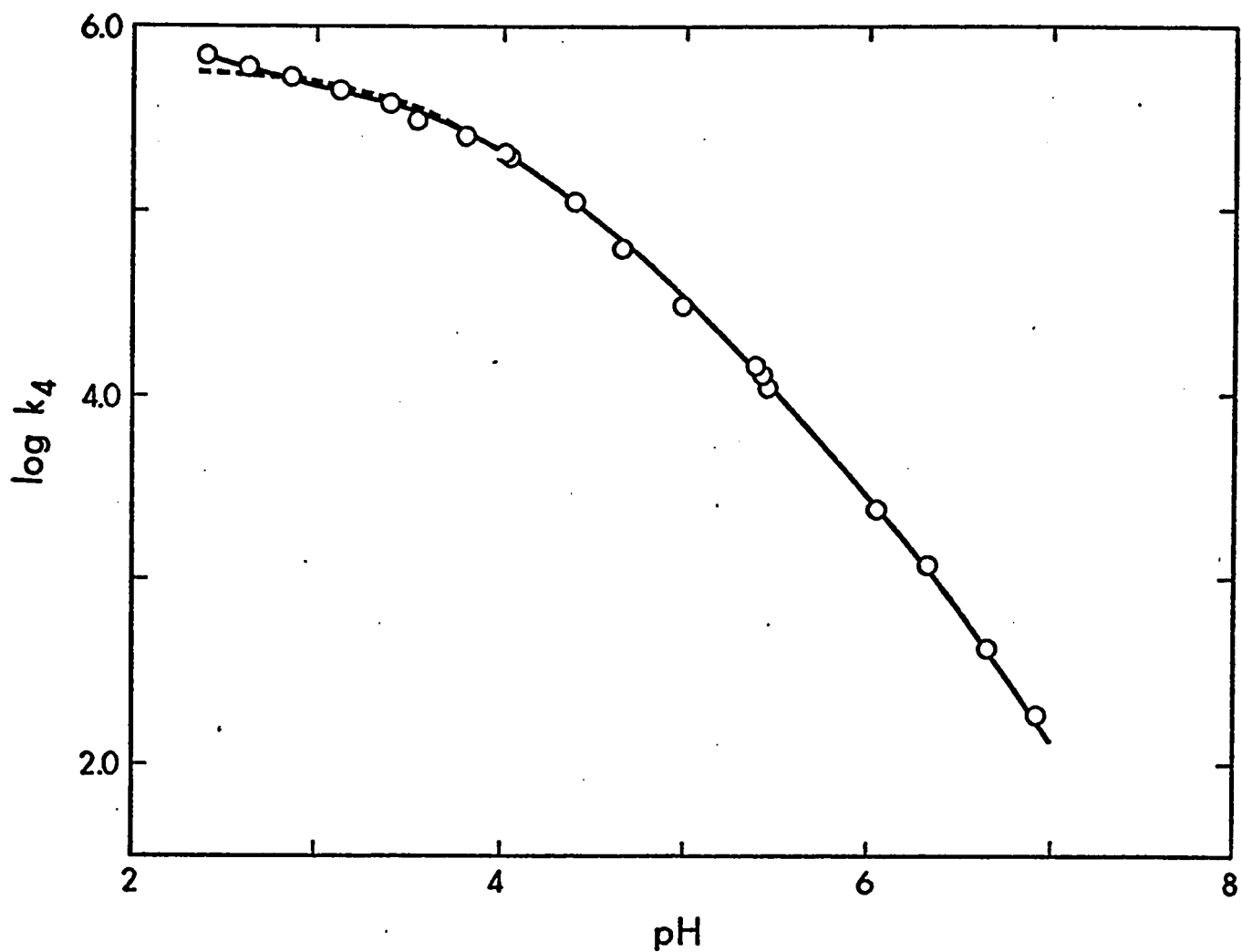


Fig. 3.04: Plot of $\log k_4$ vs. pH for the HRP-II-sulfite reaction. The solid line was calculated by a weighted nonlinear least-squares analysis of equation 3.08 and the broken line by the analysis of equation 3.09.

negative curvature at pH 4, K_s is the sulfite dissociation constant associated with the negative curvature at pH 7 and k_4' is the pH independent rate constant at pH 3. The broken line in Fig. 3.04 is the best fit to the equation

$$k_4 = \frac{k_4'}{\left(1 + \frac{K_6}{[H^+]}\right) \left(1 + \frac{K_s}{[H^+]}\right)} \quad 3.09$$

which does not involve a transition state dissociation constant. Although the fit is better to equation 3.08 than it is to equation 3.09, this difference is small. Considering the difficulty involved in measuring the rate at low pH, the kinetic data is not sufficient to distinguish between the two possibilities. The values of the parameters calculated from equations 3.08 and 3.09 are listed in Table 3.04.

Table 3.04

Ground State and Transition State Ionization Constants
Obtained by the Nonlinear Least-Squares Analyses of
Equations 3.08 and 3.09 for the HRP-II-Sulfite Reaction

	Equation 3.08	pK _a values	Equation 3.09	pK _a values
K_6 (M)	1.3×10^{-4}	3.9	1.7×10^{-4}	3.8
K_s (M)	1.9×10^{-7}	6.7	1.5×10^{-7}	6.8
K_4^\ddagger (M)	8.1×10^{-3}	2.1		
k_4' (M ⁻¹ sec ⁻¹)	4.8×10^5		5.8×10^5	

The decay of the transient enzyme species formed from the reaction between HRP-II and sulfite was studied from pH 7 to pH 4 at both 411 nm and 403 nm. The observed first-order rate constants for this reaction are presented in Table 3.05. In all cases the concentration of sulfite was sufficiently high to ensure that the formation of the species was at least ten times faster than its decay. The values of the observed first-order rate constants for the decay of the transient species, as a function of sulfite concentration, pH and wavelength, agreed within experimental error under the conditions that the reaction was monitored.

Table 3.05

Observed First-Order Rate Constants for the Decay
of the Transient Enzymatic Species Formed from
the HRP-II-Sulfite Reaction

pH	Wavelength (nm)	[Sulfite]	First-order rate constant (sec ⁻¹)
6.92	403,411	4×10^{-3}	0.27
6.92	403,411	2×10^{-2}	0.31
4.99	403,411	1×10^{-4}	0.28
4.99	403,411	1×10^{-3}	0.27
4.03	403,411	2.5×10^{-5}	0.23

Reaction Sequence of the HRP-I-Sulfite Reaction

Fig. 3.05 illustrates the spectrum of the steady-state concentration of the enzymatic intermediate present in a mixture of HRP, hydrogen peroxide and sulfite. From Fig. 3.02 and Fig. 3.04 it can be seen that the values of k_3 and k_4 at pH 6.0 are the same. Thus with an excess of hydrogen peroxide the steady-state intermediate would be expected to be a 1:1 mixture of HRP-I and HRP-II if HRP-I reacted to form HRP-II. The spectrum in Fig. 3.05 closely resembles the spectrum of HRP-I obtained under similar conditions with iodide as a substrate. It is possible that HRP-I could form HRP-II which in turn could form the transient enzyme species producing a steady-state spectrum that resembled that for HRP-I. In the present case however, this appears unlikely since the concentration of sulfite was sufficiently low that the reactions of HRP-I and HRP-II were slower than the observed decay of the transient species. Although it is possible that this species could make a small contribution to the spectrum of the steady-state intermediates if HRP-I reacted to HRP-II, the agreement between the spectrum observed for sulfite and that observed for iodide is so close that this possibility is unlikely. The largest deviation at any wavelength between the spectrum in Fig. 3.05 and the spectrum of HRP-I in Fig. 2.13 is 8% at 440 nm, however the deviation between the two spectra at the HRP-I maximum, 400 nm, is less than 1%.

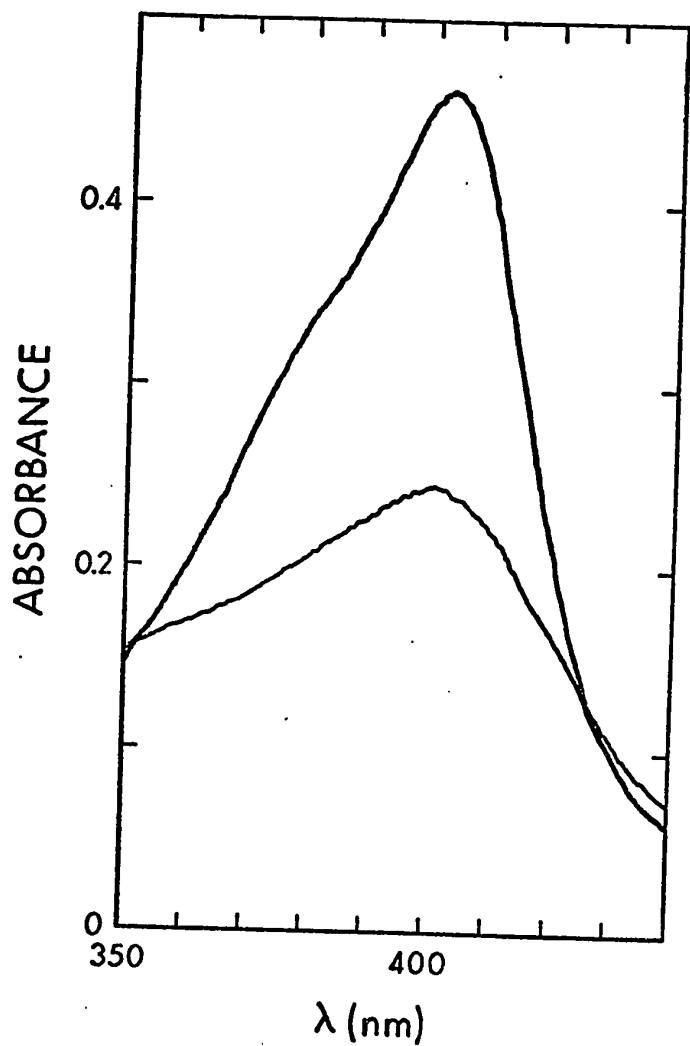
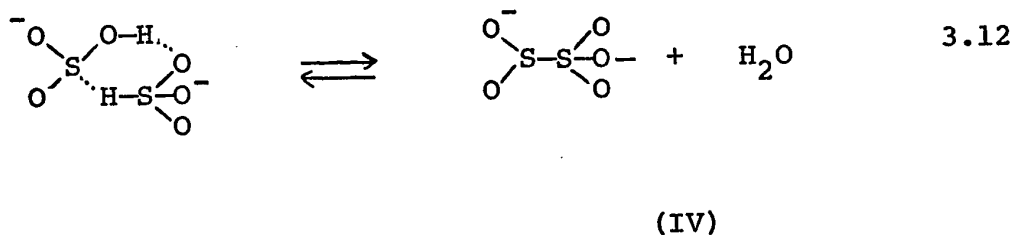
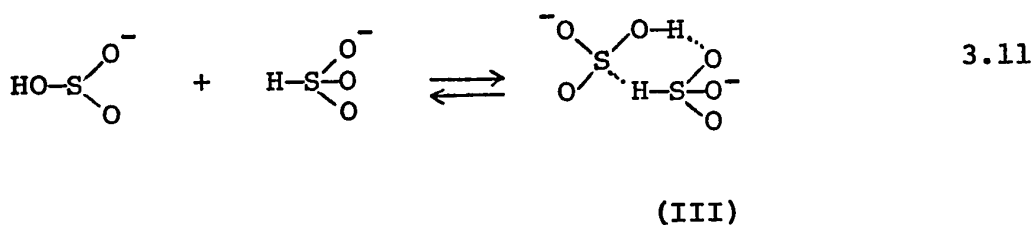
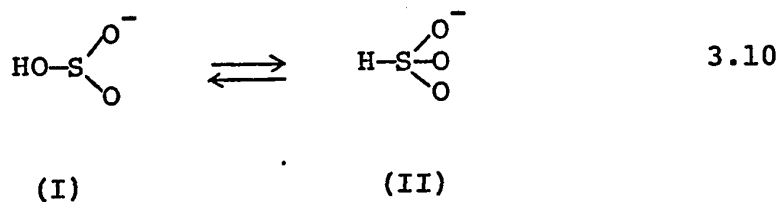


Fig. 3.05: Spectrum of the enzymatic species present in the steady state, for the HRP-catalyzed oxidation of sulfite, compared to the spectrum of HRP. The steady-state spectrum was scanned over a period of 40 seconds following the addition of hydrogen peroxide to a solution of HRP and sulfite.

The spectrum of the enzymatic species present in the steady state illustrated in Fig. 3.05 offers good evidence that HRP-I is converted directly to HRP without the intermediate formation of HRP-II. This evidence was confirmed by studying the reaction of sulfite with a 1:1 mixture of HRP-I and HRP-II at 427 nm. If HRP-I reacted to form HRP-II such a mixture would be expected to result in distinctly non-first-order kinetics for the HRP-II reaction with sulfite at this wavelength, since HRP-II formation and decay would occur simultaneously. For such mixtures an exact first-order decay of HRP-II was always observed. Because of the similarity in rate between the reactions of HRP-I and HRP-II with sulfite, many of the techniques used to confirm the direct transfer of two electrons as observed in the HRP-I-iodide reaction were not applicable to the corresponding sulfite reaction.

3.04 Discussion

Since sulfurous acid is a weak acid, its state of protonation in its reactions with HRP cannot be defined unambiguously as was possible for the iodide reactions. An additional complication concerning the nature of the sulfite species in aqueous solution results from the multiple forms bisulfite can take at different concentrations. Golding (1960) has shown that the u.v. spectra of various concentrations of bisulfite solutions can be explained by the series of equilibria



He predicts that the two tautomers I and II are present in approximately equal concentration. The hydrogen bonded species, III, is spectrally distinct and is only present in detectable concentrations in bisulfite solutions with concentrations greater than 3×10^{-3} M. The formation of pyrosulfite, IV, takes place in concentrated solutions of bisulfite. If bisulfite is the kinetically important protonated species for the HRP-I and HRP-II reactions over the pH range where these reactions were studied, different

rates of reaction might be expected from the four forms of bisulfite. The highest concentration of sulfite used in the kinetic studies was 4×10^{-3} M, thus the dominant species in solution for these studies were the tautomers I and II. The linear nature of the k_{obs} vs. [sulfite] plots indicates that either I or II or perhaps both I and II must be the reacting species in the observed reactions. The reaction of either III or IV would be expected to result in distinct nonlinearity on such plots, since each of these structures are formed from two molecules of bisulfite.

The plots of both $\log k_3$ vs. pH and $\log k_4$ vs. pH show an increase in slope of approximately -2 to -1 at a pH value close to pK_s . This indicates the probability that the same protonated species is kinetically important in the reactions of both HRP-I and HRP-II. Whether SO_3^- is the reacting species in the HRP-II-sulfite reaction can be decided by considering the value of k_4 at the lowest pH of the study. Assuming that SO_3^- is the reacting species equation 3.07 can be rewritten

$$k_{4,\text{obs}} = k_4'[\text{SO}_3^-] \quad 3.13$$

from which k_4' can be calculated to be approximately $3 \times 10^{10} \text{ M}^{-1} \text{ sec}^{-1}$ if SO_3^- is the reacting species. Since k_4' exceeds the diffusion controlled limit, SO_3^- cannot be the reacting species with HRP-II. The pH dependence of the HRP-I-sulfite reaction is more complicated than that for the corresponding HRP-II reaction. It is tempting, however, to assume a pairing of the transition state

with pK_a^\ddagger 4 to the ground state with pK_a 3.3 for HRP-I because of the similarity in the two ionization constants. Such a pairing implies that the enzyme pK_a at 3.3 has a small accelerating effect on the rate. If this assumption is made, HSO_3^- can be shown to be the reacting species in the HRP-I-sulfite reaction over the pH range where the reaction was studied, by a method analogous to that used for the HRP-II-sulfite reaction. Thus the similar effect of pK_s on the plots of $\log k_3$ and $\log k_4$ vs. pH has a reasonable explanation if bisulfite is the kinetically important species for both reactions.

Kinetically it is not possible to distinguish between bisulfite and sulfurous acid as possible reacting species. However, if sulfurous acid is the reacting species, the increase in rate with decreasing pH must be due to increasing concentration of sulfurous acid. Such a situation necessarily implies that the heme-bound group observed for the reactions of HRP-I and HRP-II with iodide has no effect on the reactions with sulfite. Since there is no evidence that the reactions of HRP-I and HRP-II with sulfite proceed via a different mechanism than the reaction with iodide, it is simpler to assume that the heme-bound groups should have a similar effect on the sulfite reaction. If this is the case, then both the ground and transition state pK_a 's associated with the first sulfurous acid ionization constant must be outside the pH range of the kinetic study and bisulfite can be assumed to be the reacting species over

this pH range.

Like the reactions of iodide and ferrocyanide with HRP-I, the kinetic pH dependence of the sulfite reaction shows the effects of an ionization with pK_a value of approximately 5. In order to compare the enzyme pK_a values observed for various substrates, an accurate estimate of the error limits of these values is desirable. One method for estimating these errors involves the analysis of the kinetic pH dependence for a particular reaction with the desired pK_a fixed at a discrete set of values. Such an analysis has been performed for the enzyme pK_a approximately equal to 5 observed for the reactions of sulfite, iodide and ferrocyanide with HRP-I and is described in Appendix 3. The results of these analyses indicate for the iodide reaction pK_2 is 4.6 ± 0.2 , for the sulfite reaction pK_4 is 5.1 ± 0.2 and for the ferrocyanide reaction the pK_a is 5.3 ± 0.8 . The difference between the pK_a values observed for sulfite and iodide is just outside the error limits on the two values. It is possible that this small difference could result if the pK_a observed for one substrate was an overlap of two enzyme pK_a 's with approximately the same value, thus causing an apparent shift in the observed pK_a . Since this difference is small, it seems a reasonable assumption that the same ionizing group on HRP-I influences the reaction rate with all three substrates.

Sulfite is the only substrate for HRP studied to date in which the reaction of HRP-II is faster than the reaction of HRP-I. In the present study this occurs over the pH range 2 to 6. Brill (1966) has reported that, in general, the reactions of HRP-I are faster by a factor of 30 to 100 than the corresponding reactions of HRP-II. Since sulfite is a much stronger reducing agent than iodide or ferrocyanide, yet reacts more slowly, the ease of oxidation of a substrate does not seem to have any simple relationship to the observed rates for the reduction of HRP-I and HRP-II. Further evidence of this phenomenon is illustrated by the HRP-II-sulfite reaction where HSO_3^- has been shown to react in preference to $\text{SO}_3^{=}$, even though the latter is a better reducing agent. The insensitivity of the reactions of HRP-I and HRP-II to the reducing ability of the substrate is in agreement with the conclusions of Critchlow and Dunford (1972b), who have proposed a mechanism for the reaction of HRP-II which involves the slow displacement of a group bound in the sixth co-ordination position of the iron followed by rapid electron transfer. At pH 7 the ratio of the rate of the HRP-I reaction to that of HRP-II is 500 for iodide, 30 for nitrite and 1.2 for sulfite. If the displacement of a group from the active site in HRP-I and HRP-II is the rate determining step, then the difference in the reaction ratio for the two compounds must be the result of a difference in shape, size or hydrogen bonding ability for the three substrates.

A unified mechanism for the reaction of HRP-II with ferrocyanide, iodide and p-cresol, which accounts for the kinetic pH dependences of the three substrates and is consistent with their rates observed in D_2O has been proposed by Critchlow and Dunford (1972b). In this mechanism substrates like p-cresol, which react very rapidly, exhibit rate determining proton transfers, while the reaction rates for substrates like iodide, which react much more slowly, are controlled by specific acid catalysis. The HRP-II-ferrocyanide reaction, which has a reaction rate intermediate between the rates of the iodide and p-cresol reactions, exhibits rate determining proton transfer in alkaline solution and specific acid catalysis below pH 6. Since the rate of the reaction between HRP-II and sulfite is intermediate between iodide and ferrocyanide, a linear increase in rate with increasing acidity below pH 6, as observed for the iodide and ferrocyanide reactions, would also be expected for the sulfite reaction. The rate influencing enzyme dissociation with pK_a of 4 observed for the HRP-II-sulfite reaction was not detected for the other two substrates. In order that the kinetic pH dependence of the HRP-II-sulfite reaction be compatible with the proposed unified mechanism observed for all other substrates studied to date, sulfite must have a stronger interaction with a group on the enzyme with pK_a of 4, than do iodide or ferrocyanide. The protonation of this group thus has a large effect on the rate of the sulfite reaction and a very small

effect on the rates of the iodide and ferrocyanide reactions. This interpretation implies that at some pH lower than 4 the effect of this dissociation will become relatively smaller and the rate of the HRP-II-sulfite reaction will begin increasing again, like the reactions with iodide and ferrocyanide. The pK_a of 4 for the group on the enzyme suggests that this group might be a carboxylic acid and the electronegative character of the bisulfite ion makes a hydrogen bonding enzyme-substrate interaction an attractive hypothesis.

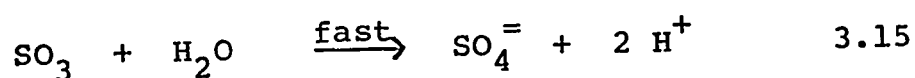
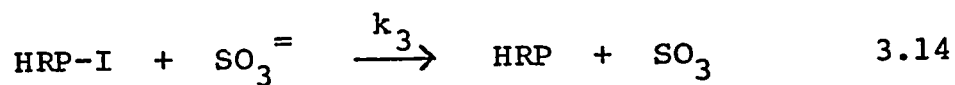
The formation of a transient enzyme species as observed for the HRP-II-sulfite reaction at 411 nm was not detected for the reactions of HRP-II with iodide or nitrite. There are a variety of possible explanations for such a phenomenon, however we believe that a complex between HRP and a sulfite species offers a simple explanation that is in accord with experimental observation. The mechanism proposed for the reaction of HRP-II by Critchlow and Dunford (1972b) assumes a rate determining displacement of a group in the active site of the enzyme followed by rapid electron transfer and radical departure. For the HRP-II-sulfite reaction we propose that the radical departure is slow enough to be observed. This proposal for the transient species is in agreement with the kinetic observations that the reaction is a first-order decay which is independent of both pH and sulfite concentrations. In principle, unless the radical departure is diffusion controlled, the same

sort of phenomenon could be observed for the reactions of HRP-II with the other two substrates at sufficiently high substrate concentration. In the present study, however, these conditions were outside the range of observable experiments.

The slow secondary reaction observed for the HRP-II-sulfite system at 427 nm (on the Cary 14 spectrophotometer) was also not observed for the reactions of iodide or nitrite. To determine whether this reaction could result from the strong reducing character of sulfite, the decay of sulfite was monitored in the presence and absence of HRP. Native HRP, which is in the ferric state, can be reduced with strong reducing agents like dithionite to ferrous HRP. In the presence of oxygen, ferrous HRP undergoes a rapid reaction to native HRP. If such a reaction occurred with sulfite, a decay of sulfite concentration would be expected in aerobic solutions. The decay of a sulfite solution in the presence of a 2×10^{-6} M solution of HRP was almost identical to the decay observed in the absence of HRP, indicating that sulfite does not reduce HRP to an appreciable extent. The slow secondary reaction observed for the HRP-II-sulfite system is possibly due to the reaction of sulfite oxidation products with native HRP. The observation that the absorbance change of this reaction increased with increasing concentrations of native HRP in HRP-II solutions is evidence to support this view. The possible nature of such a reactive product is unknown. Kinetic experiments

performed in the presence of sulfate and dithionate, the expected final reaction products, resulted in identical kinetic behavior to the reactions performed in the absence of these ions. This product would appear to be associated with the single electron transfer observed for the HRP-II reaction however, since no spurious reactions were observed with the HRP-I-sulfite system.

One of the main reasons sulfite was chosen as a substrate for HRP was to determine whether the two electron transfer observed for the HRP-I-iodide reaction could be observed for another substrate. The spectrum of the species present in the steady state illustrated in Fig. 3.05 along with the kinetic measurements made in a mixture of HRP-I and HRP-II indicate that the HRP-I-sulfite reaction most probably involves a two electron transfer to HRP-I without the observable formation of HRP-II. Due to the presence of the slow secondary reaction associated with the HRP-II-sulfite system, the titrations of HRP-I and HRP-II with sulfite, as performed for the iodide reactions were not possible. However it seems reasonable to assume that the stoichiometry observed for the reactions of HRP-I and HRP-II with iodide also applies to the reaction with sulfite. Thus the overall reaction with sulfite could be described by



Chapter 4

Oxidation of Nitrite by Horseradish Peroxidase
Compounds I and II

4.01 Introduction

The reactions of HRP-I and HRP-II with nitrite were first reported by Chance (1952c), who observed that the reaction of HRP-I with nitrite produced HRP-II. It was felt that it would be of interest to investigate further this reaction in light of the two electron transfers observed for the reactions of HRP-I with iodide and sulfite.

4.02 Experimental

Materials

Horseradish peroxidase was obtained from Boehringer-Mannheim as a highly purified suspension in aqueous ammonium sulfate and was dialyzed and passed through a Millipore filter prior to use. The concentration of HRP was determined as described previously.

Stock solutions of nitrite were prepared by weight and their concentrations checked at 355 nm using a molar absorptivity value of $23.0 \text{ M}^{-1} \text{ cm}^{-1}$ (Altshuller and Wartburg, 1960). Solutions from 0.1 M to 10^{-4} M were stable for several weeks when stored in the dark. Hydrogen peroxide, 30% by weight obtained from the Fisher Scientific Co., was stored in the dark as an approximately 5×10^{-2} M solution, and diluted before use; its concentration was checked periodically by the HRP-catalyzed oxidation of

iodide.

Kinetic investigations were carried out on the stopped-flow apparatus using similar techniques and conditions to those described previously.

Stoichiometric Experiments

The overall reaction stoichiometry for the HRP-catalyzed oxidation of nitrite by hydrogen peroxide was determined spectrophotometrically at pH 4.95 by monitoring the decrease in nitrite concentration at 355 nm and the production of nitrate at 300 nm. The spectra of sodium nitrite and potassium nitrate were obtained from 400 nm - 270 nm on the Cary 14. The molar absorptivity of the sulfite maximum at 355 nm agreed with the published value to within 1% (Altshuller and Wartburg, 1960). Potassium nitrate had no observable absorbance at 355 nm. The nitrate spectrum had a maximum at 300 nm with a molar absorptivity of $7.3 \text{ M}^{-1} \text{ cm}^{-1}$. The sulfite spectrum had a molar absorptivity of $8.9 \text{ M}^{-1} \text{ cm}^{-1}$ at the same wavelength. The reaction was initiated by the addition of hydrogen peroxide from a Hamilton microliter syringe to a cuvette containing 2.0 ml of a solution of $1.0 \times 10^{-2} \text{ M}$ sodium nitrite, $2.2 \times 10^{-6} \text{ M}$ HRP and pH 4.95 acetate buffer of ionic strength 0.01. The dilution caused by the addition of the hydrogen peroxide in amounts ranging from 10 to 100 μl , was compensated by measuring the decrease in absorbance caused by the addition of equivalent volumes of water to solutions identical to the ones used in the stoichiometry experiments.

The stoichiometry of the reaction between HRP-I and nitrite was determined by a titration of HRP-I monitored at 411 nm. Solutions of HRP-I were prepared in the usual manner by the addition of hydrogen peroxide to 2.0 ml of a solution of 2.2×10^{-6} M HRP in pH 5.05 citrate buffer of ionic strength 0.01. The initial rapid spontaneous decay of HRP-I was monitored until the rate of this reaction was slower than the reaction with nitrite (about 10% of the HRP-I was consumed), then solutions of sodium nitrite, from 2-10 μ l, were added with a Hamilton microliter syringe and the changes in absorbance were measured.

Steady-State Spectra

The spectrum of the enzymatic species present in the steady state for the HRP-catalyzed oxidation of nitrite was determined in a similar manner to the spectra obtained for the reactions of iodide and sulfite. The reaction was initiated by the addition of 3 μ l of 6.6×10^{-2} M hydrogen peroxide to 2.0 ml of solution containing 5.0×10^{-6} M HRP and 1.0×10^{-2} M sodium nitrite in a pH 6.90 phosphate buffer of ionic strength 0.01. The spectrum of the resulting steady-state mixture was scanned on a Cary 14 spectrophotometer from 350-450 nm at a rate of 2.5 nm/sec. An identical experiment was performed where the absorbance was monitored at 431 nm to ensure that steady-state conditions did exist during the time taken to scan the spectrum. It was estimated that the reaction had completed

ten cycles by the time taken to scan the spectrum.

3.03 Results

Kinetics of the HRP-I-Nitrite Reaction

The kinetic behavior of the HRP-I-nitrite reaction is consistent with a reaction that is first order in both HRP-I and nitrite. Under pseudo-first-order conditions the observed differential rate expression is

$$-\frac{d[\text{HRP-I}]}{dt} = k_{5,\text{obs}}[\text{HRP-I}] \quad 4.01$$

The validity of equation 4.01 was verified by semilogarithmic plots of the change in voltage vs. time. Values of the second-order rate constant, k_5 , were obtained from the equation

$$k_{5,\text{obs}} = k_5[\text{nitrite}] \quad 4.02$$

where [nitrite] refers to the total concentration of sodium nitrite without regard to its state of protonation. Equation 4.02 was verified by measuring $k_{5,\text{obs}}$ over a range of nitrite concentrations at pH 6.93. This plot is illustrated in Fig. 4.01. The values of k_5 as a function of pH are listed in Table 4.01 along with the ranges of nitrite concentrations and buffers used at each pH. The values of k_5 in Table 4.01 increase linearly with increasing hydrogen ion concentration. The plot of the logarithm of k_5 vs. pH has a slope of -1.0 ± 0.1 as analyzed by linear least-squares analysis.

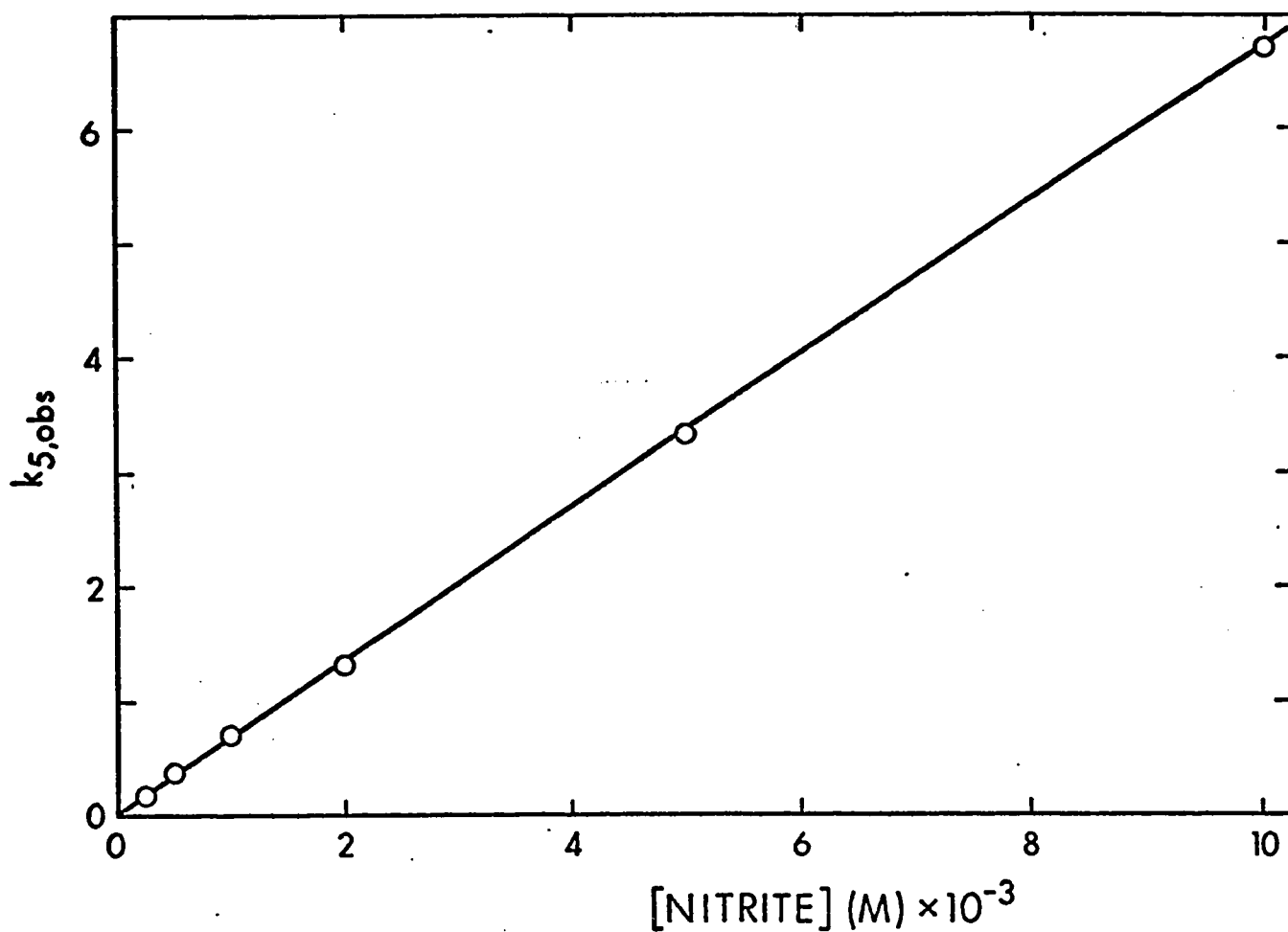


Fig. 4.01: Plot of $k_{5,obs}$ vs. [nitrite] for the HRP-I-nitrite reaction at pH 6.92. The solid line was calculated by a linear least-squares analysis. The slope, k_5 , with its standard error is $(6.7 \pm 0.2) \times 10^3 \text{ M}^{-1} \text{ sec}^{-1}$.

Table 4.01
 Second-Order Rate Constants for the HRP-I-Nitrite
 and HRP-II-Nitrite Reactions at 25°.

PH	k_5 ($M^{-1} \text{sec}^{-1}$)	k_6 ($M^{-1} \text{sec}^{-1}$)	Range of [nitrite] (M)	Buffer*
5.97	6.5×10^3	(1.8 to .04) $\times 10^2$	$0.5 - 2.5 \times 10^{-3}$	P
5.98			$0.1 - 4 \times 10^{-2}$	P
6.83		2.5×10	$0.1 - 1 \times 10^{-1}$	P
6.93	$(6.7 \pm 0.2) \times 10^2$		$0.025 - 1 \times 10^{-2}$	P
7.53			$0.2 - 1 \times 10^{-1}$	P
8.21	3.7×10	4.5	$0.2 - 2 \times 10^{-2}$	B
8.84	8.2		$0.2 - 10^{-1}$	B

*B, sodium tetraborate - HNO_3 ; P, Potassium dihydrogen phosphate-disodium hydrogen phosphate.

Kinetics of the HRP-II-Nitrite Reaction

The kinetic behavior of the HRP-II-nitrite reaction, like that for the HRP-I-nitrite reaction, is consistent with a reaction that is first order in both HRP-II and nitrite. Under pseudo-first-order conditions the observed differential rate expression is

$$-\frac{d[\text{HRP-II}]}{dt} = k_{6,\text{obs}}[\text{HRP-II}] \quad 4.03$$

The validity of equation 4.03 was verified by semilogarithmic plots of the change in voltage vs. time. Values of the second-order rate constant, k_6 , were obtained from the equation

$$k_{6,\text{obs}} = k_6[\text{nitrite}] \quad 4.04$$

A plot of $k_{6,\text{obs}}$ vs. [nitrite] at pH 5.98 is illustrated in Fig. 4.02. The values of k_6 as a function of pH are listed in Table 4.01 along with the ranges of nitrite concentrations and buffers used at each pH. The plot of the logarithm of k_6 vs. pH has a slope of -1.0 ± 0.01 .

Reaction Sequence of the HRP-I-Nitrite Reaction

Fig. 4.03 illustrates the spectrum of the enzymatic species present in the steady state for the HRP-catalyzed oxidation of nitrite. As observed for the HRP-catalyzed oxidations of ferrocyanide and ascorbic acid, the steady-state spectrum closely resembles that of HRP-II (Critchlow

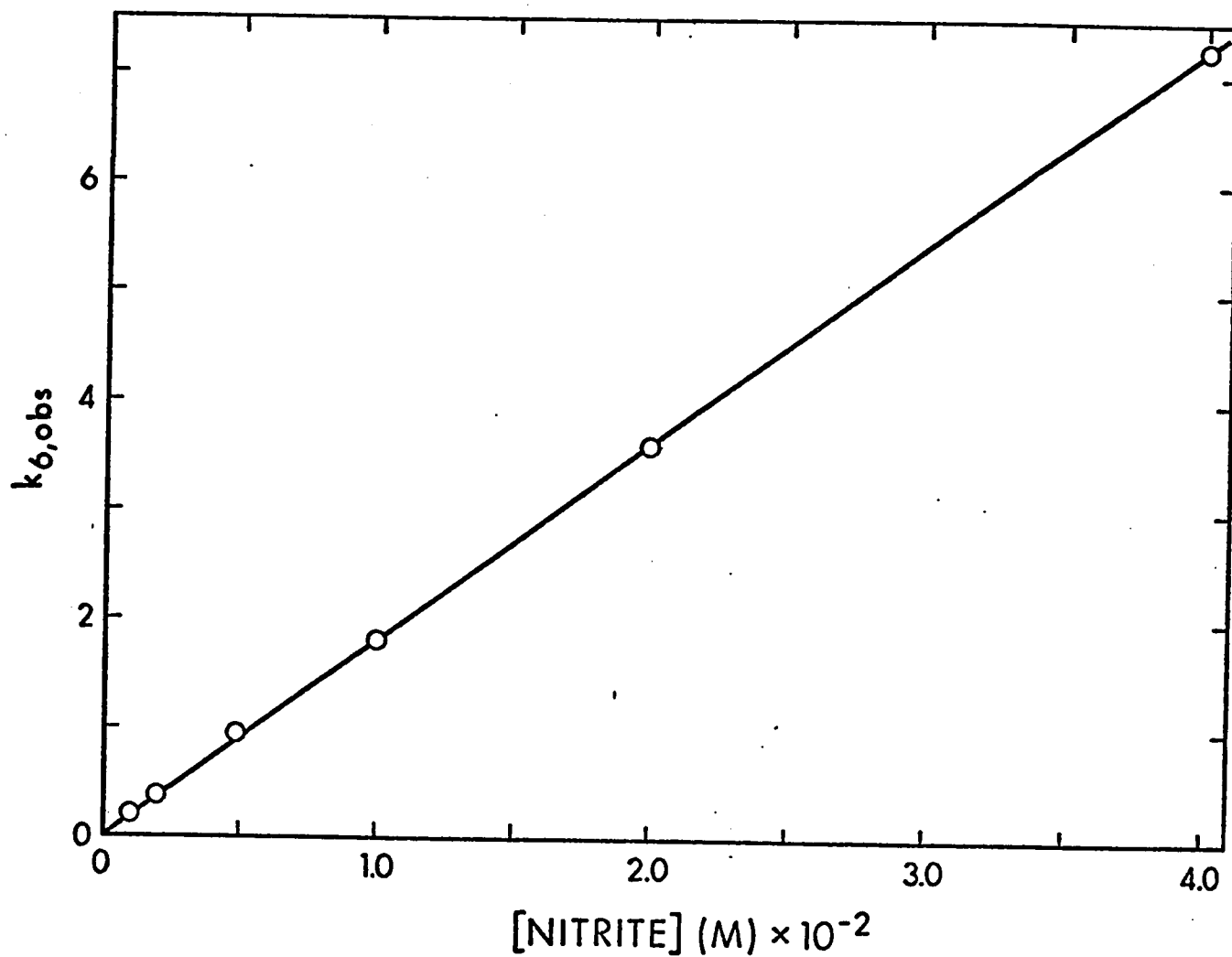


Fig. 4.02: Plot of $k_{6,obs}$ vs. [nitrite] for the HRP-II-nitrite reaction at pH 5.98. The solid line was calculated by a weighted linear least-squares analysis. The slope, k_6 , with its standard error is $(1.8 \pm 0.04) \times 10^2 \text{ M}^{-1} \text{ sec}^{-1}$.

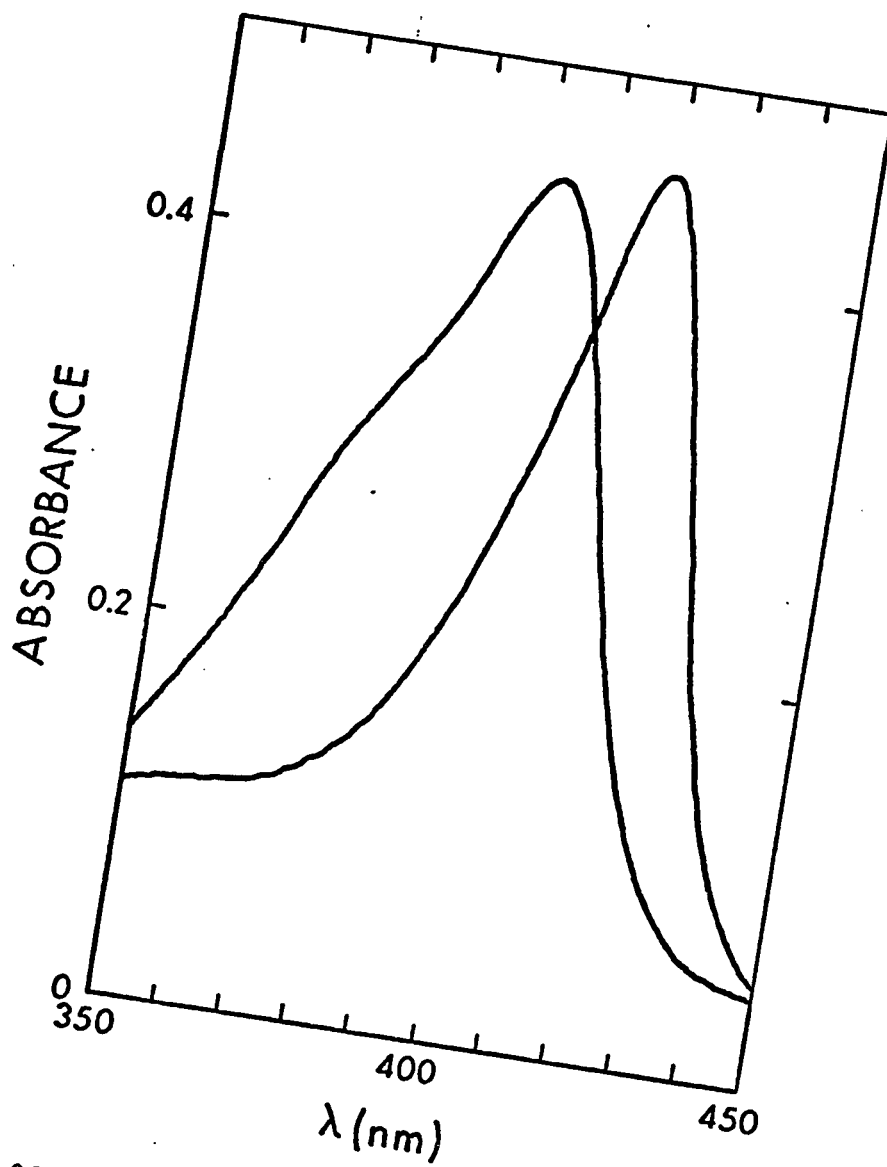
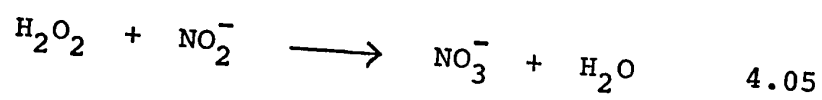


Fig. 4.03: Spectrum of the enzymatic species present in the steady state, for the HRP-catalyzed oxidation of nitrite, compared to the spectrum of HRP. The steady-state spectrum was scanned over a period of 40 seconds following the addition of hydrogen peroxide to a solution of HRP and nitrite.

and Dunford, 1972b). Since the difference in rate between HRP-I and HRP-II at pH 7 is only a factor of 30, an accurate spectrum for HRP-II would require compensation for the 3% of HRP-I present in the steady state. This steady-state spectrum, however, provides clear evidence that HRP-I reacts with nitrite in a one electron transfer forming HRP-II.

The overall stoichiometry of the HRP-catalyzed reaction between hydrogen peroxide and nitrite is described by the equation



Equation 4.05 was established by measuring the absorbance changes at 355 nm and 300 nm resulting from the steady-state oxidation of nitrite with various concentrations of hydrogen peroxide. Fig. 4.04 illustrates a plot of the changes in absorbance at 355 and 300 nm vs. the concentration of hydrogen peroxide added to a solution of HRP and sodium nitrite. The solid line in Fig. 4.04 was calculated from the linear analysis of the absorbance changes observed at 355 nm vs. the concentration of hydrogen peroxide. The slope of the line is $22.8 \pm 0.4 \text{ M}^{-1} \text{ cm}^{-1}$ in good agreement with the value of the molar absorptivity difference, $23.0 \text{ M}^{-1} \text{ cm}^{-1}$, computed on the basis of one mole of nitrite being consumed for every mole of peroxide. The broken line in Fig. 4.04 was calculated from a linear analysis of the absorbance changes observed at 300 nm vs. the concentration

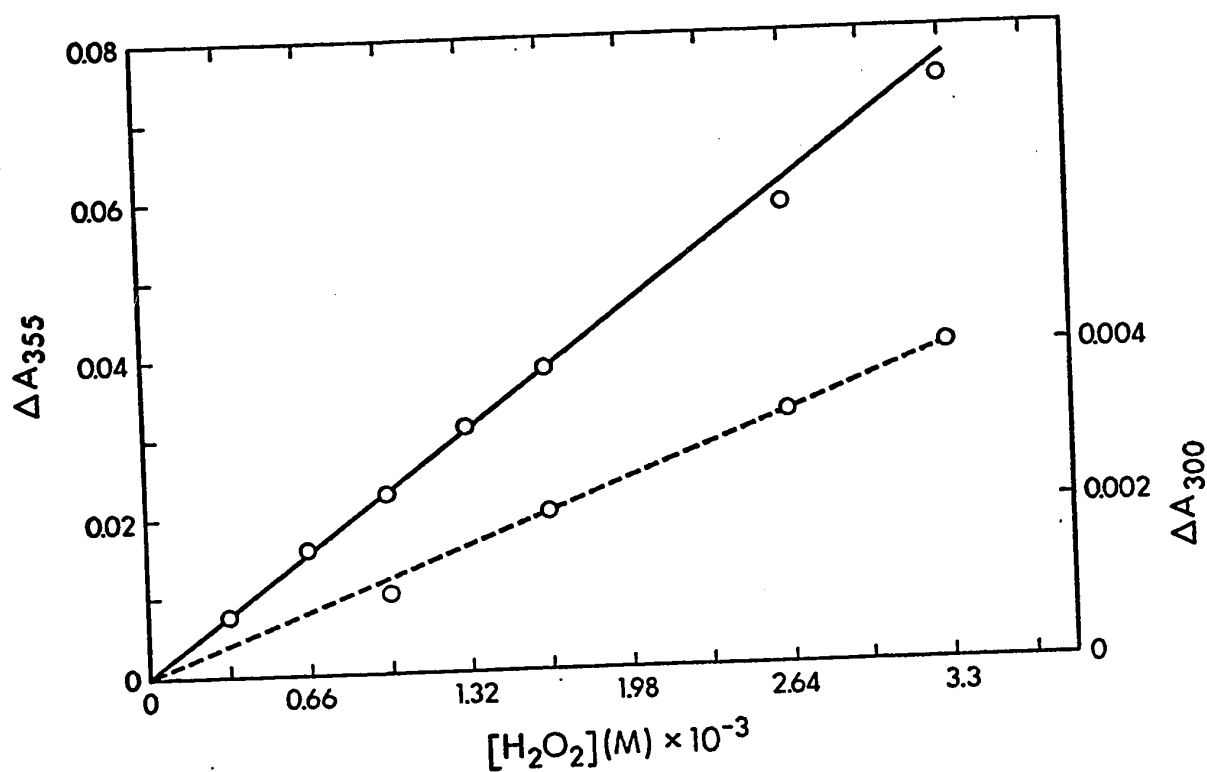


Fig. 4.04: Plot of the changes in absorbance at 355 nm and 300 nm vs. the concentration of hydrogen peroxide, for the HRP-catalyzed reaction between nitrite and hydrogen peroxide. The solid line was calculated by weighted linear least-squares analysis of the observed absorbance changes at 355 nm and the broken line by the analysis of the observed absorbance changes at 300 nm. The slope of the solid line is $22.8 \pm 0.4 \text{ M}^{-1} \text{ cm}^{-1}$ and that for the broken line is $1.3 \pm 0.5 \text{ M}^{-1} \text{ cm}^{-1}$.

of hydrogen peroxide. The slope of the line is $1.3 \pm 0.5 \text{ M}^{-1} \text{ cm}^{-1}$ in reasonable agreement with the difference in molar absorptivity expected if one mole of nitrate is formed for every mole of nitrite consumed ($1.6 \text{ M}^{-1} \text{ cm}^{-1}$).

A titration of HRP-I with nitrite was performed using the method employed for the titration of HRP-I with iodide. The result of the titration as illustrated in Fig. 4.05 indicates that each mole of nitrite reacts with two moles of HRP-I.

4.04 Discussion

Chance (1952c) interpreted the increase in rate with decreasing pH for the reactions of HRP-I and HRP-II with nitrite as an indication that nitrous acid is the reactive species. However an alternative explanation for the fact that the slopes of -1 for the plots of the logarithm of k_5 and k_6 vs. pH are the same as those observed for the reaction of iodide with HRP-I and HRP-II over the same pH range is that in the nitrite reactions this slope is due to the same enzyme groups bonded to the heme observed for the iodide reactions. This interpretation provides a self-consistent mechanism for the three inorganic substrates. Unlike the corresponding reactions with sulfite and iodide however, the reaction of HRP-I with nitrite involves the transfer of a single electron from nitrite to HRP-I forming HRP-II. The 2:1 ratio of HRP-I to nitrite observed for the titration of HRP-I with nitrite and the 1:1 ratio between

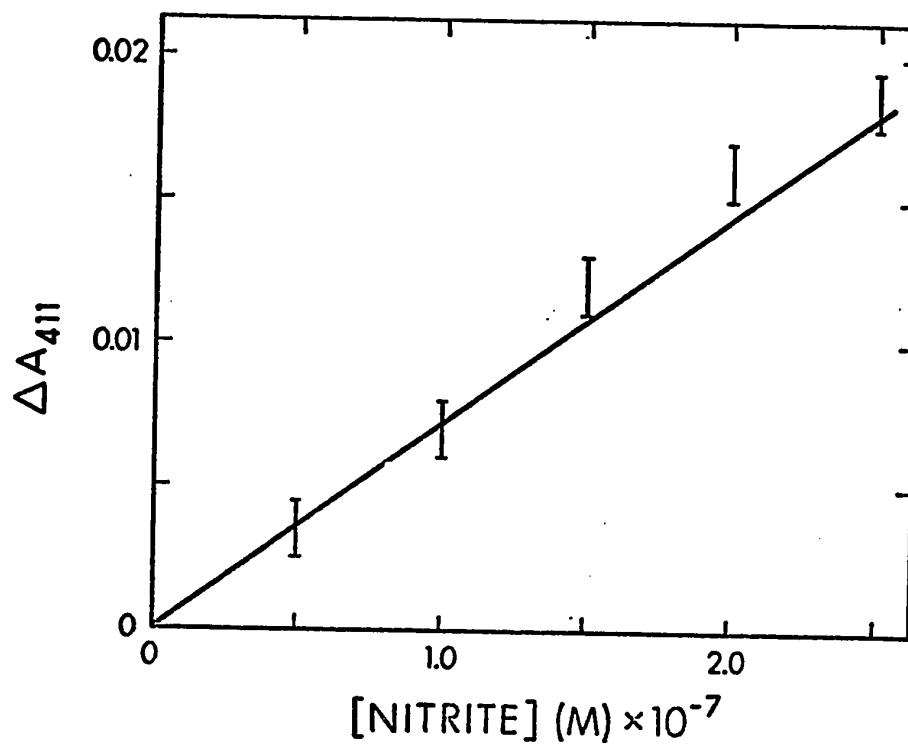
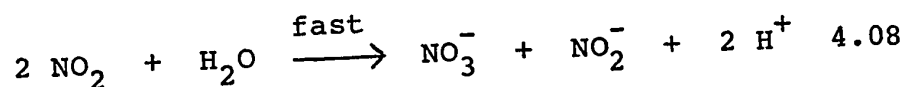
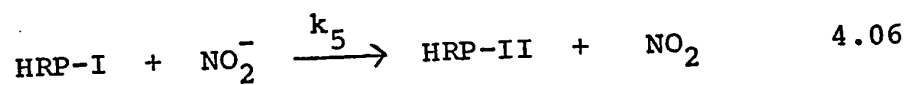


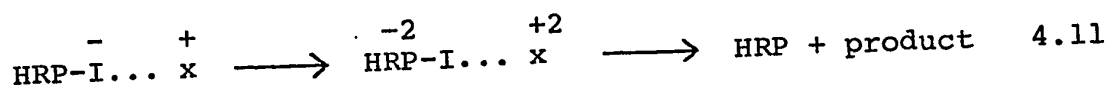
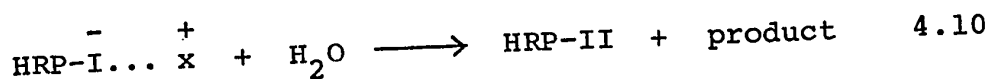
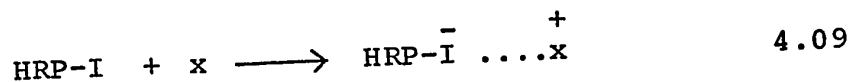
Fig. 4.05: Plot of the change in absorbance at 411 nm vs. the concentration of nitrite for the titration of HRP-I with nitrite. The solid line was calculated assuming a 2:1 ratio between HRP-I and nitrite using a difference in molar absorptivity of $3.6 \times 10^4 \text{ M}^{-1} \text{ cm}^{-1}$ interpolated from Fig. 2.13.

hydrogen peroxide and nitrite determined for the overall reaction indicates that the titration ratio between HRP-II and nitrite must also be 2:1. A simple mechanism for nitrite oxidation which incorporates the observed kinetics and stoichiometry for the reactions is



where a free NO_2 radical does not necessarily exist in aqueous solution.

It is somewhat surprising that nitrite reacts with HRP-I to produce HRP-II since it has been reported that compound I of catalase oxidizes nitrite in a direct two electron transfer without the production of compound II. In addition the reaction between nitrite and hydrogen peroxide produces nitrate via a mechanism that is analogous to that for the reaction of sulfite with hydrogen peroxide (Halperin and Taube, 1952). The following mechanism offers a simple rationale for the observed behavior of HRP-I with iodide, sulfite and nitrite



In the proposed mechanism the rate determining step is reaction 4.09 which is followed either by reaction 4.10 or 4.11. For the reactions of iodide and sulfite the products of a single electron oxidation, $I\cdot$ and SO_3^- , do not react rapidly with water so that step 4.11 predominates. For the nitrite reaction however, the reaction between NO_2 and water is rapid (Cotton and Wilkinson, 1966) so that reaction 4.10 predominates. In the reaction of compound I of catalase, the two electron transfer from nitrite could be due to the more transient nature of the initial enzymatic complex or perhaps to a more hydrophobic reaction site than HRP, which would hinder the reaction analogous to 4.10.

Chapter 5

High Resolution NMR Studies on HRP

5.01 Introduction

The NMR spectra for most proteins and enzymes are too complex for rigorous analyses, due to the large number of overlapping resonances observed in such spectra. The observation of Kowalsky (1965) that heme proteins had resonances well removed from the range normally observed for protons in NMR spectra indicated that a quantitative analysis of part of the NMR spectra for these proteins might be possible. Since these shifted resonances were due to the presence of the heme group, NMR experiments could be used to probe the site that is associated with the biological function of hemoproteins. The observations of Kowalsky were verified and extended by Kurland and Davis (1968) who published the NMR spectra of several iron porphyrins, including ferriprotoporphyrin IX, as well as metmyoglobin (My) and methemoglobin (Hb). These authors reported shifts of 30-90 ppm downfield from those observed for the diamagnetic porphyrins. The spectra of My and Hb were not as well resolved as those for the simple porphyrins, where line widths from 2-3 ppm were observed, thus no attempt was made to interpret the protein spectra.

The problems of large shifts and wide line widths that complicated the NMR spectra of My and Hb were to a large extent overcome by converting the high spin iron in these

proteins to low spin through the formation of the protein-cyanide complexes. The NMR spectrum of cyanometmyoglobin (My-CN) exhibited shifts of only 5-20 ppm and line widths of less than 0.3 ppm (Wüthrich et al., 1968a). The NMR spectrum of My-CN can be thought of as being divided into three sections: the section from 0 to -10 ppm (the internal reference was sodium 2,2-dimethyl-2-silapentane-5-sulfonate and was taken to be zero ppm) where the majority of the 950 protons of My-CN resonate, the section from 0 to 5 ppm where ten resonances were observed with intensities from one to three protons and the section from -10 to -27 ppm where nine well separated resonances were observed with intensities from one to three protons. The NMR spectra of all low spin heme proteins and porphyrins reported to date have displayed resonances shifted to high and low field similar to those observed for My-CN (Wüthrich, 1970).

There are three possible explanations for the observed shifts in the NMR resonances for heme proteins. One explanation is that the unpaired electron from the iron is delocalized in the π orbitals of the porphyrin ring and, in the case of My-CN and Hb-CN, into the imidazole ring of the histidine residue co-ordinated to the iron. From the study of aromatic radicals it has been established that the odd electron in these compounds occupies a molecular π orbital delocalized over the carbon framework of the molecule. This results in a coupling of the σ electrons in the C-H bond to the π electrons of the ring, referred to as the

contact interaction. This contact interaction causes a slight spin polarity in the C-H bond resulting in a negative spin density at the proton (Carrington and McLachlan, 1967). In the case of a methyl group bonded to an aromatic carbon, the methyl protons are coupled to the aromatic carbon via hyperconjugation so that these protons have a positive spin density. The second explanation is that the resonances could be shifted via pseudocontact interactions resulting from an anisotropic g tensor for the unpaired electron.

The g value is referred to as the spectroscopic splitting value for electron spin resonances and can be considered to be roughly analogous to the chemical shift in NMR experiments. In the present case the g values along the two principal axes in the plane of the heme group are different than the g value that is perpendicular to the heme, with the result that different protons will have different interactions with the unpaired electron depending on their spatial orientation. The third explanation is that the resonances could be shifted via interactions with the ring currents produced by the aromatic amino acids and the porphyrin ring.

The shifts arising from contact inversions can be expressed by

$$\Delta \nu_c = -A \frac{|\gamma_e|}{|\gamma_H|} s(s+1) \frac{\nu}{3kT}$$

where $\Delta\nu_c$ is the upfield shift from the corresponding diamagnetic molecule, γ_e and γ_H are the gyromagnetic ratios for the electron and proton, k is Boltzmann's constant, T the absolute temperature, S the electron spin, ν the operating frequency of the NMR instrument and A the contact inversion constant for the proton (Wüthrich et al. 1968b). The pseudocontact interaction can be expressed by

$$A_{\text{eff}} = A + \left(\frac{3\cos^2\psi - 1}{3r^3} \right) (g_{\parallel} - g_{\perp}) g_N \beta \beta_N \quad 5.02$$

where A_{eff} is the effective contact inversion constant, r is the distance from the unpaired electron to the nucleus, ψ is the angle between the paramagnetic ion-nucleus vector and the axis of the porphyrin, g_{\parallel} and g_{\perp} are the parallel and perpendicular g tensor components and β , g_N and β_N are constants (Carrington and McLachlan, 1967). Shifts arising from interactions between protons and the ring currents can be expressed by

$$\Delta\nu_r = \frac{\gamma_H n e^2 H_0 a^2 (3 \cos^2 \theta - 1)}{8\pi^2 m c^2 d^3} \quad 5.03$$

where d is the distance between the center of the ring and the proton in question, θ is the angle between d and the applied field H_0 , n is the number of delocalized π electrons with charge e and mass m , c the velocity of light and a the radius of the ring (Wüthrich et al., 1968a).

Since $\Delta\nu_r$ is independent of temperature and $\Delta\nu_c$ is not, a plot of $\Delta\nu$ observed vs. $\frac{1}{T}$ should distinguish between the two. Wüthrich (1970) reports that for My-CN, Hb-CN, the

ferriprotoporphylin IX-cyanide complex, cytochrome c and the cytochrome c-cyanide complex all the resonances at low field and those at high field except at 0 ± 1 ppm were shifted by contact or pseudocontact interactions. Wüthrich and co-workers state that the observed shifts appear too large to have resulted from pseudocontact interactions and thus to a good approximation the shifts can be considered to arise from contact interactions (Wüthrich et al., 1968a, 1969). More recently the work of Shulman et al. (1971) has shown that the pseudocontact interactions are appreciable and can be estimated if the values of g_{\parallel} and g_{\perp} in equation 5.02 are known.

The value of A, which can be calculated from equation 5.01, can be related to the unpaired spin density on the ring carbons of the porphyrin by McConnell's relation

$$A = Q \rho_c^{\pi} \quad 5.04$$

where Q is a proportionality constant which has the value of -6.3×10^7 Hz for protons on the porphyrin and 3.0×10^7 Hz for the protons of methyl groups attached to the porphyrin and ρ_c^{π} as the percent spin density on the aromatic ring carbon atom (Wüthrich et al., 1969). Using this relationship the authors were able to calculate the spin densities for the porphyrin carbon atoms of ferriprotoporphylin IX. The calculations were repeated by Shulman et al. (1971) with the contribution from the pseudocontact interactions taken into account.

The published NMR studies have been performed on proteins whose structures are known from X-ray crystallography. We thought that the NMR technique could also be useful in elucidating conformational details for heme proteins, like HRP, where the tertiary structure is unknown. Comparison of the NMR spectrum for such a compound to that for a compound of known structure, like My, could yield information concerning the protein environment surrounding the heme. The studies of Wüthrich et al. (1970) indicate that the NMR spectrum of My-CN is more sensitive to changes in the protein environment than to modification of the heme group. Ideally it might be possible to calculate the spin densities for a protein like HRP and compare them to the values calculated for My. Such a comparison might help explain the vastly different chemical functions of HRP and My. In addition it might also be possible to identify the ligand in the fifth co-ordination position of the iron in a protein of unknown structure. The presence of a histidine group co-ordinated to the iron in My (Wüthrich et al., 1970) and a methionine group in cytochrome c (Wüthrich, 1969) were verified by the NMR spectra of these two compounds.

5.02 Experimental

The NMR spectra were obtained on a Varian HA-100-15 MHz spectrometer with either 5 mm or 12 mm sample tubes. The ferriprotoporphyrin IX-cyanide complex was prepared by

dissolving 4 mg of protoporphyrin IX iron (III) chloride obtained from Eastman Organic Chemicals, with 30 mg potassium cyanide in 0.1 ml of D₂O and 0.4 ml of pyridine-d₅. When larger volumes of sample were required, the amounts of reagents used were increased accordingly. NMR spectra of the ferriprotoporphyrin IX-cyanide complex were recorded over a temperature range from -15° to 20°. The My-CN solution was prepared by dissolving 340 mg of My, lyophilized sperm whale myoglobin obtained from Mann Research, 50 mg of potassium cyanide, 8 mg of potassium dihydrogen phosphate and 14 mg of dipotassium hydrogen phosphate (to buffer the solution at pH 7) in 3 ml of D₂O. The concentration of My in the solution was 4×10^{-3} M. The solution was lyophilized from D₂O three times to remove the majority of exchangeable protons. The NMR spectra of My-CN was recorded at 18°. The HRP-cyanide complex (HRP-CN) solution was prepared by dissolving 2.0 gm of Grade II lyophilized HRP with P.N. of 0.9 obtained from Boehringer-Mannheim, 50 mg of potassium cyanide, 8 mg of potassium dihydrogen phosphate and 14 mg of dipotassium hydrogen phosphate in 3 ml of D₂O. The concentration of HRP in solution was 6.7×10^{-3} M. This solution was also lyophilized from D₂O three times. The NMR spectra of HRP-CN were recorded over the temperature range from 18° to 60°.

5.03 Results

The NMR spectrum of the low field region of the ferri-protoporphyrin IX-cyanide complex observed at -15° is illustrated in Fig. 5.01a. The spectrum of the ferriprotoporphyrin IX diethylester-cyanide complex obtained on a 220 MHz NMR spectrometer by Wüthrich *et al.* (1969) over the same frequency range is reproduced in Fig. 5.01b. The four sharp peaks at low field in Fig. 5.01a and 5.01b are the methyl resonances from the four methyl groups on the porphyrin ring. As evident from Fig. 5.01a and 5.01b the signal-to-noise ratio of the two spectra are comparable.

The low field NMR spectra obtained for My-CN at 18° is illustrated in Fig. 5.01d. The spectrum of My-CN at 35° obtained by Wüthrich *et al.* (1968a) on the 220 MHz spectrometer is reproduced in Fig. 5.01c. The shifts of the peaks in the two spectra are not identical, since the spectra were recorded at two different temperatures, but clearly the resolution of the 100 MHz instrument is approaching that for the 220 MHz instrument.

Figs. 5.02, 5.03 and 5.04 illustrate the NMR spectra observed for HRP-CN in the low field region, the intermediate region and the high field region. No resonances outside the normal range of proton resonances could be detected from -50 to 77 ppm of TMS over a temperature range from 18° - 60° .

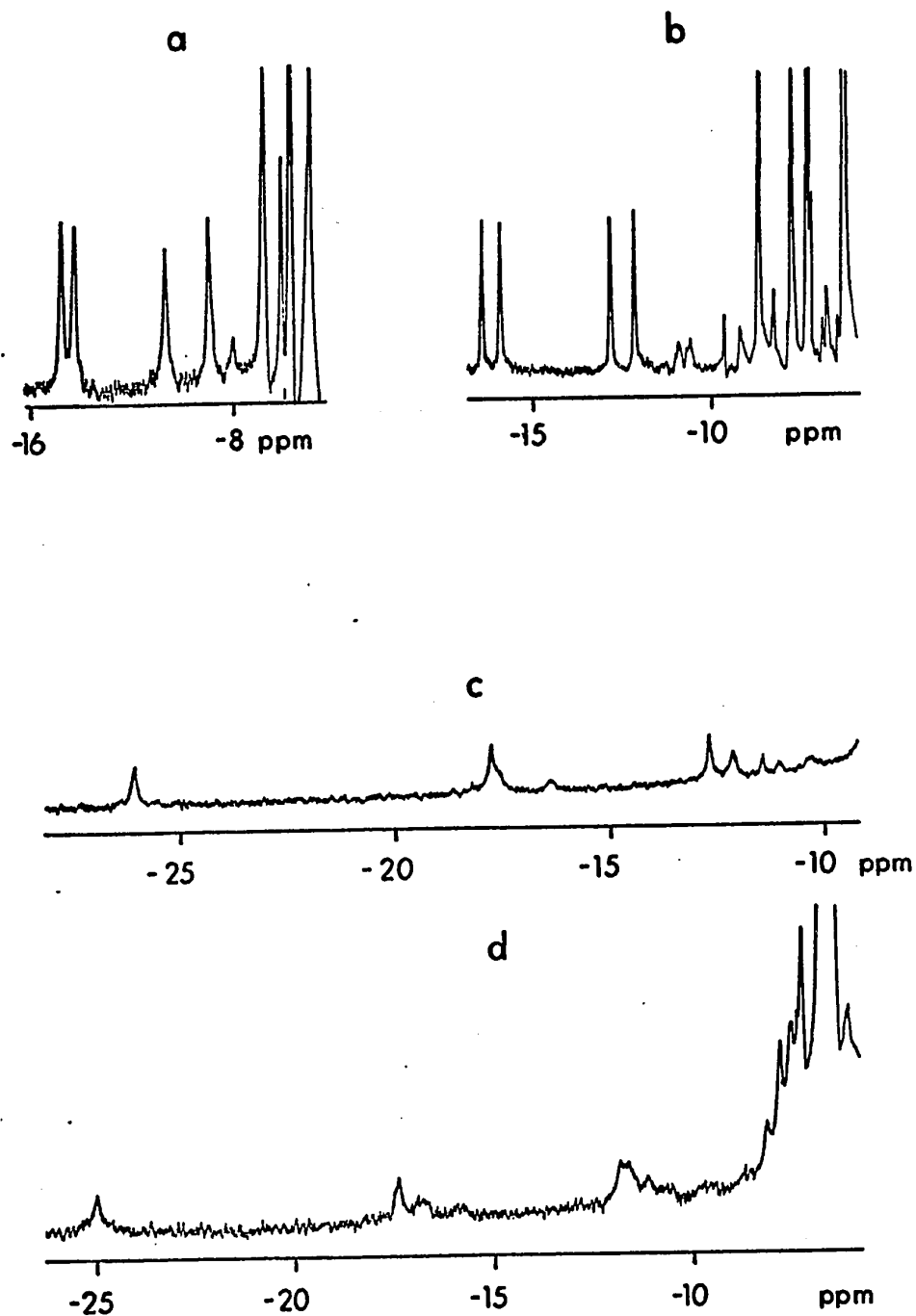


Fig. 5.01: NMR spectra obtained on a 100 MHz instrument compared to those obtained on a 220 MHz instrument. The spectra in (a) and (d) were obtained on a 100 MHz instrument and the spectra in (b) and (c) were obtained on a 220 MHz instrument. The spectra (a) and (b) are of the ferriprotoporphyrin IX-cyanide complex and the spectra (c) and (d) are of My-CN.

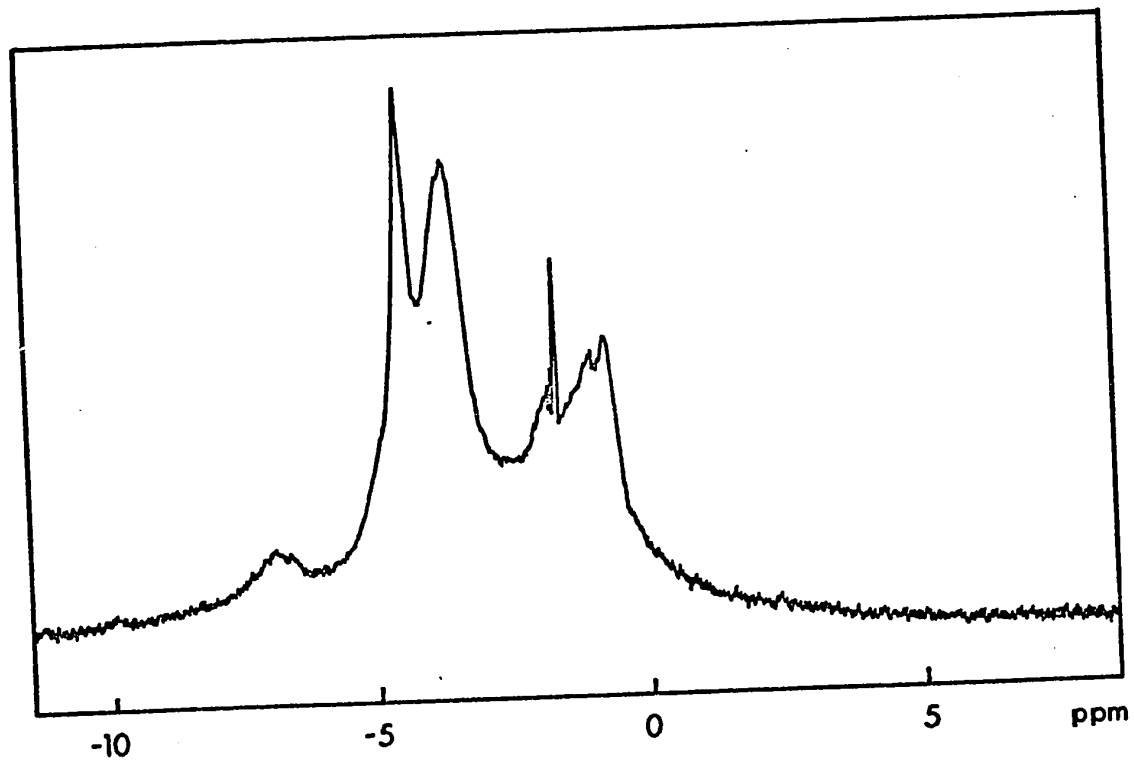


Fig. 5.02: NMR spectrum of HRP-CN over the range where normal proton resonances are observed.

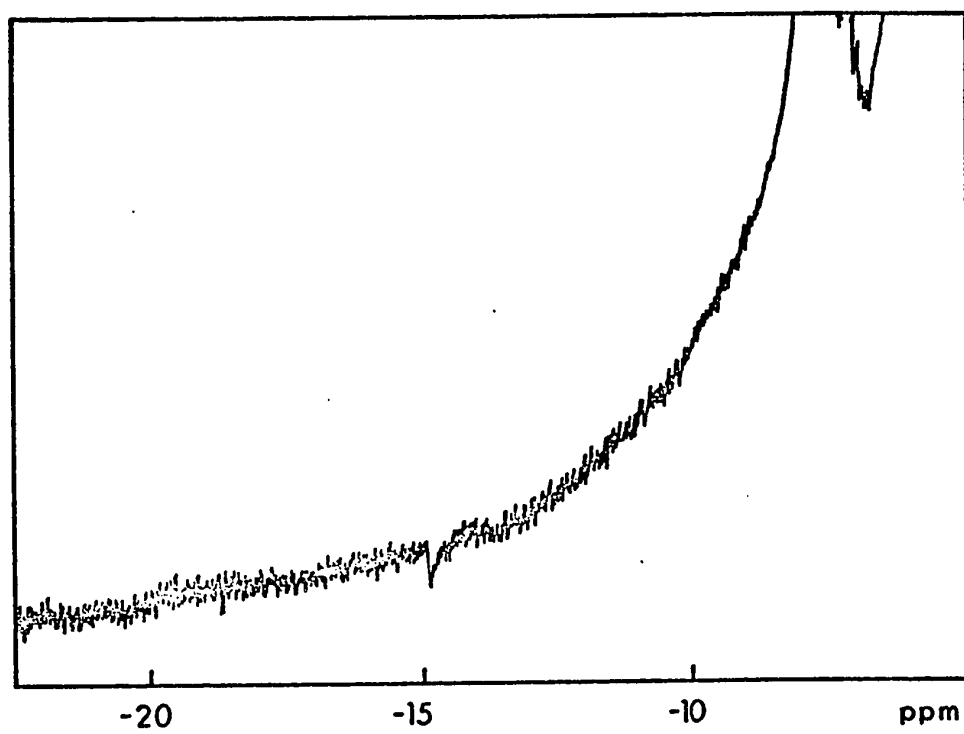


Fig. 5.03: NMR spectrum of HRP-CN at low field.

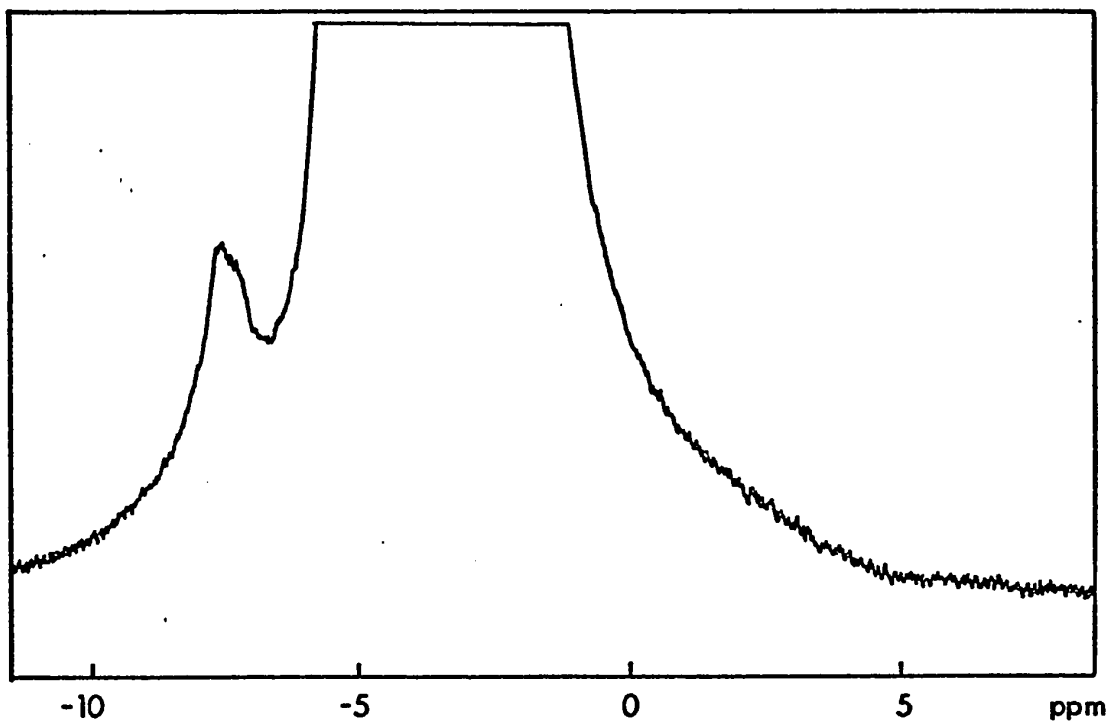


Fig. 5.04: NMR spectrum of HRP-CN at high field.

5.04 Discussion

Because of the similarity of the magnetic and spectral properties of HRP to other heme proteins it is reasonable to assume that the resonances shifted by the paramagnetic iron, observed for the other proteins, are also present for HRP. It seems unlikely that the absence of these resonances in the spectrum of HRP could be due to a difference in sensitivity between the 100 MHz and 220 MHz NMR spectrometers. The signal-to-noise ratio of a NMR spectrometer is proportional to the square of the frequency, thus the 220 MHz instrument would have a 4.8 fold enhancement in the signal-to-noise ratio compared to the 100 MHz instrument. The 100 MHz NMR spectrometer used in the present studies, however, had the capacity for 12 mm sample tubes compared to the 5 mm tubes used in the 220 MHz NMR spectrometer. A five fold increase in volume can be achieved with the 12 mm tubes, yielding a five fold increase in the signal-to-noise ratio, thus the sensitivity of the 100 MHz and the 220 MHz instruments should be approximately equal. The similar sensitivity of the two spectrometers is evident by comparing the spectra in Fig. 5.01a and 5.01b and 5.01c and 5.01d.

The most probable reason for the absence of any observable resonances shifted to high and low field for HRP-CN is that these resonances are so broad that they cannot be distinguished from the baseline. One explanation for such broadening is that the electronic relaxation time

for the unpaired electron in HRP-CN is sufficiently slow to broaden the observed line widths. The line broadening for a given proton resonance in contact with an unpaired electron is

$$\delta\nu_e = \frac{S(S+1)}{3\pi} \left(\frac{A^2 T_{1e}}{h^2} + \frac{\gamma_e^2 \gamma_H^2 h^2}{5r^6} \left[7\tau_c + \frac{13\tau_c}{1+\omega_s \tau_c^2} \right] \right) \quad 5.05$$

where $\delta\nu_e$ is the resulting line broadening in Hz at half height for a given proton resonance, T_{1e} is the longitudinal electronic relaxation time, τ_c is the correlation time for dipole-dipole coupling, ω_s is the resonance frequency of the electron in radians/sec, h is Planck's constant and the other terms have been previously defined (Wüthrich, 1970). If T_{1e} is sufficiently short, τ_c is proportional to T_{1e} and equation 5.05 indicates that the unpaired electron will not broaden the proton resonances appreciably. This is the case for My-CN where a value for T_{1e} of 2×10^{-12} sec has been reported (Wüthrich, 1970). The line width, $\delta\nu$, for the resolved lines in the NMR spectra of the heme proteins is

$$\delta\nu = \delta\nu_e + \delta\nu_{H-H} \quad 5.06$$

where $\delta\nu_{H-H}$ is the line broadening from dipolar coupling between protons modulated by the random tumbling of the entire protein molecule (Wüthrich *et al.*, 1968b). For large proteins $\delta\nu_{H-H}$ can be considered to vary with τ_r , the correlation time for rotational tumbling of the molecule.

The line width of an ESR resonance varies as the inverse of the electronic relaxation time, that is, for very short relaxation times the ESR resonance is broadened into the base line. In general if an ESR resonance can be observed at a given temperature, the value of T_{1e} is sufficiently slow that the NMR resonance shifted by the paramagnetic species will be too broad to be detected. The ESR spectrum for HRP-CN has been reported by Blumberg et al. (1968). The spectrum was measured at 1.4°K and even at this temperature the resonances were fairly broad thus indicating a small value for the electronic relaxation time. This fact implies that at room temperature the electronic relaxation time should be sufficiently short not to broaden the NMR resonances.

Although one cannot be certain that the NMR resonances for HRP-CN are not broadened by the electronic relaxation time without observing its ESR spectra over a range of temperature, the work of Blumberg et al. would indicate that some other explanation is probably necessary to account for the absence of shifted resonances in the HRP-CN NMR spectrum.

An alternative explanation for the broadening of the shifted resonances in HRP-CN is that this broadening is the result of an increased rotational correlation time compared to My-CN and Hb-CN. The formula for the rotational correlation time for a perfect sphere is

$$\tau_r = \frac{4\pi \eta a^3}{3kT}$$

5.07

where a is the radius of the sphere and η is the viscosity of solution. The rotational correlation time can be thought of as the average time taken by a molecule tumbling randomly in solution to return to a given orientation. The rotational correlation time for a protein depends on the viscosity of the solution. At sufficiently high concentrations, the protein will contribute a significant portion of the viscosity and hence result in broadening of the NMR resonances. Such a situation was reported by Wüthrich et al (1968a) for My-CN. The spectrum of My-CN reproduced in Fig. 5.01c was measured for a solution of 5×10^{-3} M. The authors report that significant line broadening was observed if My-CN concentrations greater than 8×10^{-3} M were used. HRP-CN which has a molecular weight almost $2\frac{1}{2}$ times that of My-CN would be expected to have a larger effect on the viscosity of solution than a My-CN solution of the same concentration. In addition the crude HRP used for the NMR studies contained only 30% HRP with about 70% of the enzyme added to solution being comprised of extraneous protein (as estimated from the P.N. of the crude HRP). This extraneous protein would tend to further increase the viscosity of the HRP-CN solutions and hence broaden the resonances as compared to My-CN at the same concentration. Spectra of HRP-CN were recorded at lower

enzyme concentrations and at higher temperatures than illustrated in Figs. 5.02 - 5.04 in order to reduce the viscosity of solution, however, in no case were any shifted resonances observed.

The shifted NMR resonances observed for Hb-CN are broader and less well defined than the corresponding My-CN resonances (Wüthrich et al., 1968b) . The reason for the line broadening is due to the increased rotational correlation time for Hb-CN as compared to My-CN. The correlation time for Hb has been measured to be 8.5×10^{-8} sec and that for My to be 2.9×10^{-8} sec (Cohn and Edsall, 1943). The three fold increase in line width observed for Hb-CN compared to My-CN corresponds closely to the increase in the rotational correlation times for the two species. In addition to the size of a protein the rotational correlation time also depends on the shape of the molecule. Since both My and Hb are very nearly spherical, the correlation times for these two species represent an approximate minimum value that would be expected for proteins of their molecular weight. Thus if HRP is a spherical protein it would be expected to have a correlation time approximately two times that of My. Since the shape of HRP is not precisely known, it is possible that its correlation time could be greater than that for My by a factor even greater than two. The fact that HRP contains about 18% of its molecular weight in the form of eight carbohydrate side chains (Welinder and Smillie, 1972) also indicates the possibility that HRP could have a longer

rotational condition time than a spherical protein of the same molecular weight.

Both the increased viscosity of the HRP-CN solution and the increased molecular weight compared to My-CN would broaden the shifted NMR resonances of HRP-CN. The problem of the increased viscosity of the HRP-CN solution could have been partially overcome by using a highly purified sample of HRP. Considering the amount of HRP required for a single NMR experiment, the cost involved by using purified HRP would be prohibitively high. From our present results, it would appear, at best, that pure HRP and perhaps higher temperatures would only show an indication of the shifted resonances, with a well resolved spectrum being beyond the sensitivity of present NMR spectrometers. Since a meaningful interpretation of the shifted NMR spectrum could only result from the assignment of resonances to particular protons and the possible calculation of spin densities, further attempts to observe these resonances for HRP-CN were not undertaken.

Summary, Conclusions and Suggestions for Further Work

A thorough understanding of the mechanism for HRP catalysis requires knowledge of the active sites for HRP-I and HRP-II. As evident from Chapter 1, at the present time our available knowledge concerning this area is limited and often contradictory. We hope that our kinetic results will enable us to define, at least partially, the active site of the two compounds.

The pH dependence of the HRP-II-iodide reaction indicates the presence of an acid group in HRP-II which is in intimate association with the heme group and which has a major effect on the observed rate of reaction. This acid group is described as being bonded to the heme. Although the possibility exists that the ionization of this group is an ionization of the heme, the more attractive assumption is that this group is co-ordinated to the iron. Protonation of such a group would reduce its attraction for the positively charged iron and thus facilitate the approach of a reducible substrate.

The pH dependence for the HRP-I-iodide reaction is more complex than that for the HRP-II reaction due to the presence of a kinetically important enzyme ionization with a pK_a value of approximately 5. However, the explanation for the kinetic pH dependence of the HRP-I reaction also requires that a group be bonded to the heme. In HRP-I, this group may ionize with a pK_a of 4.6 or, like HRP-II, the group may

ionize at lower pH. In either case, the presence of a second ionization implies that another group in the active site of the enzyme has an influence on the reaction. Unlike a group that is bonded to the heme, which would be expected to influence the reactions with all substrates, the smaller kinetic effect of a secondary group in the active site could be expected to be very susceptible to different substrates. For example, if the group with a pK_a of 4.6 observed for the HRP-I-iodide reaction is not bonded to the heme but rather exerts its kinetic effect through a steric interaction with the iodide ion, a smaller substrate would be expected to display a smaller kinetic effect to the ionization of this group. Thus the comparison of the pH dependences for a variety of different substrates should allow us, in principle, to determine the nature of the interactions of these secondary ionizable groups in the active site of the enzyme.

The pH dependences for the reactions of HRP-I and HRP-II with sulfite are more complicated than those for the corresponding reactions with iodide and, in addition, the interpretation of the sulfite reactions are complicated by the kinetic ambiguity introduced by the various possible protonated forms of the substrate. The assumption that the groups bonded to the heme in HRP-I and HRP-II have a similar effect for the reactions of both sulfite and iodide leads to a considerable simplification in the interpretation of the sulfite reactions, since with this assumption it is possible to show that bisulfite ion is the reacting species

in the reactions with HRP-I and HRP-II. Over the range of pH where the reactions of HRP-I with both iodide and sulfite were studied, the kinetic pH profiles are very similar. The HRP-II-sulfite reaction, on the other hand, is influenced by an enzyme ionization with a pK_a value of 3.9 that has no influence on the HRP-II-iodide reaction. Although the identification of the nature of the interaction of this group from the behavior of only two substrates is very speculative, hydrogen bond formation between the bisulfite ion and a carboxyl group on the enzyme is a reasonable hypothesis.

In addition to information concerning the nature of secondary groups in the active site of the enzyme, the HRP-I-sulfite reaction could potentially be used to elucidate the nature of the heme-bound group in HRP-I. As mentioned previously, the work of Halperin and Taube (1952) has shown that sulfate formed from the reaction of oxygen-18 labelled hydrogen peroxide and sulfite contained both atoms of labelled oxygen. Thus if the product analysis for the reaction of HRP-I formed from oxygen-18 labelled hydrogen peroxide and sulfite indicates that the sulfate contains oxygen-18, it would provide strong evidence that the heme-bound group in HRP-I is a peroxide fragment. Unfortunately the absence of any labelled oxygen in the sulfate would not necessarily indicate that there was no peroxide fragment present in HRP-I, since the oxygen acquired by the oxidized sulfite species could also come from the aqueous solution.

The steady-state concentrations of HRP-I and HRP-II that were observed for the HRP-catalyzed reactions of iodide, sulfite and nitrite could provide a convenient method for obtaining a known concentration of these labile compounds. This could be a major advantage for future physical measurements on these compounds. In this regard the HRP-nitrite system seems ideally suited for the production of known concentrations of HRP-II, since the HRP-II-nitrite reaction is slow. Experiments were performed, concerned with obtaining the steady-state spectrum illustrated in Fig. 4.03, which indicated that stable solutions of HRP-II can be maintained for 30 minutes or longer.

In order to gain insight into the general mechanism of HRP catalysis it is necessary to compare the kinetics of the three inorganic substrates, iodide, sulfite and nitrite, to the other possible substrates of HRP. Such a comparison has been made for the reactions of HRP-II with iodide, ferrocyanide and p-cresol (Critchlow and Dunford, 1972b). In addition to phenols, there are two other types of organic compounds, aromatic amines and ene-diols, which have proved to be common substrates for HRP. A complete picture of the mechanism of HRP catalysis would thus require a detailed kinetic study of these classes of compounds and in this regard a study of the oxidation of HRP-I and HRP-II with p-amino benzoic acid is now underway in our laboratory.

In addition to the information provided concerning the mechanism of the reactions of HRP-I and HRP-II, the kinetic

studies involving the three inorganic substrates are important with regard to the peroxidase-catalyzed oxidation in the thyroid gland. The experiments in Chapter 2 provide the first clear evidence that I^+ is the initial iodine containing product formed in the HRP-catalyzed oxidation of iodide, although such a product has previously been suggested for thyroid peroxidase (White *et al.*, 1964). In addition, Hager and Brown (1967) reported, based on product analysis for the chlorination of anisole, that chloroperoxidase oxidizes chloride via a two electron transfer to produce Cl^+ . The study of the HRP-I-sulfite reaction illustrated that a two electron transfer from substrate to enzyme was not unique to iodide. The fact that nitrite undergoes a single electron oxidation in its reaction with HRP-I, even though it undergoes a two electron transfer in its reaction with hydrogen peroxide (Halperin and Taube, 1952), is rationalized in the mechanism postulated for the reaction of HRP-I with inorganic substrates illustrated in Chapter 4.

Although the studies with iodide, sulfite and nitrite present a reasonably consistent model for the oxidation of iodide in the thyroid, the possibility that thyroid peroxidase serves an additional function in the synthesis of thyroxine, remains open to investigation. For example a kinetic study of the reactions of HRP-I and HRP-II with tyrosine would provide basic information concerning the feasibility of the involvement of a peroxidase in the iodination of tyrosine residues. A kinetic study of the

oxidation of iodinated tyrosines with respect to product formation, could possibly verify the function of thyroid peroxidase in the coupling of the two tyrosine residues necessary in thyroxine formation. A kinetic study of the HRP-catalyzed oxidation of thyroxine could provide information on the possible feedback mechanism for the control of thyroxine levels involving peroxidases. Finally, if all the simpler reactions were understood, the production of thyroxine from a mixture of peroxidase and thyroglobulin could be studied, thus providing a good model for thyroxine production in situ. Although the problem of obtaining an accurate model for the production of thyroxine is clearly quite complex, a reasonable solution should be possible if a systematic approach to the problem is employed.

Bibliography

1. Abel, E. (1951), Monatsh. Chem. 82, 815.
2. Alberty, R. A. and Bloomfield, V. (1963), J. Biol. Chem. 238, 2804.
3. Alberty, R. A. and Hammes, G. G. (1958), J. Phys. Chem. 62, 154.
4. Altshuller, A. P. and Wartburg, A. F. (1960), Anal. Chem. 32, 174.
5. Bach, A. N. and Chodat, R. (1903), Ber. dtsh. chem. Ges. 36 B, 606.
6. Battelli, F. and Stern, L. (1908), Biochem. Z. 13, 44.
7. Bell, R. P. (1959), in "The Proton in Chemistry", Cornell University Press, Ithaca, N.Y., p. 89.
8. Björkstén, F. (1968), European J. Biochem. 5, 133.
9. Björkstén, F. (1970), Biochim. Biophys. Acta 212, 396.
10. Blumberg, W. E., Peisach, J., Wittenberg, B.A. and Wittenberg, J. B. (1968), J. Biol. Chem. 243, 1854.
11. Brill, A. S. (1966), Comp. Biochem. 14, 447.
12. Brill, A. S. and Sandberg, H. E. (1968), Biochemistry 7, 4254.
13. Brill, A. S. and Williams, R.J.P. (1961), Biochem. J. 78, 253.
14. Brown, S. B. and Jones, P. (1968), Trans. Far. Soc. 64, 994.
15. Caldwell, E. S. and Steelink, C. (1969), Biochim. Biophys. Acta 184, 420.

16. Carrington, A. and McLachlan, A. D. (1967), in "Introduction to Magnetic Resonance", Harper and Row, New York, N.Y.
17. Chance, B. (1949), Arch. Biochem. Biophys. 22, 224.
18. Chance, B. (1952a), J. Biol. Chem. 197, 577.
19. Chance, B. (1952b), Arch. Biochem. Biophys. 37, 235.
20. Chance, B. (1952c), Arch. Biochem. Biophys. 41, 416.
21. Chance, B., De Vault, D., Legallais, U., Mela, L. and Yonetani, T. (1967), in Nobel Symposium V, "Fast Reactions and Primary Processes in Chemical Kinetics", Interscience, New York, N.Y., p. 437.
22. Chapman, N. B. and Saunders, B. C. (1941), J. Chem. Soc., 496.
23. Chen, J. (1968), Ph.D. Thesis, University of California, Riverside, Calif.
24. Cohn, E. J. and Edsall, J. T. (1943), in "Proteins, Amino Acids and Peptides", Reinhold, New York, N.Y., p. 557.
25. Cotton, M. L. and Dunford, H. B. (1972), submitted for publication.
26. Cotton, M. L., Dunford, H. B. and Raycheba, J. (1972), submitted for publication.
27. Critchlow, J. C. and Dunford, H. B. (1972a), in press.
28. Critchlow, J. C. and Dunford, H. B. (1972b), in press.
29. Critchlow, J. C. and Dunford, H. B. (1972c), submitted for publication.
30. Critchlow, J. C. and Dunford, H. B. (1972d), in "Second Symposium on Oxidases and Related Oxidation-Reduction Systems", in press.

31. Daniels, D.G.H., Naylor, F. T. and Saunders, B. C. (1951), J. Chem. Soc., 3433.
32. Dixon, M. and Webb, E. C. (1964), in "Enzymes", 2nd ed., Longmans, Green, London, p. 124.
33. Dolman, D. and Dunford, H. B. (1972), in preparation.
34. Dolphin, D., Forman, A., Borg, D. C., Fajer, J. and Felton, R. H. (1971), Proc. Nat. Acad. Sci. U.S. 68, 614.
35. Ellis, W. D. (1968), Ph.D. Thesis, University of Alberta, Edmonton.
36. Ernest, A. and Berger, H. (1907), Ber. dtsh. chem Ges. 40, 467.
37. Fox, R. L., Purves, W. K. and Nakada, H. J. (1965), Biochemistry 4, 2754.
38. Fridovich, I. and Handler, P. (1961), J. Biol. Chem. 236, 1836.
39. Frost, A. A. and Pearson, R. G. (1961), in "Kinetics and Mechanism", 2nd ed., John Wiley and Sons Inc., New York, N.Y., p. 29.
40. George, P. (1953a), J. Biol. Chem. 201, 413.
41. George, P. (1953b), Biochem. J. 54, 267.
42. Golding, R. M. (1960), J. Chem. Soc., 3771.
43. Hager, L. P. and Brown, D.R. (1967), J. Am. Chem. Soc. 89, 719.
44. Halperin, J. and Taube, H. (1952), J. Am. Chem. Soc. 74, 380.
45. Hammond, G. S. (1955), J. Am. Chem. Soc. 77, 334.

46. Hasinoff, B. B. (1970). Ph.D. Thesis, University of Alberta, Edmonton.
47. Hasinoff, B. B. and Dunford, H. B. (1970), Biochemistry 9, 4930.
48. Higginson, W.C.E. and Marshall, J. (1957), J. Chem. Soc., 447.
49. Hinman, R. L. and Lang, J. (1965), Biochemistry 4, 144.
50. Hosoya, T. (1968), Gunma Symp. Endocrinol. 5, 219.
51. Keilin, D. and Hartree, E. F. (1951), Biochem. J. 49, 88.
52. Keilin, D. and Mann, T. (1937), Proc. Roy. Soc. B 122, 199.
53. Kendrew, J. C. (1962), Brookhaven Symposia in Biology 15, 216.
54. Kitto, G. B., Wassarman, P. M. and Kaplan, N. O. (1966), Proc. Nat. Acad. Sci. U.S. 56, 579.
55. Klebanoff, S. J. (1961), Biochim. Biophys. Acta 48, 93.
56. Kolthoff, I. M. and Sandell, E. B. (1963), in "Textbook of Quantitative Inorganic Analysis", 3rd ed., MacMillan Co., New York, N.Y., p. 544.
57. Kowalsky, A. (1965), Biochemistry 4, 2382.
58. Kuhn, R., Hand, D. B. and Florkin, M. (1931), Z. physiol. chem. 201, 225.
59. Kurland, R. J., Davies, D. G. and Ho, C. (1968), J. Am. Chem. Soc. 90, 2700.
60. Kurozumi, T., Inada, Y. and Shibata, K. (1961), Arch. Biochem. Biophys. 594, 464.
61. Lee, T. and Hager, L. P. (1970), Fed. Proc. 29, 599.

62. Linossier, M.G.C.R. (1898), Soc. Biol. Paris 50, 373.
63. Maehly, A. C. (1951), in "Enzymes and Enzyme Systems", Edsall, J. T. Ed., Cambridge, Mass., Harvard University Press, p. 77.
64. Maehly, A. C. (1955), in "Methods in Enzymology", Vol. 2, Colowich, S. P. and Kaplan, N. O. Eds., Academic Press, New York, N.Y., p. 801.
65. Maguire, R. J. and Dunford, H. B. (1972a), in press.
66. Maguire, R. J. and Dunford, H. B. (1972b), submitted for publication.
67. Markert, C. F. and Moller, F. (1959), Proc. Nat. Acad. Sci. J.S. 45, 653.
68. Moss, T. H., Ehrenberg, A. and Bearden, A. J. (1969), Biochemistry 8, 4159.
69. Nunez, J. and Pommier, J. (1968), European J. Biochem. 5, 114.
70. Ovenston, T.C.J. and Rees, W. T. (1950), Anal. (London) 75, 204.
71. Paul, K. G. (1960), in "The Enzymes", Vol. 3, 2nd ed., Boyer, P. D., Hardy, H. and Myrback, K. Eds., New York, N.Y., p. 293.
72. Paul, K. G. (1963), in "The Enzymes", Vol. 8, Part B, 2nd ed., Boyer, P. D., Hardy, H. and Myrback, K. Eds., New York, N.Y., p. 227.
73. Paul, K. G., Gewitz, H. S. and Volker, W. (1959), Acta Chem. Scand. 13, 1240.
74. Paul, K. G. and Stigbrand, T. (1970). Acta Chem. Scand. 24, 3607.

75. Peisach, J., Blumberg, W. E., Wittenberg, B. A. and Wittenberg, J. B. (1968), J. Biol. Chem. 243, 1871.
76. Phelps, C., Forlani, L. and Antonini, E. (1971), Biochem. J. 124, 605.
77. Planche (1810), Bull. Phar. 2, 578.
78. Ramette, R. W. and Sandford, R. W. (1965), J. Am. Chem. Soc. 87, 5001.
79. Roman, R. and Dunford, H. B. (1972), in press.
80. Roman, R., Dunford, H. B. and Evett, M. (1971), Can. J Chem. 49, 3059.
81. Rombauts, W. A., Schroeder, W. A. and Morrison, M. (1967), Biochemistry 6, 2965.
82. Saunders, B. C., Holmes-Siedle, A. G. and Stark, B. P. (1964), in "Peroxidases", Butterworths, London.
83. Schönbein, C. F. (1855), Verch. naturf. Ges. Basel 1, 339.
84. Seo, E. T. and Sawyer, D. T. (1964), J. Electroanal. Chem. 7, 184.
85. Shannon, L. M., Kay, E. and Lew, J. Y. (1966), J. Biol. Chem. 241, 2166.
86. Shulman, R. G., Glarum, S. H. and Karplus, M. (1971), J. Mol. Biol. 57, 93.
87. Smith, D. W. and Williams, R.J.P. (1969), in "Structure and Bonding", Vol. 7, Springer-Verlag, New York, N.Y., p. 1.
88. Swedin, B. and Theorell, H. (1940), Nature 145, 71.
89. Taurog, A. (1970), Arch. Biochem. Biophys. 139, 212.
90. Theorell, H. (1941), Enzymologia 10, 250.
91. Theorell, H. (1942), Arkiv. Kemi Miner. Geol. 16A, No. 2.

92. Theorell, H. (1943), Arkiv Kemi Miner. Geol. 16A, No. 14.
93. Theorell, H. and Akeson, A. (1943), Arkiv Kemi Miner. Geol. 16A, No. 8.
94. Theorell, H., Bergstrom, S. and Akeson (1942), Arkiv. Kemi Miner. Geol. 16A, No. 13.
95. Thomas, J. A., Morris, D. R. and Hager, L. P. (1970), J. Biol. Chem. 245, 3129.
96. Tohjo, M., Nakamura, Y., Kurihara, K., Samejima, T., Huchimori, Y. and Shibata, K. (1962), Arch. Biochem. Biophys. 99, 222.
97. Watson, H. C. (1968), in "Progress in Stereochemistry", Vol. IV, Aylett, A. and Harris, M. M. Eds., Butterworths, London, p. 299.
98. Welinder, K. G. and Smillie, L. B. (1972), submitted for publication.
99. Welinder, K. G., Smillie, L. B. and Schonbaum, G. R. (1972), submitted for publication.
100. White, A., Handler, P. and Smith, E. L. (1964), in "Principles of Biochemistry" 3rd, ed. McGraw-Hill New York, N.Y., p. 83.
101. Wüthrich, K. (1969), Proc. Nat. Acad. Sci. U.S. 63, 1071.
102. Wüthrich, K. (1970), in "Structure and Bonding", Vol. 8, Springer-Verlag, New York, N.Y., p. 53.
103. Wüthrich, K., Shulman, R. G. and Peisach, J. (1968a), Proc. Nat. Acad. Sci. U.S. 60, 373.
104. Wüthrich, K., Shulman, R. G. and Yamane, J. (1968b), Proc. Nat. Acad. Sci. U.S. 61, 1199.

105. Wüthrich, K., Shulman, R. G., Wyluda, B. J. and Caughey, W. S. (1969), Proc. Nat. Acad. Sci. U.S. 62, 636.
106. Wuthrich, K., Shulman, R. G., Yamane, T., Wyluda, B. J. Hugli, T. E., Gurd, F.R.N. (1970), J. Biol. Chem. 245, 1947.
107. Yamazaki, T., Mason, H. S. and Piette, L. (1960), J. Biol. Chem. 235, 2444.
108. Yang, S. F. (1970), Biochemistry 9, 5008.
109. Yonetani, T. (1970), in "Advances in Enzymology", Vol. 33, Nord, F. F. Ed., Interscience Publishers, New York, N.Y., p. 309.

Appendix 1

Purification of Crude HRP

In order to determine the isozyme content of the HRP used in the kinetic studies (obtained from Boehringer-Mannheim) a crude batch of the enzyme was purified on a Sephadex carboxy methyl cellulose (CM C-50) column. This column material separates compounds by both size and charge. In general larger molecules are eluted faster than small ones and negatively charged molecules are eluted faster than positively charged ones. The purification technique was a modification of that used by Shannon et al. (1966). These authors isolated and purified to homogeneity seven isozymes of HRP from horseradish roots. It was hoped that by using the chromatography conditions of Shannon et al. that it would be possible to correlate the isozymes present in the Boehringer-Mannheim preparation with those determined by the former authors.

Experimental Procedure

The column material was prepared by adding 4 g of CM C-50 Sephadex to 750 ml of pH 4.4 acetate buffer of ionic strength 0.005. The Sephadex was kept in contact with the buffer for 24 hours with several changes of supernatant liquid to ensure the complete equilibration with the buffer and the elimination of the finest Sephadex particles. The equilibrated Sephadex was poured into a 2.5 × 45 cm column (Sephadex Laboratory Column type K 25/45) and the excess

buffer drained off.

Between 40 and 500 mg of Grade II lyophilized HRP from Boehringer-Mannheim was dissolved in 2 ml of pH 4.4 acetate buffer of ionic strength 0.005 and carefully applied to the column. The column was then eluted with a linear gradient consisting of 500 ml of pH 4.4 acetate buffer of ionic strength 0.005 and pH 4.4 acetate buffer of ionic strength 0.1. The flow rate of the column was usually about 1 ml/min and fractions of approximately 10 ml were collected. Just before this elution system was exhausted a second elution system consisting of a linear gradient of 300 ml of pH 4.4 acetate buffer of ionic strength 0.1 and 300 ml of pH 4.9 acetate buffer of ionic strength 0.25 was begun.

The absorbance of each sample was determined on a Beckman DU spectrophotometer at 403 nm and 280 nm. Fig. A 1.01 illustrates a plot of absorbance vs. fraction number for a 500 mg sample of HRP. The absorbance at 403 nm monitors the concentration of HRP and the absorbance at 280 nm monitors the aromatic amino acids in both HRP and extraneous proteins.

For kinetic studies, fractions of the main peak with P.N. of 2.8 or greater were pooled and precipitated at -10° in a centrifuge by dissolving 53 gm of ammonium sulfate per 100 ml of enzyme solution. Following centrifugation, the supernatant liquid was decanted and the precipitated enzyme was dissolved in a small volume of water and dialyzed against distilled water. After dialysis the

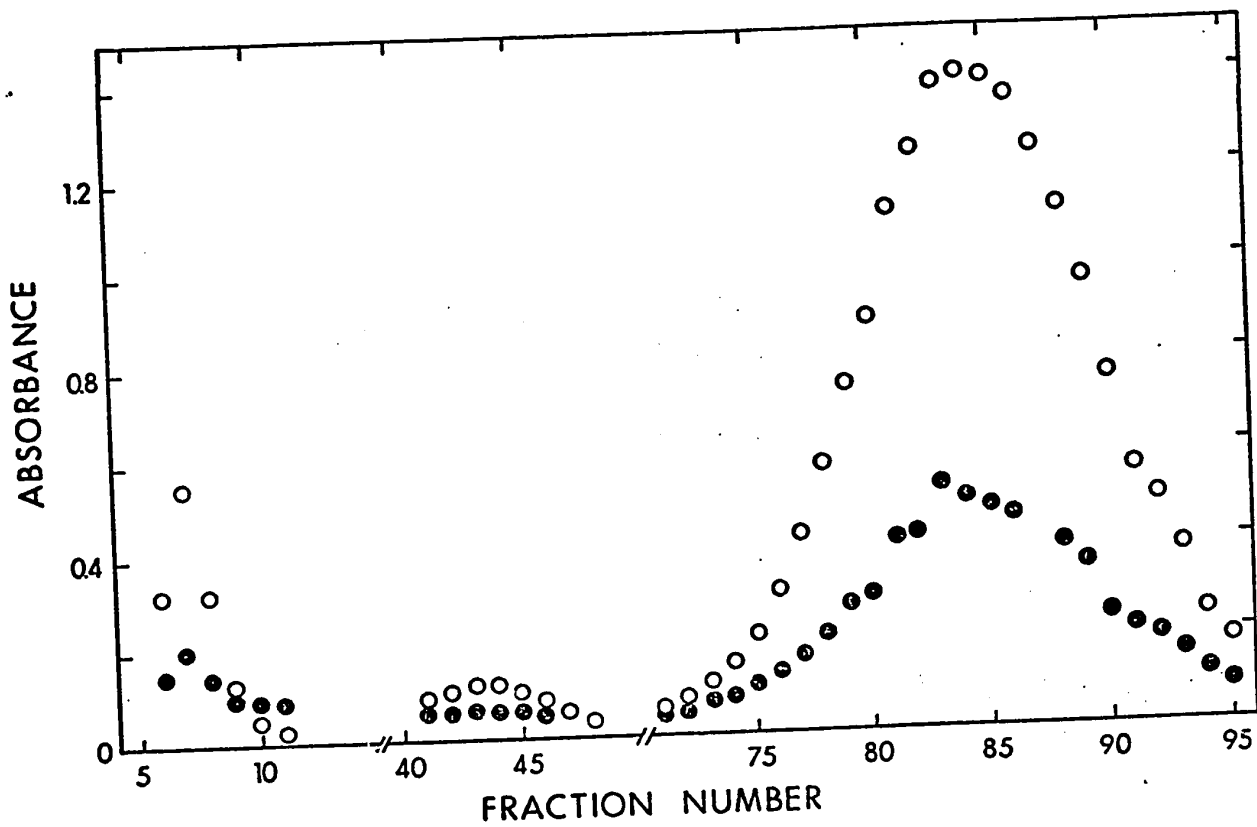


Fig. A 1.01: Plot of the absorbance of various fractions from the HRP purification. The open dots represent the absorbance at 403 nm and the solid dots represent the absorbance at 280 nm.

the enzyme was passed through a 8 μ Millipore filter and stored in the cold until it was used in the kinetic studies.

Discussion

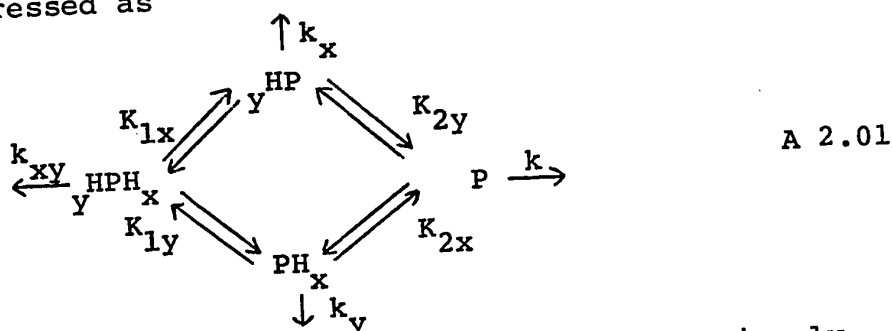
Shannon et al. (1966) reported that the main fraction of their enzyme preparation eluted at approximately the same position as the main peak illustrated in Fig. A 1.01. Further chromatographic separation by these authors revealed that this peak contained two components which they labelled isozyme B and C in order of their elution rate from the column. The B fraction represented 23% of the total HRP recovered and the C fraction 42%. In the present separation the main peak never revealed any indication of heterogeneity, even when HRP samples as small as 40 mg were applied under the same chromatographic conditions. This could indicate either that the peak represents only one isozyme or that a single chromatographic separation is insufficient to reveal the presence of a second isozyme. If the main peak is a single isozyme, the small peak observed between fractions 40 and 50 could be the B isozyme observed by Shannon et al. Shannon et al. also observed the presence of HRP isozymes which eluted rapidly from the column. Further purification of these fractions resulted in the isolation of three A isozymes. The other two isozymes reported by Shannon et al. eluted after the main peaks and represented about 12% of the total recovered HRP. These peaks were not observed for our sample of HRP under the present elution system. A third linear gradient consisting

of pH 4.9 acetate buffer of ionic strength 0.25 and pH 5.4 acetate buffer of ionic strength 0.6 revealed the presence of a small amount of HRP of low P.N. that may correspond to these isozymes. Overall the agreement with the results of Shannon et al. were reasonable and indicated that the HRP used in the kinetic studies consists primarily of B and C isozymes or perhaps only isozyme C.

Appendix 2

The pH Dependence of the Second-Order Rate Constant
for the Reaction of HRP-I with Iodide

The mechanism for the reaction illustrated in Fig.2.03
may be expressed as



where P , ${}_y\text{HP}$, PH_x and ${}_y\text{HPH}_x$ have been defined previously. The group ionization constants K_{1x} , K_{1y} , K_{2x} and K_{2y} are defined in an analogous manner to those for the unsymmetrical dibasic acid described by Dixon and Webb (1964). The symbols k , k_x , k_y and k_{xy} represent the second-order rate constants for the reactions of the various protonated HRP-I species with iodide, although for simplicity the iodide ions have not been included in equation A 2.01. The symbols k and k_{xy} represent the pH independent rate constants at high and low pH as illustrated in Fig. 2.03.

Equilibrium relations can be written for the four group ionization constants and rearranged to solve for any particular form of the enzyme. In the present case it was found convenient to solve in terms of P , the unprotonated form of HRP-I. The expressions are

$$K_{2y} = \frac{[P][H^+]}{[{}_yHP]} \therefore [{}_yHP] = \frac{[P][H^+]}{K_{2y}} \quad \text{A 2.02}$$

$$K_{2x} = \frac{[P][H^+]}{[PH_x]} \therefore [PH_x] = \frac{[P][H^+]}{K_{2x}} \quad \text{A 2.03}$$

$$K_{1y} = \frac{[PH_x][H^+]}{[{}_yHPH_x]} \therefore [{}_yHPH_x] = \frac{[PH_x][H^+]}{K_{1y}} = \frac{[P][H^+]}{K_{1y}K_{2x}} \quad \text{A 2.04}$$

$$K_{1x} = \frac{[{}_yHP][H^+]}{[{}_yHPH_x]} \therefore [{}_yHPH_x] = \frac{[{}_yHP][H^+]}{K_{1x}} = \frac{[P][H^+]}{K_{1x}K_{2y}} \quad \text{A 2.05}$$

From equations A 2.04 and A 2.05 we can deduce the equality

$$K_{1y}K_{2x} = K_{1x}K_{2y} \quad \text{A 2.06}$$

The conservation relationship that applies to the reaction is

$$[P]_t = [P] + [{}_yHP] + [PH_x] + [{}_yHPH_x] \quad \text{A 2.07}$$

where $[P]_t$ is the total concentration of HRP-I present in solution. Rewriting equation A 2.07 in terms of $[P]$ results in

$$[P]_t = [P] + \frac{[P][H^+]}{K_{2y}} + \frac{[P][H^+]}{K_{2x}} + \frac{[P][H^+]^2}{K_{1x}K_{2y}} \quad \text{A 2.08}$$

The differential rate expression for the reaction of HRP-I is given by

$$-\frac{d[P]_t}{dt} = k_1 [P]_t [I^-] = k [P] [I^-] + k_x [HP] [I^-] + k_y [PH_x] [I^-] + k_{xy} [y^{HPH_x}] [I^-] \quad \text{A 2.09}$$

Substituting the values of equations A 2.02 - A 2.05 into equation A 2.09 we obtain

$$k_1 [P]_t = k [P] + k_y \frac{[P][H^+]}{K_{2x}} + k_x \frac{[P][H^+]}{K_{2y}} + k_{xy} \frac{[P][H^+]^2}{K_{1x} K_{2y}} \quad \text{A 2.10}$$

Dividing both sides of equation A 2.10 by the value of $[P]_t$ in equation A 2.08 and cancelling the value for the $[P]$ from every term we obtain

$$k_1 = \frac{k + \frac{k_y [H^+]}{K_{2x}} + \frac{k_x [H^+]}{K_{2y}} + \frac{k_{xy} [H^+]^2}{K_{1x} K_{2y}}}{1 + \frac{[H^+]}{K_{2x}} + \frac{[H^+]}{K_{2y}} + \frac{[H^+]^2}{K_{1x} K_{2y}}} \quad \text{A 2.11}$$

In order to facilitate the comparison of equation A 2.11 with the equation derived from the transition state approach, the equation can be rewritten as

$$k_1 = \frac{k \left(1 + \frac{k_y [H^+]}{k K_{2x}} + \frac{k_x [H^+]}{k K_{2y}} + \frac{k_{xy} [H^+]^2}{k K_{1x} K_{2y}} \right)}{1 + \frac{[H^+]}{K_{2x}} + \frac{[H^+]}{K_{2y}} + \frac{[H^+]^2}{K_{1x} K_{2y}}} \quad \text{A 2.12}$$

Appendix 3

Error Estimates of the Parameters Calculated From
the Nonlinear Least-Squares Analysis of the
Kinetic pH Dependence

The pH dependence of the second-order rate constant for a given substrate is usually analyzed by obtaining the best fit to a predicted kinetic equation using a nonlinear least-squares analysis. In the conventional analysis, using the matrix inversion method, initial guesses for all adjustable parameters, including the pK_a values, are inserted into the computer program, which then minimizes the difference between the experimental and computed rate curves by varying these parameters. Using the transition state approach, the number of variable parameters is equal to the number of inflections in the pH profile plus one for the limiting rate constant at high or low pH. Generally all of these parameters are adjusted. However, if one parameter is known by independent measurement it can be fixed, for example in the analysis of the HRP-I-ferrocyanide reaction the ferrocyanide ionization constant was fixed.

Since the kinetic pH dependence for the various substrates are often quite different, there has been no set procedure devised (1) to distinguish between two different interpretations for the kinetic pH dependence, that is, to determine whether an observed inflection warrants

inclusion in the pH dependence and (2) to establish the errors associated with the various observed inflections. The purpose of this discussion is to propose a procedure for determining these two characteristics of the kinetic analysis.

Because of the complex nature of the equations being analyzed and the number of adjustable parameters involved, there will always be a certain arbitrariness associated with the procedure used. Thus the procedure employed in the present studies gives reasonable results for the reactions with iodide, sulfite and ferrocyanide, however this does not imply that this procedure will not have to be altered when more information becomes available on different substrates.

Along with the optimum values for the adjustable parameters calculated from the nonlinear least-squares analysis, our particular program provides various estimates of the error between experimental and calculated points. Among the error estimates calculated are the "standard deviations" of the various adjustable parameters. Although these "standard deviations" may have meaning as relative values, for example in comparing the deviation of two parameters from the same analysis, they are meaningless in an absolute sense. This point is perhaps best illustrated with an example. It is not unusual to find the standard deviation on an ionization constant to be less than 5%,

however this implies that the pK_a value is known to within ± 0.02 units. A careful look at any of the pH profiles in the present study will show that this error is unrealistically low. It was decided that a more reasonable approach to estimating the error on an individual parameter could be obtained if the analysis was performed with the parameters in question being held invariant. If the analysis is repeated with a variety of different invariant values for the parameter, the increase in the error between experimental and calculated values as the fixed parameter is varied away from its minimizing value provides a means for estimating the error of this parameter.

In the error estimates provided by the computer program, the one entitled "average absolute relative deviation" appears to provide the most meaningful estimate of the error between experimental and calculated values. The relative deviation calculated for each experimental point is defined as the difference between the observed and calculated values divided by the observed value. The "average absolute relative deviation" is an average of the absolute values for the relative deviations on each point. The inclusion of an additional adjustable parameter in a given analysis will always reduce the value of the "average absolute relative deviation". Within the context of the present studies, it was felt that if the deletion of a parameter resulted in an increase of 50% or greater in the value of the "average absolute relative deviation", then the parameter

warranted inclusion in the analysis.

In the HRP-I-iodide reaction a distinction was made in the analysis of the kinetic pH dependence between two interpretations differing by the inclusion of a transition state pK_a^\ddagger . The "average absolute relative deviation" for the interpretation illustrated by the solid line in Fig. 2.02 is 7.0%; that for the interpretation illustrated by the broken line is 12.2%, a percentage increase of 75%. An important difference between the two interpretations illustrated in Fig. 2.02 is that the broken line, in addition to having a larger average error per point, has a systematic deviation from the experimental points at low pH. Such systematic deviations are not taken into account by a simple comparison of the "average absolute relative deviation" for two interpretations and this is probably the major disadvantage to the use of this approach. Unfortunately it is not obvious at the present time how a consideration of this type of systematic deviation can be incorporated in a consistent manner into the procedure for distinguishing between two interpretations for the kinetic pH dependence.

The interpretation illustrated by the solid line in Fig. 3.02 for the HRP-I-sulfite reaction has an "average absolute relative deviation" of 3.8% and that for the broken line in the same figure has a value of 28%. The large average error for the broken line is obvious from the deviation between calculated and experimental points in Fig. 3.02. The "average absolute relative deviation" for the

interpretation represented by the solid line in Fig. 3.04 for the HRP-II-sulfite reaction is 5.2% and that for the broken line is 7.2%. Using the same criterion for the difference between these interpretations, the 38% increase in the value of the "average absolute relative deviation" is not sufficient to warrant inclusion of an additional parameter. Again this conclusion is in agreement with that made by visual inspection of Fig.3.04, which would indicate that the two interpretations were sufficiently similar to make distinction between them difficult.

In order to get an estimate of the errors associated with each parameter, the criterion of a 50% increase in the value of the "average absolute relative deviation" over that observed for the minimizing values of the parameters was again used. Table A 3.01 presents the values of the "average absolute relative deviations" obtained by holding the term K_2 in equation 2.18 for the HRP-I-iodide reaction constant at pK_a values from 4.3 to 4.9. Table A 3.01 also contains another estimate of error supplied by the computer program, the "root mean square deviation". The changes in the "root mean square deviation" generally parallel those for the "average absolute relative deviation". For purposes of comparison, the values of the standard deviations calculated for the adjustable parameters are also included in Table A 3.01. These error estimates have the disadvantage that the extent of the change in these values depends on their relation to the fixed parameter. That is, the

standard deviation of one parameter may vary greatly for a certain value of K_2 , while that for another parameter changes only slightly.

The variation of the "average absolute relative deviation" in Table A 3.01 indicated that pK_2 has a value between 4.5 and 4.8, thus this value can be written 4.6 ± 0.2 . Inspection of the values in Table A 3.01 indicates that the error is not symmetrical about the pK_a value. In such cases the error limits on the pK_a value are represented as the larger of the two errors, in this case the difference between 4.6 and 4.8. The results of a similar analysis for equation 3.04 with K_5 as an invariant parameter, for the HRP-I-sulfite reaction, are illustrated in Table A 3.02. The value of pK_5 deduced from this table is 5.1 ± 0.2 . The results for the analysis of the HRP-I-ferrocyanide reaction are presented in Table A 3.03. The pH dependence of this reaction was analyzed according to the equation

$$k_7 = \frac{k_7' \left(1 + \frac{[H^+]}{K_5^\ddagger} + \frac{[H^+]^2}{K_5^\ddagger K_6^\ddagger} \right)}{\left(1 + \frac{[H^+]}{K_7} \right) \left(1 + \frac{[H^+]}{K_a} \right)} \quad \text{A 3.01}$$

where the experimental values of k_7 were obtained from the work of Hasinoff and Dunford (1970). In this analysis the value of the ferrocyanide ionization constant, K_a , was held constant as had been done in the original analysis

Table A 3.01

Errors Resulting from the Analysis of Equation 2.18 with K_2 as an Invariant Parameter for the Reaction of HRP-I with Iodide

K_2 (M)	pK_2	Percent Average Absolute Relative Deviation	Root Mean Square Deviation	Percent Standard Deviation of Adjustable Parameters K_1	k K_1
5.0×10^{-5}	4.3	21	5.6	5.5	1.2×10^4
3.2×10^{-5}	4.5	12	2.6	2.3	63
2.5×10^{-5}	4.6	7.5	1.4	1.2	17
2.3×10^{-5a}	4.64	7.0	1.3		
2.0×10^{-5}	4.7	7.4	1.5	1.4	14
1.6×10^{-5}	4.8	10	2.7	2.4	18
1.3×10^{-5}	4.9	15	3.9	3.5	23

^aThe minimizing value of K_2 calculated with K_2 as an adjustable parameter.

Table A 3.02

Errors Resulting from the Analysis of Equation 3.04 with K_5 as an Invariant Parameter for the Reaction of HRP-I with Sulfite

K_5 (M)	pK_5	Percent Average Absolute Relative Deviation	Root Mean Square Deviation	K_3^{\dagger}	Percent Standard Deviation of Adjustable Parameters	K_4	K_5
3.2×10^{-5}	4.5	25	12	99	63	152	35
2.5×10^{-5}	4.6	13	11	159	144	244	26
2.0×10^{-5}	4.7	11	10	93	58	140	33
1.6×10^{-5}	4.8	7.9	3.5	28	19	43	7.7
1.3×10^{-5}	4.9	5.6	2.9	16	10	23	6.0
1.0×10^{-5}	5.0	4.1	2.3	10	7.1	15	4.6
8.5×10^{-6a}	5.07	3.8	2.3				
7.9×10^{-6}	5.1	4.1	2.2	8.8	6.4	13	4.2
6.3×10^{-6}	5.2	5.1	2.6	9.6	7.1	14	4.7
5.0×10^{-6}	5.3	6.4	3.3	12	8.8	18	5.9
4.0×10^{-6}	5.4	7.9	4.1	15	11	22	7.1
3.2×10^{-6}	5.5	9.3	4.9	18	13	26	8.6

^aThe minimizing value of K_5 calculated with K_5 as an adjustable parameter.

Table A 3.03

Errors Resulting from the Analysis of Equation A 3.01 with K_7 as an Invariant Parameter for the Reaction of HRP-I with Ferrocyanide

K_7 (M)	pK_7	Percent Average Absolute Relative Deviation	Root Mean Square Deviation	Percent Standard Deviation of Adjustable Parameter k_7	k_5	k_6
5.0×10^{-4}	3.3	21	0.29	6.4	16	1.3×10^4
7.9×10^{-5}	4.1	15	0.20	4.4	11	528
5.0×10^{-5}	4.3	14	0.18	4.1	10	81
3.2×10^{-5}	4.5	13	0.16	3.7	9	41
2.0×10^{-5}	4.7	11	0.14	3.3	8.1	25
1.3×10^{-5}	4.9	10	0.13	3.0	7.3	18
1.0×10^{-5}	5.0	9.3	0.12	2.8	6.9	15
7.9×10^{-6}	5.1	9.0	0.12	2.7	6.7	14
6.3×10^{-6}	5.2	8.8	0.11	2.7	6.6	12
5.1×10^{-6a}	5.29	8.8	0.11			
5.0×10^{-6}	5.3	8.8	0.11	2.7	6.6	12
4.0×10^{-6}	5.4	8.9	0.11	2.7	6.6	11
3.2×10^{-6}	5.5	9.0	0.12	2.8	6.9	11
2.0×10^{-6}	5.7	9.3	0.13	3.1	7.5	11
1.3×10^{-6}	5.9	9.7	0.14	3.4	8.3	12
7.9×10^{-7}	6.1	10	0.15	3.8	9.3	12
3.2×10^{-7}	6.5	13	0.18	4.6	11	19

^aThe minimizing value of K_7 calculated with K_7 as an adjustable parameter.

by these authors. The results in Table A 3.03 indicate that the value of pK_7 is 5.3 ± 0.8 .

The analysis of the kinetic pH dependence for the HRP-I-sulfite reaction indicates that there are two pK_a 's, pK_4 and pK_5 , with values of 3.1 and 5.1. The value of the standard deviation calculated by the computer program indicates that the error in K_4 is about 50% greater than in K_5 . In order to check if these values of the standard deviation have relative meaning, an analysis of equation 3.02 was performed with K_4 as the invariant parameter. The results of this analysis are illustrated in Table A 3.04 and indicate that the value of pK_4 is 3.3 ± 0.3 . The error on pK_4 is thus about 50% greater than the error on pK_5 , 0.2, indicating that the values of the standard deviation calculated for the adjustable parameters may be useful in relating the errors of different parameters in the same analysis.

Table A 3.04
 Errors Resulting from the Analysis of Equation 3.04 with
 K_4 as an Invariant Parameter for the
 Reaction of HRP-I with Sulfite

K_4 (M)	PK ₄	Percent		Root Mean		Percent Standard Deviation of Adjustable Parameters			
		Average Absolute Relative Deviation	Square Deviation	Average Absolute Relative Deviation	Square Deviation	k_3 [†]	k_3 '	K_5	K_s
3.2×10^{-3}	2.5	41	43	165	124	77	-16		
2.0×10^{-3}	2.7	9.1	3.4	12	8.8	8.3	10.2		
1.3×10^{-3}	2.9	7.4	3.1	7.1	7.3	8.5	9.7		
7.9×10^{-4}	3.1	5.1	2.6	9.3	5.4	8.8	9.1		
6.3×10^{-4}	3.2	4.0	2.4	8.5	4.6	8.8	8.9		
5.0×10^{-4}	3.3	3.7	2.2	7.9	4.0	8.9	8.8		
4.6×10^{-4a}	3.34	3.8	2.3						
4.0×10^{-4}	3.4	4.7	2.3	8.0	3.8	9.7	9.5		
3.2×10^{-4}	3.5	6.8	2.5	8.8	4.0	11	11		
2.0×10^{-4}	3.7	12	3.4	12	4.8	17	16		
1.3×10^{-4}	3.9	16	4.3	15	5.4	22	21		
7.9×10^{-5}	4.1	21	5.1	19	5.8	29	26		

^aThe minimizing value of K_4 calculated with K_4 as an adjustable parameter.

Appendix 4

Descriptions of Photomultiplier Circuit Modifications
and the Analog-to-Digital Converter used with the
Stopped-Flow Apparatus

The analog-to-digital converter used in the kinetic studies on the stopped-flow apparatus was designed and constructed by the Technical Services Electronic Shop at the University of Alberta. The device converted the voltage output at the photomultiplier to digital readings at predetermined time intervals. In a typical kinetic experiment the analog-to-digital converter was activated by the voltage surge from the pneumatic solenoid valve used to trigger the drive on the stopped-flow apparatus. In order to optimize the number of data points taken in the region of changing absorbance, the initial reading was delayed until the driving time (the time taken to drive the syringe plungers from stop to stop) had been completed. This was accomplished by directing the voltage surge resulting from the triggering of the solenoid into a time delay circuit that could be adjusted from 6 to 90 milliseconds. The resulting delayed pulse was used to trigger the initiation of the voltage readings as well as the oscilloscope. Thus the visual representation of the voltages being measured were available on the oscilloscope providing a convenient method of monitoring the reaction.

The digital voltage meter used in the analog-to-digital converter is capable of reading voltages from +10 to -10

volts to an accuracy of 10 millivolts. In order to minimize the error in the voltage readings an amplification of the photomultiplier output was necessary. The normal total change in voltage obtained from the photomultiplier output for the experimental conditions used for the kinetic studies is approximately 200 millivolts. When the digital voltage meter is used, this signal is usually amplified to give a change of 4-8 volts. A circuit diagram of this amplifier is illustrated in Fig. A 4.01. The input to the amplifier, labelled BNC input, is from the photomultiplier. The photomultiplier circuit is basically the same as that described by Ellis (1968), however the addition photomultiplier power supply used to furnish the "bucking voltage" in the previous instrument was replaced by a series of three balance controls coupled to the amplifier power supply in the present instrument. In addition to the balance controls the amplifier is also equipped with a gain control (the maximum gain of the amplifier is 1000), a filter control (to reduce noise levels) and a moving coil voltmeter (with a scale from -10 to +10 volts) to give a qualitative indication of the voltage changes.

The amplified photomultiplier voltage from the BNC output leads to a unit containing the digital voltage meter, a master clock and the memory circuits. The master clock determines the frequency of voltage measurements. These can be varied from 600 readings/sec to 0.75 readings/sec. The thirty voltage readings are stored and if the visual

inspection of the voltage trace on the storage oscilloscope shows it to be satisfactory, the printer is activated and the voltages are printed out. The printer is a Hewlett-Packard model 5055A Digital Recorder that can print up to ten lines/sec. The circuitry involved in the storage of the voltage readings is complex and will not be discussed here. However more detailed information and circuit diagrams are available on request.